# ESTIMATION OF STATISTICAL ENERGY ANALYSIS PARAMETERS FOR STRUCTURAL ELEMENTS

*A thesis submitted for the award of the degree of*

**DOCTOR OF PHILOSOPHY**

*in*

**Mechanical Engineering**

*by*

**MARUTI BHAGWAN MANDALE**
**Roll No. 701137**

*Under the guidance of*

**Prof. P. BANGARU BABU**
Department of Mechanical Engineering
National Institute of Technology (NIT), Warangal-506004

&

**Prof. S.M.SAWANT**
Department of Mechanical Engineering
R.I.T.Rajaramnagar, Islampur.

.


**DEPARTMENT OF MECHANICAL ENGINEERING**
**NATIONAL INSTITUTE OF TECHNOLOGY**
**WARANGAL – 506004**
**INDIA**
**2018**

Thesis Approval Sheet

# Estimation of statistical energy analysis parameters for structural elements

*By*

**Mr. MARUTI BHAGWAN MANDALE**

**is approved for the degree of**

## Doctor of Philosophy

---

**Dr. A.T.Chavan**
(External Examiner)
Senior Software Technical Consultant
Parametric Technology Corporation India Pvt. Ltd, Pune

---

**Prof P. Bangaru Babu**
(Supervisor)
Department of Mechanical Engineering
National Institute of Technology
Warangal-506004

---

**Prof. S.M.Sawant**
(Co-Supervisor)
Department of Mechanical Engineering
R.I.T.Rajaramnagar, Islampur, Dist-Sangli, Maharashtra

---

**Prof Selvaraj N**
Head & Chairman DSC
Department of Mechanical Engineering
National Institute of Technology
Warangal-506004

# Department of Mechanical Engineering
# NATIONAL INSTITUTE OF TECHNOLOGY
# WARANGAL-506004

## CERTIFICATE

This is to certify that the dissertation work entitled **"ESTIMATION OF STATISTICAL ENERGY ANALYSIS PARAMETERS FOR STRUCTURAL ELEMENTS**" which is being submitted by **Mr. MARUTI BHAGWAN MANDALE (Roll No.701137)**, his bonafide work is submitted to National Institute of Technology, Warangal, in partial fulfilment of requirement for the award of degree of **Doctor of Philosophy in Mechanical Engineering**. To the best of our knowledge, the work incorporated in this thesis has not been submitted elsewhere for the award of any degree.


**Prof P. Bangaru Babu**
Supervisor
Department of Mechanical Engineering
National Institute of Technology
Warangal-506004

**Prof. S.M.Sawant**
Co-Supervisor
Department of Mechanical Engineering
R.I.T.Rajaramnagar, Islampur,
Dist-Sangli, Maharashtra.

**Prof Selvaraj N**
Head & Chairman DSC
Department of Mechanical Engineering
National Institute of Technology
Warangal-506004

# DECLARATION

This is to certify that the work presented in the thesis entitled "**ESTIMATION OF STATISTICAL ENERGY ANALYSIS PARAMETERS FOR STRUCTURAL ELEMENTS"** is a bonafide work done by me under the supervision of Dr P. Bangaru Babu, Professor, Department of Mechanical Engineering, N.I.T.Warangal and Prof.S.M.Sawant, Department of Mechanical Engineering, R.I.T.Rajaramnagar, Islampur and was not submitted elsewhere for the award of any degree.

I declare that this written submission represents my ideas in my own words and where others ideas or words have been included; I have adequately cited and referenced the original sources. I also declare that I have adhered to all principles of academic honesty and integrity and have not misrepresented or fabricated or falsified any idea/data/fact/source in my submission. I understand that any violation of the above will be a cause for disciplinary action by the institute and can also evoke penal action from the sources which have not been properly cited or from whom proper permission has not been taken when needed.

**Maruti Bhagwan Mandale**
Roll No. - 701137
Date:

*Dedicated with all humility and devotion*

*to*

*My teachers, my family and who were responsible*

*for completion*

# ACKNOWLEDGEMENTS

Research is, but, one of the numerous means to expound the mysterious ways of the Almighty. I thank him with all veneration and modesty for granting me this opportunity.

I express my deepest gratitude to my research supervisor **Prof. P. Bangaru Babu**, for his invaluable guidance and care that helped me tread my path in this journey. I express my sincere thanks to my external research supervisor Prof.S.M.Sawant, Department of Mechanical Engineering, R.I.T.Rajaramnagar, Islampur, for his valuable suggestions and guidance in spite of his busy schedule.

I am grateful to my Doctorial Scrutiny Committee (DSC) members, Prof. T.D.Gunneswara Rao, Department of Civil Engineering and Prof.R.V.Chalam, Department of Mechanical Engineering, National Institute of Technology, Warangal, for their support and suggestions at every level from starting to completion of the work.

I am very much thankful to Prof. L.Krishnanand, Prof.C.S.P.Rao, Prof. P.Bangaru Babu and Prof.Selvaraj N, Chairman's of DSC at various periods for extending their support in completing the research work.

I wish to express my sincere thanks to Prof. Mrs. S. S. Kulkarni, Director, R. I.T., Rajaramnagar. I am also thankful to Dr. S. S.Gawade, Dr. S.D.Patil and Dr. S.K.Patil of R. I.T., Rajaramnagar, for their continuous support during my research work.

Words fail to express my profound gratitude to my beloved wife Mrs. Rohini and my two children Rucha and Ruturaj, for their love and affection, wishes and patiently bearing me during my research work. I also express my whole hearted thanks to all my family members, whose love, affection and blessings are the backbone for my success.

**Maruti Bhagwan Mandale**

# Abstract

The statistical energy analysis (SEA) method has been developed for middle and high audio-frequencies. It is a useful tool for designers to predict power transmission paths and radiation of complex mechanical systems, such as airplanes, ships, buildings, transport vehicles and electromechanical equipments. In statistical energy analysis, damping loss factor, coupling loss factor and modal density are the essential parameters for vibro-acoustic analysis of complicated structures.

Damping is usually characterized by the amount of energy dissipated and the most common measure of this dissipation is damping loss factor. The effects of materials used for plate on damping loss factors are described. Half-power bandwidth method had used for determining damping loss factors of aluminium, mild steel and stainless steel rectangular plates with free-free, simply supported and clamped free condition. Also this method had used for determining damping loss factors of composite plates with different fiber orientations. Damping loss factor values of composite plates are higher than aluminium, stainless steel and mild steel plates for free-free boundary condition.

In statistical energy analysis the resonant modes are grouped into different frequency bands. Modal density gives the relation between number of resonant modes in selected frequency band and frequency range. Modal densities had determined and compared by theoretical and experimental methods for rectangular plates of different materials like mild steel, aluminium, stainless steel and composites. Also modal densities of unidirectional, quasi isotropic and cross ply fiber orientations of composite plates had compared. The effect of graphene addition in composite plate on modal density had verified.

In industries, the use of appropriate junctions between components is of paramount interest. The values of coupling loss factor had calculated and compared for different

junctions. The screwed and bolted junctions had examined for thin rectangular aluminium plates of same size. The energy level difference method had used to find coupling loss factors because of its simplicity. These experimentally found coupling loss factors had later compared with analytical solutions. It is noticed that the analytical results are in qualitative agreement with experimental results. It is also observed that coupling loss factors for bolted junction are relatively higher than that of screwed junction. Also the values of coupling loss factor had estimated by using energy level difference method by varying tightening torque applied at junction. Higher values of coupling loss factor have been observed for higher tightening torque on bolted junction.

The values of coupling loss factor had determined for different structural junctions of composite plates. The riveted and bolted junctions had examined for rectangular composite plates of same size and in same plane. It is observed that coupling loss factors for bolted junction are relatively higher than that for riveted junction of composite plates. The values of coupling loss factors are found to increase with increasing tightening torque applied at structural junctions of composite plates. It is also noticed that the experimental results of coupling loss factors for point junctions vary with changes in fiber orientations of composite plates.

It is firmly believed that the various findings of the statistical energy analysis parameters in the current thesis help for vibro-acoustic analysis of complicated structures.

**Keywords**: Statistical energy analysis, Modal density, Damping loss factor, Coupling loss factor, Structural junctions, Power flow equation.

# Table of Contents

# List of Figures

# List of Tables

# NOMENCLATURE

| | |
|---|---|
| $B$ | The flexural rigidity |
| $C_{gl}$ | Group speed of longitudinal wave |
| $E$ | Modulus of elasticity |
| $E_p$ | Vibration energy of subsystem ‘p’ |
| $E_s$ | Vibration energy of subsystem ‘s’ |
| $\boldsymbol{E}_i$ | The time-averaged total energy stored in subsystem i. |
| $f$ | Frequency in Hz |
| $G_{pA}$ | Input conductance of subsystem ‘p’ at ‘A’. |
| $h$ | Thickness of plate |
| $I_n$ | Intensity component |
| $k_p$ | Bending wave number of subsystem ‘p’ |
| $k_s$ | Bending wave number of subsystem ‘s’ |
| $L_1$ and $L_2$ | Dimensions of rectangular plate |
| $L_j$ | Junction length |
| $l_p$ | Sinusoidal force of rms amplitude |
| $M_p$ | Mass of the subsystem ‘p’ |
| N | The number of available modes of subsystem |
| $R_{sj}$ | Input resistance of subsystem ‘s’ at the junction |

| | |
|---|---|
| $R_{pj}$ | Input resistance of subsystem ‘p’ at the junction |
| $r$ | Amplitude reflection coefficient at the interface |
| $S$ | Surface area of plate under consideration |
| $Z_{pj} + Z_{sj}$ | The total impedance at the junction |
| $\prod_{1,in}$ | Power input to subsystem 1 from external excitation |
| $\prod_{1,diss}$ | Power dissipated from subsystem 1 by the internal damping |
| $\prod_{in}^{p}$ | Power input to subsystem ‘p’ from external excitation |
| $\prod_{diss}^{p}$ | Power dissipated from subsystem ‘p’ by the internal damping |
| $\prod_{12}$ | Power transmitted from subsystem 1 to subsystem 2 |
| $\prod_{p,in}$ | Power input to subsystem ‘p’ |
| $\prod_{p,diss}$ | Power dissipated from subsystem ‘p’ |
| $\prod_{ps}$ | Power transmitted from subsystem ‘p’ to subsystem ‘s’ |
| $\prod_{p}^{(1)}$ | Input power of subsystem ‘p’ when it is being excited |
| $\prod_{s}^{(2)}$ | Input power of subsystem ‘s’ when it is being excited |
| $\prod_{coup}^{ps}$ | Net power transferred from subsystem ‘p’ to subsystem ‘s’ through dynamic coupling |
| $\prod_{tra}$ | Transmitted power |
| $\prod_{inc}$ | Incidence power |
| $\prod_{ref}$ | Reflected power |
| $\omega$ | The central frequency of the chosen percentage band |

| | |
|---|---|
| $\eta_p$ | The damping loss factor of subsystem ‘p’. |
| $\eta_s$ | The damping loss factor of subsystem ‘s’. |
| $\eta_{ps}$ | The coupling loss factor from subsystem ‘p’ to subsystem ‘s’. |
| $\eta_{12}$ | The coupling loss factor from subsystem ‘1’ to subsystem ‘2’. |
| $\eta_{sp}$ | The coupling loss factor from subsystem ‘s’ to subsystem ‘p’. |
| $v_j$ | The rms velocity at the junction |
| $v'_{pA}$ | The rms velocity of subsystem ‘p’ at the point ‘A’ |
| $\tau(f)_{ps}$ | The transmission coefficient as a function of frequency f. |
| $\tau_{ps,\infty}$ | Infinite system transmission coefficient |
| $\delta f_p$ | Average frequency spacing of subsystem ‘p’ |
| $\delta f_s$ | Average frequency spacing of subsystem ‘s’ |
| $\beta_p$ | Modal overlap factor of subsystem ‘p’ |
| $\beta_s$ | Modal overlap factor of subsystem ‘s’ |
| $\beta_{corr}$ | Corrected overlap factor |
| $\beta_{p,net}$ | Net overlap factor of subsystem ‘p’ |
| $\beta_{s,net}$ | Net overlap factor of subsystem ‘s’ |
| $n(\omega)$ | Modal density of subsystem |
| $C_{gl}$ | Group speed of wave |
| $\upsilon$ | Poisson’s ratio |
| $\rho$ | Density of the material |

# ABBREVATIONS

| | |
|---|---|
| SEA | Statistical energy analysis |
| CLF | Coupling loss factor |
| DLF | Damping loss factor |
| MD | Modal density |
| CSEA | Classical statistical energy analysis |
| EILFs | Effective internal loss factors |
| ESEA | Experimental statistical energy analysis |
| ESEM | Energy spectral element method |
| EFA | Energy flow analysis |
| ASEA | Advanced statistical energy analysis |
| FEM | Finite element method |
| ELD | Energy level difference method |
| PIM | Power injection method |
| FFT | Fast Fourier Transform |
| DAS | Data acquisition system |

Chapter 1

# INTRODUCTION

## 1.1 Background

Statistical Energy Analysis (SEA) was evolved in the early 1960's, to model high frequency vibro-acoustic interaction in the rocket launch vehicle structures. The word SEA was coined due to the subsequent reasons. 'Statistical' notes that the systems under study are assumed to be drawn from populations of similar construction with a known distribution of their dynamic parameters. This enables one to account for the manufacturing tolerance that exists in practical systems. ‘Energy’ is the primary variable considered in SEA. Displacement, velocity, acceleration and sound pressure are all can be derived from energy. SEA basically consists of computing the storage and flow of energy. The term "analysis" is used to underline that SEA is a framework of study and not a particular technique.

Though the vibrational modes of structures could be predicted computationally, the size of the models and the computational speed limit the engineers to predict a few of the lowest modes. Traditionally, in analysis of mechanical vibrations, the lowest modes are significant because these modes produce maximum response. But while designing large and lightweight structures, it is necessary to account higher order modes for the purpose of envisaging equipment failure, structural fatigue and noise production. Information about mode shapes and natural frequencies of structures at higher frequencies are necessary for modal analysis. The natural frequencies and mode shapes become highly sensitive to small variation in material properties, construction and geometry of the structure due to smaller wavelengths. Therefore, one has to precisely describe material properties, construction and geometry of the structure and compute the natural frequencies and mode shapes accurately.

Such an accurate description is practically impossible, since the above parameters can only be defined in terms of tolerance limits. Hence SEA that uses the statistical model of dynamic systems continues to be a useful technique for many vibration and noise applications in the high frequency region.

SEA has been widely used in a growing number of applications. It has been used in predicting cabin noise of automobiles and calculating the transmission loss of partitions. It has also been successful in predicting the average vibrational amplitudes and sound pressures in aircraft, ships, buildings, space vehicles and large machines. Thus, SEA has evolved as a beneficial technique for predicting vibration and noise in a large number of applications. It has thus replaced the empirical approach that was used earlier.

The SEA procedure consists of three steps for analysis purpose. In first step, SEA model of system is to be developed to calculate the flow of dynamical and storage energy in a system. The subsystems are groups of similar modes. The input energy comes from each of the storage elements from a set of external sources. In SEA model, the subsystem or fundamental element is group of similar energy storage modes. Same type of mode such as flexural, torsional and longitudinal that exist in complex system is called as subsystem. Similarity and significance criteria are used for selecting the modal group. In similarity criteria, mode groups are excited with nearly equal excitation force by the source which results in same energy of vibration. In significance criteria, mode group plays an important role in dissipation and transmission of energy.

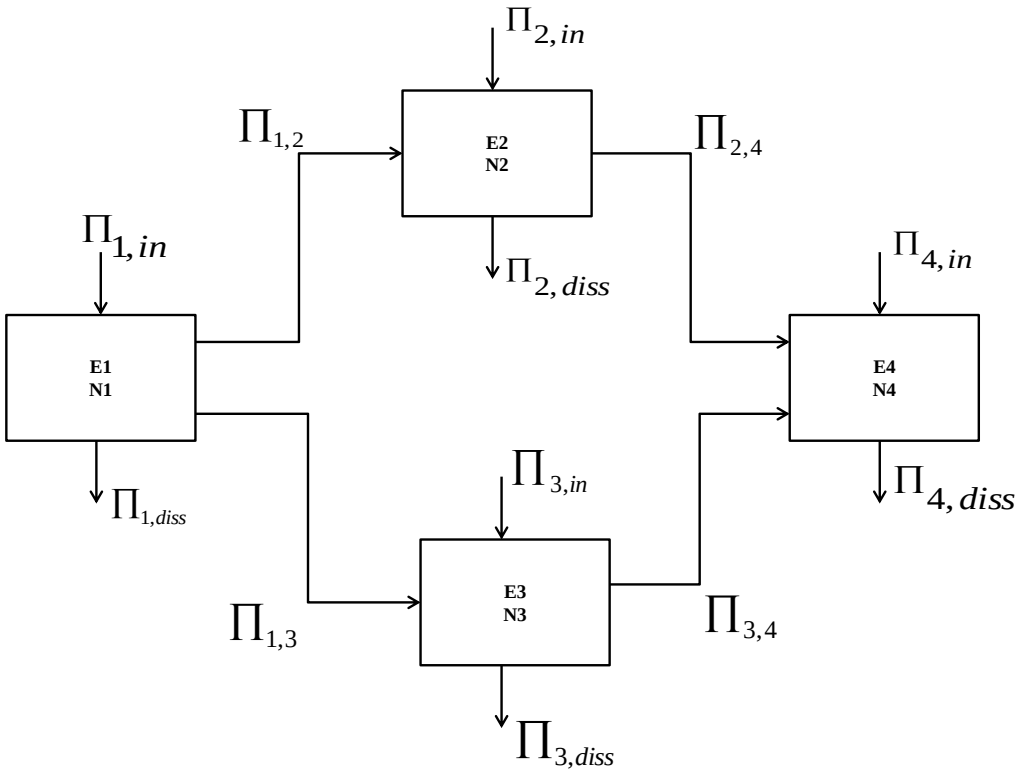


Figure 1.1: Distinctive form of statistical energy analysis model of the system

The SEA parameters of the subsystems are evaluated in second step. The quantities shown in figure 1.1 can be evaluated by knowing certain parameters called as SEA parameters. They are grouped as energy transfer and energy storage parameters. The number of available modes $N_1$, $N_2$....for each subsystem in particular frequency range gives the storage of energy. The ratio of number of available modes to the frequency band is called the modal density. It is frequently used in calculations of statistical energy analysis instead of the mode count. The modal density can be measured by exciting the subsystem with pure sound and varying the frequency. From frequency domain chart, number of peaks can be counted for modal density. Theoretical formulae's are also used to calculate the modal density of different subsystems.

$\prod_{diss}$ represents dissipation of energy for each subsystem. It can be dissipated by friction or radiate into the structure or the ambient air. This dissipated power cannot be returned to the subsystem. The dissipation of energy into the subsystem is measured by loss factor called as damping loss factor. It is defined as ratio of energy dissipated per cycle of oscillation to the total energy in the subsystem. Dissipation mechanism varies with respect to viscosity, surface friction, acoustical radiation, rotational flows, turbulence, mechanical and magnetic hysteresis. While analyzing complex system, it is noticed that some damping mechanisms are measurable effects and other forms are negligibly small. As far as vibration and noise control is concerned, structural damping is most pertinent type of damping. Damping loss factor of system is measured by decay rate and half power bandwidth method.

$\prod_{in}$ is the input power from the environment as shown in figure 1.1. It is computed for full or one-third octave band. Force applied on the subsystem and impedance corresponding to that force is used for calculating the input power. Also input power is measured by using dissipated power.

$\prod_{12}$ represents transmitted power between subsystems 1 and 2. The transmitted power depends on the modal energy difference of the subsystems and the strength of the coupling between the subsystems. The coupling loss factor is the parameter governing the transmitted power. This is the ratio of the energy transferred per oscillation cycle to the total energy in the subsystem. It is also related to transmission loss, radiation efficiency, junction impedances of mechanical systems, orientation, thickness and material properties of the structure.

To calculate the response, SEA model and parameters of subsystems are required. The vibrational energy (E) of different mode groups or energy storage elements is obtained by solving linear algebraic equations. These linear algebraic equations depend on number of

subsystems. The average vibrational energy depends upon the modal density, input power, damping and coupling loss factors.

There are physical interconnections between subsystems through joints in machines such as automobiles, aerospace and ships. To predict the response of such systems, determination of coupling loss factor for various systems with bolted, riveted and screwed joints becomes necessary. The modal density and damping loss factors depends on material properties of the system. This present work focuses on estimation of statistical energy analysis parameters of idealized subsystems.

### 1.2 Organization of the Thesis

The present thesis comprises a total of seven chapters inclusive of the current chapter. In what follows, the prominent features of various chapters are enunciated.

**Chapter 1:**'**Introduction**' deals with the present research problem tackled in this work. This chapter further describes the broad organization of the thesis indicating what is in store in each of the chapters.

**Chapter 2:** '**Literature Review**' presents an exhaustive review of the literature pertaining to the research problem taken up in the present work. Based on gaps identified in literature, objectives and the scope of the research work are presented in this chapter.

**Chapter 3:** '**Theoretical models and computations of statistical energy analysis parameters**' deals few cases of idealized subsystem. The theoretical and experimental methods of estimating statistical energy analysis parameters of idealized subsystem are included in this chapter.

**Chapter 4:** '**Experimental setup for the estimation of statistical energy analysis parameters'** deals with arrangement of instrumentation for measurement of statistical energy

analysis parameters for idealized subsystems. In this chapter details of the instruments used for the experimentation are included.

**Chapter 5: 'Damping loss factor and modal density estimation for plates'** reports the experimental setup for measurement of damping loss factor and modal density of the plates with different boundary conditions. This chapter summarises the results of the experimentation for modal density and damping loss factor.

**Chapter 6:'Coupling loss factor estimation for different structural junctions of idealized subsystems'** reports the result of experimentation for coupling loss factor of perpendicular and in same plane plates with different structural junctions.

**Chapter 7:'Conclusions'** outlines the overall outcome of the present study. This chapter also includes the scope for further study in the area of statistical energy analysis.

### 1.3 Closer

The background and the motivation pertaining to the research problem taken for study in the present research work is presented. Subsequently various important features of each of the seven chapters of the thesis are provided enabling the reader to know, a priori, as to what could be expected in these chapters.

# Chapter 2

# LITERATURE REVIEW

## 2.1Introduction

In this chapter, a review of the past investigations carried out in the field of statistical energy analysis has been discussed in brief, for identification of the research gaps, and for identifying the new research work listed in the present study. Review of literature is presented in four categories such as general statistical energy analysis, modal density, damping loss factors and coupling loss factors.

## 2.2 Literature related to statistical energy analysis

Statistical energy analysis (SEA) is extensively used vibro-acoustic method for predicting the transmission of vibration and sound through different structural systems. Such a complex systems are generally divided in to subsystems. The effective prediction of sound and vibration levels in such systems depends on precise estimation of SEA parameters. R.H.Lyon is credited to be the originator of SEA. The first paper on SEA was written by R.H.Lyon et al. [1].Authors proved that power flow is directly proportional to the modal energy difference between coupled oscillators and indicated that the direction of the power flow depends on the energy levels of two oscillators. They also applied the idea to two randomly excited multimodal systems. The articles by R. H. Lyon form the basis of SEA techniques, which have grown enormously in the last fifty-five years, both in terms of the number of publications and useful applications.

Initial work in statistical energy analysis assumed a weak coupling between subsystems. E.E.Ungar [2] applied statistical energy analysis to strongly coupled case. An expression has been developed by C. A. Mercer et al. [3] using a perturbation analysis for the

flow of energy between two oscillators coupled by a weak coupling and subjected to the transient load. It is concluded that the energy flow between the coupled oscillators is directly proportional to the magnitude of the transient load as well as the energy difference.

To calculate the internal loss factor and coupling loss factors for plates, Bies et al. [4] applied the power input method. It has been resolved that good agreement was obtained between predicted and measured values.

A review of theoretical background of SEA has been presented by J.Woodhouse [5]. SEA has been illustrated by simple example and also explained the procedure for dividing structure into subsystems. B.M.Gibbs et al. [6] have investigated theoretical and experimental low frequency reflection and transmission of vibrational energy at an L-junction of square section rods.

R. J. M. Craik [7] incorporated random errors into the statistical energy analysis model. For large systems, this creates uncertainty about energy levels. The shape of the system is important because error depend on it. A small statistical energy analysis model having short paths was less affected than statistical energy analysis model controlled by long paths. It is concluded that large statistical energy analysis models can be used with assurance based on approximate data.

M.J. Sablik et al. [8] applied statistical energy analysis method for a beam network in building structure. A method related to structural resonance was introduced. One beam was vibrationally excited in a beam network and transfer function was computed over wide frequency range. They concluded that by taking resonance effects into account, the predictions of statistical energy analysis can be made to display the fine details found in the frequency dependence of transfer functions for real building structures.

F.J.Fahy et al. [9] reported that power flow averaged over time between two oscillators attached by damping and spring elements, subjected to white sound sources, was not only proportional to the energy difference of two oscillators averaged over time, but also the energy of individual oscillators averaged over time.

Numerical procedure for solving measured matrix from experimental method related to loss factors were documented by C. H. Hodges et al. [10].

R. J. M. Craik et al. [11] presented a theoretical model for predicting the transmission of bending waves through dual walls, the two sheets being coupled by line junctions. The model assumes that the joint has four semi-infinite plates joined to its edges by a rigid beam without inertia, and allows the structural loss of transmission between the plates to be calculated. It is concluded that the predicted results were consistent with the measurements made on both a masonry cavity wall and a drywall tested in a transmission suite.

Bosmans et al. [12] presented wave propagation approach and modal summation approach for two plates connected by a rigid junction. The wave and modal approach have been used for prediction of structure borne sound transmission between the plates. Both semi-infinite plates as well as finite-sized plates were orthotropic. The results for an orthotropic plate were compared to those of isotropic plates. The discussion has been carried out for orthotropic plate model in the environment of statistical energy analysis.

Rotational inertia and transverse shear is very important when wavelength of the structure is comparatively less than thickness of the same structure at high frequencies. The direct dynamic stiffness method has been extended to comprise rotational inertia and shear deformation by A. N. Bercin [13]. The method suggested in this paper and the approach to statistical energy analysis was used to study the effects of shear deformation and rotational inertia on bending energy transmission of structure made of stiffened plate. It has been shown

that the energy flow decreases considerably compared to the transmitted energy calculated according to the conventional theory of thin plates.

M. P. Sheng et al. [14] used statistical energy analysis to analyze the random vibrations of structures. The aim of the authors was to present the energy balance mechanism for non-conservatively coupled systems. More focus has been given by authors to the difficulties of the energy balance mechanism. A method for calculating coupling loss factors and effective internal loss factors for non-conservatively coupled systems has been introduced. The reasons for negative loss factor have been studied for non-conservatively coupled systems. In addition, the effect of stiffness and damping on effective internal loss factors and coupling loss factors were studied for non-conservatively coupled systems. To reveal the accuracy of the method, an application example has been included.

Y.C. Ma et al. [15] applied experimental statistical energy analysis for the identification of noise sources, noise levels and vibration levels encountered in the heating, ventilation and air conditioning (HVAC) industry. In HVAC industry, use of compressor is most important. It is required to identify path of energy flow in the HVAC system. Authors used experimental statistical energy analysis for estimation of modal density, damping loss factor and coupling loss factor of rotary compressor components rather than theoretical statistical energy analysis. Mobility method for modal density and half power bandwidth method for damping loss factor have been used.

C. Hopkins [16] used the concept of the experimental energy statistical analysis set to facilitate the use of Statistical Energy Analysis with plate subsystems with low modal density and low modal overlap. It has been found that for low modal overlap and low modal density plate systems, relatively low uncertainty in physical properties has resulted in large differences in Statistical Energy Analysis parameters.

L. Maxit et al. [17] proposed statistical modal energy distribution analysis approach for analysis of structures. Equipartition of modal energies in selected systems were not assumed in statistical modal energy distribution analysis approach. Authors obtained modal energy equations by using basic power flow equations between two oscillators. It is possible to find out the modal energy of the coupled subsystems from the information of the modes of the uncoupled subsystems. The relation between statistical energy analysis and statistical modal energy distribution analysis was established and allowed to mix the two approaches: statistical modal energy distribution analysis for the subsystems for which equipartition was not verified and statistical energy analysis for the other subsystems. Coupling of systems with low modal overlap, coupling of heterogeneous systems, and localized excitations configurations of structures described by statistical modal energy distribution analysis improves prediction of energy as compared to statistical energy analysis. Method proposed by authors is possible to apply for complex structure along with finite element method.

Initially vibro-acoustic source and transmission path is required to identify and then it is possible to control it effectively. For hermetic rotary compressor, so many approached were used to control noise and vibration. However, the identification proved to be difficult because the characteristics of the compressor noise are complicated due to the interaction of the compressor parts and the gas pulsation. To identify vibro-acoustic source and transmission path for hermetic rotary compressor due to the external sound field, the statistical energy analysis approach was used by Seon-Woong Hwang [18].

Resonant parts of the structural response are considered in conventional statistical energy analysis. Chieh-Yuan Cheng et al. [19] used isotropic and orthotropic plates for statistical energy analysis. The non-resonant responses of isotropic and orthotropic plates due to acoustically induced vibrations were measured in a reverberation chamber. Authors

introduced a new SEA model for predicting the non-resonant response of the plate. The new SEA model was applied for isotropic and orthotropic plates. The results of resonant and non-resonant responses of plates were compared by experimental method. These results were close to results of SEA model. Due to neglecting non-resonant part for an isotropic plate with a low dissipation loss factor, the expected response can cause large errors at frequencies close to and above the critical frequency. For same condition, more error may occur in expected response of orthotropic plate below the critical frequency. Authors concluded that non-resonant response should be considered for analysis of the isotropic and orthotropic plates.

L. Ji et al. [20] introduced randomness into the system by certain assumptions. A coupling coefficient parameter and the coupling strength parameter have been introduced. That represents the statistic of the coupling stiffness. It has been found that the variance of the excited subsystem depends mainly on the variance of the input power. The variance of the excited subsystem also depends on the number of modes of excited subsystems in selected frequency bands. The variance of the non-induced subsystem, variance of the intermodal coupling coefficients and variance of the number of modes are related to each other. Authors presented some numerical examples of two coupled plates by using springs.

Santos et al. [21] solved the energy equations using the spectral element method. The structures which are subjected to high frequencies, energy flow as well as energy density can be predicted by using the spectral element method. The author's models were generated using the spectral energy element method. The results obtained were compared with the energy densities calculated from the displacement fields predicted by the spectral element method.

The prediction of averaged energy of damped structural and acoustic systems was investigated by S. Wang et al. [22]. A simplified method of energy finite element (EFEM) has

been developed based on energy flow analysis equations. It has been implemented along with the finite volume method. The energy finite element method can be used for strongly coupled systems by incorporating into statistical energy analysis software. The energy finite element method was checked against analytical solutions for coupled beams and a single beam with weak and strong coupling. Energy finite element method was used to model moderately damped plates.

An effective method has been presented by P.Ragnarsson et al. [23] for calculating point mobility from parts of a complete structure. The results of industrial body in white BIW were presented for three different cases. The results showed that the wave-based boundary condition for point impedance calculations from a subcomponent model gives more accurate results than the results obtained with free or clamped boundary conditions.

A. Le Bot et al. [24] reported the area of validity of the statistical energy analysis. It has been defined in terms of criteria. The number of modes, the modal overlap, the normalized attenuation factor and the coupling strength are the criteria's for validity diagrams of statistical energy analysis. The validity diagrams of the statistical energy analysis were presented.

T. Lafont et al. [25] discussed about diffuse field, rain on the roof excitation and modal energy. It has been shown that for any damping and frequency band, rain-on-the-roof excitation involves a diffuse field but point force produces a diffuse field if the low damping and high frequency condition satisfies.

D. Wilson et al. [26] investigated errors that may occur with statistical energy analysis and focused on the potential of advanced statistical energy analysis for predicting vibro-acoustic analysis in the low and mid frequency ranges. Emphasis has been placed on the medium and low frequency range because the plates only support local modes with a low

number of modes. The statistical energy analysis and advanced statistical energy analysis forecasts were evaluated by comparison with finite element models. It is concluded that advanced statistical energy analysis provides better accuracy than statistical energy analysis.

Cristina Díaz-Cereceda et al. [27] presented an automatic methodology for the identification of statistical energy analysis subsystems within a vibro-acoustic system. It consists in dividing the system into cells and grouping them into subsystems through a hierarchical cluster analysis based on the natural modes of the problem. The distribution of the subsystem corresponds to the optimal grouping of the cells, defined in terms of the correlation distance between them. The method suggested by the authors makes it possible to define several subsystems in the same geometric region, if necessary. This was the case of natural modes with a very different mechanical response.

Lightweight structures are demanded in today's era due to its low weight and more rigidity. The inertia forces of lightweight structures are low which results in more vibration levels and noise level. Olaf Täger et al. [28] developed vibro-acoustic analytical simulation models that allow structural and sound radiation analysis adapted to the material of anisotropic multilayer composite plates. The vibro-acoustic analytical simulation models permits physical based and fast analysis of anisotropic composite plates as compared to finite element method or boundary element methods. Eigen frequency and modal damping properties depends on the direction for anisotropic composite plates. It is concluded that a laminated composite exhibits damping-dominating acoustic radiation behavior. The vibro-acoustic design procedure and design guidelines were proposed by authors.

### 2.3 Literature related to coupling loss factors

Different methods are available for evaluating coupling loss factor between connected subsystems. The information about transmission loss or radiation efficiency is available in

literature because of which coupling loss factor is related to it. A review of literature related to coupling loss factor is presented below,

M.J. Sablik [29] obtained transmission coefficient and coupling loss factor for an L-joint between two beams. It is found that the torsional waves have developed at the L-joint. The flexural wave to torsional wave transmission is more efficient than the flexural wave to flexural wave transmission between two beams through L-joint. An incident torsional wave at the butt joints and an incident torsional wave at the L-joint were taken into account for the analysis.

B. L. Clarkson et al. [30] measured the dissipation loss factor and coupling loss factor of two plates at individual level and connected to each other respectively. An iteration technique was used to estimate the coupling loss factor and the individual dissipation loss factors. The experimental results of plates are in good agreement with theoretical results for coupling loss and dissipation loss factors. The method was then applied to the joining of a plate and a cylinder. The loss of coupling was slightly less than that of the two-plate junction.

R.S.Langley [31] derived expression for coupling loss factor in terms of frequency and space averaged Green functions of the coupled system. Author has shown that the general form of the principle SEA equation is widely applicable provided that the coupling between the subsystem is conservative. R.S.Langley [32] introduced meaning of weak coupling by considering all existing parameters. It has been shown that, for positive coupling loss factor, two subsystems should be connected to each other even in presence of weak coupling. A general result of the coupling loss factor has been obtained involving space and Green function averaged over frequencies. It has been shown that by considering suitable assumptions, the number of existing results can be inferred from the expression similar to wave and modal approach of statistical energy analysis

To derive the transmission of vibrational energy across a structural joint, a method called as “Bishop’s receptance method” was presented by B.L.Clarkson [33]. The results of “Bishop’s receptance method” for estimation of coupling loss factor were compared with traveling wave method. F. J. Fahy et al. [34] presented the effect of geometrical and material properties of plates and beams on vibratory power flow averaged over frequency and coupling loss factor. Authors proved that two important parameters such as modal overlap factor of plate or beam and coupled modes of plates or beams affects on the power flow and coupling loss factor. It has been shown that coupling loss factor estimated by wave approach gives more value than expected when modal overlap factor is less than unity. For good estimation of coupling loss factor, at least five natural frequencies should be available in selected frequency band. It has been suggested to select carefully difference of modal energies while calculating coupling loss factor of beam or plate systems.

C.Cacciolati et al. [35] determined coupling loss factors using measured point mobility for coupled subsystems. To validate the theory, an experiment was carried out on plates coupled at three points. Agreement was reasonably good for homogeneous and non-homogeneous plates. . F.J.Fahy [36] discussed background and concepts of statistical energy analysis. Comparison and relation is made in between the modal and travelling wave approaches and also discussed the strengths and weaknesses of statistical energy analysis.

Y.K.Tso et al. [37] presented a method for calculating the transmission efficiency of beam junctions by taking into considerations, the influence of rotational inertia, shear deformation, mode coupling between bending and torsion waves and unsymmetrical bending of beam. The component used at junction of beam might not match to beam centroid and shear centre of beam. To formulate the equations for coupled bending and torsional motion of coupled beams, wave transmission theory was used. The amplitude of wave in complex form

was used to estimate power of the wave. Transmission efficiency was calculated using power of wave. At higher frequency considerable effect has been observed on transmission efficiency for bending to torsional wave coupling.

K. Shankar et al. [38] studied the behavior of two spring-coupled hinged beams with weak to strong coupling from the point of view of vibrational energies, power consumption, and transferred power by the coupling. Two configurations have been studied for beams.

FJ Fahy et al. [39] proposed an input power modulation technique for measurement of coupling loss factor and damping loss factor for statistical energy analysis of any structure. In this technique input power measurement is not required for estimation of coupling loss factor and damping loss factor as compared to power injection method. To estimate coupling loss factor and damping loss factor, two coupled plates and two coupled rooms were used for applying input power modulation technique. The results of input power modulation technique were compared with power injection method for selected systems and found close to each other.

D.N.Manik [40] presented the drawbacks for determining coupling loss factor of currently available methods. A new numerical method has been suggested by him for determining coupling loss factors. F.J.Fahy [41] suggested an alternate power transfer coefficient for coupling loss factor (CLF) and an experimental method for its determination, which obviates the need to measure input powers was proposed.

In wave approach, it is assumed that transmitted wave which is coming towards junction is not correlated to the directly transmitted wave while estimating coupling loss factor in statistical energy analysis. The structures which are subjected to low frequency, the above assumption are not satisfied because of well defined response. For calculation of better coupling loss factor of one-dimensional subsystems, C. T. Hugin [42] presented a new

method. This method is applicable for low modal overlap and does not depend on exact boundary conditions. By using statistical considerations in power flow equation, the ratio of reflected to incident wave amplitude at the junction has been calculated. This average value of ratio was used to calculate improved coupling loss factor. In this calculation re-injected and re-radiated power has been taken into consideration. The improved coupling loss factor has been used in statistical energy analysis model and responses were predicted for coupled beams at low modal overlap. The accuracy of predicted responses was good.

The structural intensity technique can directly measure and distinguish power transmissions between different structural wave types across a joint, and its applications are numerous in practical engineering. Ruisen Ming [43] proposed a new method for the measurement of coupling loss factors (CLFs) using the structural intensity technique. An outline of the method's theory was also given. Theoretically the proposed method gives an approximate estimation of CLFs. According to author, the approximate error depends on the ratios of the effective modal overlap factor of the receiving subsystem to the modal overlap factors of the subsystems coupled through the joint of interest. A series of measurements were carried out by the author to verify the outlined theory. It is concluded that this proposed method can be used to measure CLFs when the modal overlap factor of the receiving subsystem is larger than that of the source subsystem. The approximate error decreases with increasing frequency and the modal overlap factor ratio of the receiving subsystem to the source subsystem.

B. R. Mace et al. [44] analyzed a system comprising two coupled edge plates. Theoretical predictions of coupling power and coupling loss factor have been established using the traditional asymptotic wave theory and an application of an analytical wave solution on rectangular plates. These were compared to the frequency averages found by finite element

analysis of the complete system. The results were presented for different shape plates and different damping levels. It is suggested that if the damping is large enough, the response is independent of the shape of the plates and for lighter damping, the response depends significantly on the geometry of each plate. Also it is concluded that the coupling power and the coupling loss factor are both lower for rectangular plates, for which the irregularity of the subsystems is the weakest. The reasons for this behavior have been attributed to the coherence of the waves or, in modal terms, to the location of the global modes of the structure in one or other of the subsystems.

L.Maxit et al. [45] presented a technique for calculating coupling loss factors for a complicated subsystem modeled with finite element method. The technique is based on the basic modal formulation of statistical energy analysis and the use of a formulation called dual modal formulation. From modal values of individual subsystems, it is possible to calculate coupling loss factor of coupled subsystems.

I. Bosmans et al. [46] have been discussed two previously published formulations for coupling loss factor applicable to coupled anisotropic components. The first was derived in the context of coupled cylindrical panels and was based on a thorough theoretical analysis. The second, established in the context of orthotropic plates, is the result of a simpler formulation allowing to directly deducing the coupling loss factor from the transmission coefficient.

R.S.Ming et al. [47] developed the formulae to predict the approximation error resulted from the use of the energy level difference method. The effects of different parameters on the approximation error were analyzed and discussed. Two practical applications were presented. The numerical and experimental results showed that the energy level difference method could give identical results.

I. Grushetsky et al. [48] presented the method for the determination of coupling loss factors of finite element method of coupled subsystems. The coupling loss factors were determined for two beams coupled at right angles. The calculation results are in good agreement with the well-known analytical solution for such a semi-infinite beam junction. By applying the coupling loss factors derived from the finite element method simulation, the vibratory energy of structure such as "stairs" composed of four beams was calculated by statistical energy analysis, used under the name of energy method and finite element method. The exact and approximate results matched well in the octave frequency bands containing two or more resonant frequencies of the structure.

The estimation of the coupling loss factor for two right angle beams using finite element method is presented by I. Grushetsky et al. [49]. It has been shown that coupling loss factors derived from numerical simulation differ from analytical values. It is concluded that the numerical coupling loss factor in the energy balance equations for the four beam structure gives better results than the analytical coupling loss factor.

The distribution of energy between subsystems of a system can be found in terms of the modes of the system. If there are enough modes in the frequency band of interest, the system can be described by an statistical energy analysis model. However, in general, it is a "quasi-SEA" model, which involves direct and indirect coupling loss factors, the values of which depend on the modal overlap. B.R. Mace [50] explored the conditions under which the indirect coupling loss factors are zero, so that a ‘proper-SEA’ model describes the system. The author also investigated the dependence of direct and indirect coupling loss factors on the modal properties of the system and the modal overlap. It is observed that, within the low modal overlap limit, the coupling loss factors were proportional to the damping loss factor and that the energy distribution only occurs if all the modes were global. It is also observed

that if all the modes are local, the indirect coupling loss factors are all null. It is concluded that, within the high modal overlap limit, coupling loss factors relative to constants, indirect coupling loss factors becoming zero.

Panuszka et al. [51] studied the effect of joints on the measured coupling loss factors . It has been shown that the coupling loss factors measured depend on the thickness of the plates. The authors conducted several experiments to evaluate the coupling loss factors of different perpendicular connections of rectangular plates. The energy storage method was conducted under free-field acoustic conditions and a large number of thin plates with different types of junctions were examined. Two types of connections were included: welded line junctions and point junctions. In the first type of connection, the influences of the plate thickness ratio on the coupling loss factor values were tested. In the second type of connection, the influence of the distribution point at the junctions on the values of coupling loss factor was tested. It is concluded that welded line junctions tend to decrease coupling loss factors as the plate thickness ratio increases and the coupling loss factors increase with the density of the junction points.

Ruisen Ming [52] experimentally tested the feasibility of the power coefficient method for a two-plate system. The author as a reference to evaluate the accuracy of the power coefficient method used the power injection method. The measurements were made under two types of sources: constant and continuous excitation and repeated excitation by impact hammer. The estimate was made based on two data formats: autospectra velocity and velocity transfer functions. The power coefficient method has been shown to provide results comparable to the power injection method at frequencies where the modal overlap factor is greater than 1. It is concluded that for frequencies where the modal overlap factor is less than 1, the error of the power coefficient method was wide, leading to overestimation.

I. Grushetsky et al. [53] presented the technique of determining coupling loss factors taking into account the uncertainty of subsystems. Two junction beams were considered as an example. The random variables were considered for the length of the beams, which obeyed the law of normal distribution. The finite element method was used for the calculation of the coupling loss factors. Calculations were made using two techniques: finite element method and energy method. The results of both the techniques were close to each other. A.N.Thite et al. [54] established techniques for estimating coupling loss factors from finite element analysis. It was usually based on a single selected system. A slightly different system choice would give different estimates. This approach has been used for plate structures.

B. R. Mace et al. [55] have documented statistical energy analysis of two conservatively coupled oscillators, sets of oscillators, and continuous subsystems subjected to broadband excitation. The results of conventional statistical energy analysis and coupled oscillator matched well for weak coupling but diverged for strong coupling. It is concluded that for strong coupling and weak connection, the coupled oscillator results matched well with exact wave analysis and Monte Carlo simulations.

The spectral element method along with fuzzy set method was proposed by R. F. Nunes, et al. [56] for determining coupling loss factor. This method was applied for two semi-infinite beam structures connected to each other with arbitrary angle by considering uncertainties of all parameters. The results obtained by spectral element method along with fuzzy set method for semi-infinite beams were compared with results of Monte Carlo analysis.

J. W. Yoo et al. (57) have described the coupled structures of beams and plates. The Fourier technique has been explained to obtain the energies and the power flows necessary for excitation of the beam and the plate. Then, these were used in the power injection method to

obtain the effective coupling loss factors of the single beam plate system. Overlapping octave bands were used in a frequency averaging approach. On the basis of the analysis of the beam-plate structure, the beam-plate-beam structure was also studied in the framework of the statistical energy analysis. It has been found that the indirect coupling in the statistical energy analysis sense can exist for such a beam-plate-beam coupled structure. The numerical result showed that its effect was greater when the dimensions of the beams were similar.

A.N.Thite et al. [58] addressed the issue of apparent coupling loss factors for plate structures. The effects of structural changes can be estimated without the need for multiple complete re-analyses. The case studies show a good agreement between the estimates based on the proposed approaches and those based on a new analysis. The end result is that apparent coupling loss factors can be estimated once the change has been made in a manner similar to that of the conventional statistical energy analysis.

M.A. BenSouf et al. [59] investigated the effect of variability on the diffusion matrix. The reflection and transmission coefficients of two deterministic waveguides connected by an uncertain coupling element to a single random variable were processed. On the basis of hybrid numerical tools called finite element method, a formulation has been developed and validated. The statistics of the energy coefficients have been examined and explicitly formulated. Coupling loss factors were evaluated according to the mechanical and geometrical inhomogeneities of the coupling element. Numerical validations were performed using Monte Carlo simulations.

Average modal spacing, transmission coefficient, input power and coupling loss factor were determined for symmetrically coupled laminated composite plates by Abdullah Secgin [60]. For this modal approach through discrete singular convolution method was used for composite plates with 4 and 6 ply and with different orientation. Coupling loss factor were

estimated analytically for composite plates and compared with numerical results. Natural frequencies were used to find average modal spacing by analytical as well as experimental method for uncoupled composite plates. Modal impedances were used for input power measurements. It has been suggested by author to use proposed methodology in high frequency region as well as in mid frequency region for statistical energy analysis of composite plates.

In Statistical Energy Analysis modeling, it is desirable that coupling loss factors between two permanently connected subsystems can be conveniently estimated. Lin Ji et al. [61] recommended a simple statistical energy analysis modeling technique, since continuous coupling interfaces can be replaced by sets of discrete points, provided the points are spaced by an appropriate distance. On the basis of numerical investigations on modeling of two thin plates connected along a line, a point spacing criterion was recommended by adjusting the point and line connection data of the two plates. It has been shown that the spacing of the points depends not only on the wavelengths, but also on the wavelength ratio of the two coupled subsystems.

Improved energy ratio method was proposed by Jintao Guet et al.[62] for estimation of coupling loss factor. This method was used for three coupled structures. The results obtained by proposed method were compared with other existing methods. It has been concluded that improved energy ratio method is more reliable.

### 2.4 Literature related to damping loss factors

The damping loss factor is frequently obtained from experimental methods. The loss mechanism of connecting joints, damping treatments and surface absorption are comparatively more than the internal dissipation of the subsystem material. The estimated damping loss factors for different materials are reviewed as below,

The effects of damping on energy sharing in coupled systems have been studied by F.F.Yap et al. [63]. The approach adopted consisted of calculating the forced response models of various idealized systems, and then calculating the parameters of the statistical energy analysis model of the systems using the matrix inversion approach. They showed that, when the statistical energy analysis models were adjusted according to this procedure, the values of the coupling loss factors were significantly dependent on the damping, except when they were sufficiently high. For very low damped coupled systems, the variation in damping results in a direct variation of the coupling loss factor values in proportion to the internal loss factor. In the limit of zero damping, coupling loss factors tend to zero. This is a view that strongly contrasts with the "classical" statistical energy analysis, in which the coupling loss factors were determined by the nature of the coupling between subsystems, regardless of the subsystem damping. The strong dependence on damping implied in particular that the equipartition of modal energy under low damping conditions generally did not occur. It was contrary to the conventional prediction of the statistical energy analysis that modal energy equipartition always occurs if the damping can be reduced to a sufficiently small value. It has been shown that the use of this classical assumption can lead to a gross overestimate of subsystem energy ratios, especially in multi-subsystem structures.

Ahmed Maher et al. [64] investigated damping loss factor for composite beam made up of fiber reinforced plastic material. They considered volume fraction of 45% and15%. The specimen were fabricated and stated as (0/0/0), (0/45/0), (0/30/0),(0/90/0), (45/0/45)and (45/45/0) for each volume fraction. The effect of planting orientation on damping capacity has been studied.

Marek Iwaniek [65] determined of damping loss factor in plate elements. Author has tested plates made of different materials like steel, brass, plexiglass, aluminum etc. Comparison of different values of damping loss factors were made for different materials.

Nirmal Kumar Mandal et al. [66] measured damping loss factors for orthotropic plates. The half-power bandwidth method was used for estimating damping loss factor of rectangular and trapezoidal plates. Single degree of freedom system concept has been adopted by authors. Low frequency range was selected for conducting the tests.

Kranthi Kumar Vatti [67] evaluated the accuracy of the estimation of the damping loss factor for plates by the power input method and the impulse response decay method. For this, various processing parameters, such as the frequency resolution, the frequency bandwidth, the number of measurement locations and the signal-to-noise ratio have been taken into account. Two other coupling loss factor estimation algorithms were investigated, one using individual plate loss factor estimates and the other using plate loss factors estimated during plate coupling. The modal density and the coupling loss factors for the two sets of plates were estimated experimentally and compared with the theoretical results. The estimates showed a reasonable agreement between experimental and theoretical results.

A. Wang, X. et al. [68] presented the experimental method to predict damping loss factors of ship structure panels with constrained or unconstrained damping layers. Various components of thickness, material properties as well as the partial location of constrained damping layers have been investigated.

## 2.5 Literature related to modal densities

The modal density is used most often in the theoretical developments of SEA for distributed systems. Modal density is represented in form of the mode count and review of literature related to modal density is presented below,

B.L. Clarkson et al. [69] presented an indirect experimental method for estimating loss factors. The modal density of plane plates and cylinders has been estimated. Renji [70] experimentally determined the modal density of a structure from the real part of its admittance. It is found that the experimental values of modal density correspond well to the theoretical results.

Finnveden [71] used the finite element method-waveguide, to compute the propagation characteristics of waves in thin-walled structures constructed. In particular, essential features such as modal density, group velocity and waveform have been evaluated. The description of the evaluation of a dispersion relation for a channel beam, presented from the data provided by the finite element formulation and the method of determining the modal density and the group velocity from the input data of finite element, was also presented in detail for beam structure.

Wave number integration method was used to study the influence of the boundary conditions on mode number and modal density for one dimensional and two dimensional elements by Xie et al. [72]. Beam and plate were used as one dimensional and two dimensional elements respectively. The average mode count reduced from 0 to 1 for single beam vibrating in bending mode for different types of boundary conditions. The results from previously published formulae of natural frequency and finite element method were used for comparison with the results obtained by wave number integration method for beam and plate

with different boundary conditions. Accuracy in estimation of modal density for statistical energy analysis increases due to inclusion of boundary conditions for beam and plate.

Ramachandran et al. [73] developed an analytical method for predicting the radiation efficiency and modal density of a longitudinally stiffened cylinder for use in statistical energy analysis.

Statistical energy analysis subsystem formulation based on a combination of finite element, component mode synthesis and periodic structure theory has been described by V. Cotoni et al. [74]. The method efficiently calculates the statistical energy analysis parameters for very general structural panels. Expressions were calculated for modal density, damping loss factor, and engineering unit response of the panel. Using an efficient Fourier transformation approach, resonant radiation efficiency, non-resonant transmission loss, and acoustic input power were also obtained. The method was derived and a number of cases of analytical and experimental validation were presented.

Richard Bachoo et al. [75] derived an analytical expression for the modal density of fiber-reinforced composite beams coupled in bending and torsion. The variation of the modal density with the orientation of the fiber for a unidirectional composite reinforced beam has been studied and it has been found that there exists in each frequency band an orientation corresponding to a minimum modal density. The additive property of modal density for discontinuous composite beam systems has also been verified.

Jingyong Han et al. [76] presented the modal density expressions for sandwich panels made of orthotropic material. Hamilton principle was used to derive the governing equations for sandwich panels by considering in-plane rigidity of the core. Similar material and reference axes to each other for selected system were not considered. Integration of wavenumber in space was used to obtain modal density. The study has been carried out by

authors for number of modes and the effects of boundary conditions. The existing modal density expressions, finite element models and shear deformation theory were used to decide the accuracy of proposed models. To investigate the influence of transverse shear rigidity, ply angle of face sheets, boundary conditions and in-plane rigidity of the core on modal density, parametric studies has been carried out. To predict the sound transmission of sandwich panels, the proposed modal density expressions can be used because of its broader scope.

The detailed analysis of literature has been done for statistical energy analysis parameter estimation. Experimental, analytical and numerical results from literature for different case studies have been given in Table 2.5.1 for statistical energy analysis parameters.

Table 2.5.1 Comparison of selected literature for SEA parameter analysis

| **Sr. No.** | **SEA Parameter** | **Name of Author [Ref.No.]** | **Name of Structure** | **Experimental Analysis** | **Analytical/Numerical Analysis** | **Remark** |
|---|---|---|---|---|---|---|
| 1. | Coupling loss factors | B. L. Clarkson et al. [30] | Plate and cylinder | Iteration Technique used | Line Junction | Coupling loss factors are estimated for line junctions. More focus is required on structural junctions and materials of subsystems. |
| 2. | | R.S.Langley [32] | Plates | - | Differentiated weak and strong coupling | |
| 3. | | B.L.Clarkson [33]. | Beams | - | Bishop receptance method | |
| 4. | | C.Cacciolati et al. [35] | Plates | Measured Point mobility | Line Junction-modal approach | |
| 5. | | FJ Fahy et al. [39] | Plates and Rooms | - | An input power modulation technique | |
| 6. | | Ruisen Ming [52] | Plates | Power coefficient method | Power Injection method | |
| 7. | | I. Grushetsky et al. [53] | Beams | - | Finite Element method | |
| 8. | | R. F. Nunes, et al. [56] | Beams | - | Spectral element method | |
| 9. | | A.N.Thite et al. [58] | Plates | - | apparent coupling loss factors | |

| | | | | | | |
|---|---|---|---|---|---|---|
| 10. | | Jintao Guet et al.[62] | Plates | Improved energy ratio method-Line junction | Modal approach | |
| 11. | Damping Loss Factors | F.F.Yap et al. [63]. | Plates | - | Matrix inversion approach | Damping loss factors of plates with different boundary condition and different materials are required to estimate. |
| 12. | | Ahmed Maher et al. [64] | Composite Beam | - | Matrix inversion approach | |
| 13. | | Marek Iwaniek [65] | Plates | - | Power input method | |
| 14. | | Nirmal Kumar Mandal et al. [66] | Corrugated Plates | Half power bandwidth method | - | |
| 15. | | KranthiKumar Vatti [67] | Plate | Impulse response decay method | - | |
| 16. | | A. Wang, X. et al. [68] | Ship structure panels | - | Power input method | |
| 17. | Modal Density | B.L. Clarkson et al. [69] | Plate and cylinder | - | Modal approach | Effect of fiber orientation of composite plate on modal density is required to verify. |
| 18. | | Renji [70] | Beam | - | Wave approach | |
| 19. | | Finnveden [71] | Thin-walled structures | - | finite element method | |
| 20. | | Xie et al. [72]. | Plate | - | Wavenumber integration method | |
| 21. | | Ramachandran et al. [73] | Cylinder | - | Developed analytical method | |
| 22. | | V. Cotoni et al. [74]. | structural panels | Modal analysis | Finite Element method | |
| 23. | | Richard Bachoo et al. [75] | Composite Beam | - | Developed analytical method | |
| 24. | | Jingyong Han et al. [76] | Sandwich Panels | - | Wave approach | |

A detailed survey of literature on estimation of statistical energy analysis parameters for different structures brings out the point that no available study seems to address, in requisite detail, the effect of structural junctions of coupled subsystems on estimation of coupling loss factors. Another important observation is that influence of different fibre orientations on coupling loss factors, modal densities and damping loss factors are not reported for some composite plates. Further, the studies documented in the literature mostly have used the power injection method for determining statistical energy analysis parameters rather than energy level difference method which is relatively simple.

### 2.6 Objectives and scope of the present work

The primary objective of the present research work is to investigate the coupling loss factors for different types of junction between coupled subsystems experimentally. It includes estimation of coupling loss factor, damping loss factor and modal density of plate elements made up of different materials. The detailed objectives are as follows,

- To estimate damping loss factors by experimental method for plates made from different materials such as aluminium, mild steel, stainless steel and composites.
- To estimate modal densities by analytical and experimental methods for plates made from different materials such as aluminium, mild steel, stainless steel and composites.
- To study the influence of junction length of coupled subsystems on coupling loss factors.
- To investigate coupling loss factors of aluminium plates for screwed and bolted junctions.

- To compare coupling loss factors for bolted and riveted junctions of plates made from composite materials.
- To study influence of tightening torque at structural junction of plates made from aluminium and composite materials on coupling loss factors.
- To study influence of different fiber orientation angle of plate made from composite materials on coupling loss factors.

It is to be noted here that the problem taken up in the current thesis and the results presented therein are of fundamental nature, with their implications seen in the design of structural junctions.

**2.7 Closure**

The current chapter provided a thorough review of literature pertinent to coupling loss factors, modal densities and damping loss factors of different idealized subsystems. This is accompanied by the reasons that justify the selection of the current research problem. Subsequently, all the prominent objectives of the present research work have been listed.

# Chapter 3

# THEORETICAL MODELS AND COMPUTATIONS OF STATISTICAL ENERGY ANALYSIS PARAMETERS

## 3.1 Introduction

In this chapter, the expressions for coupling loss factor, damping loss factor and modal density of idealized subsystems are presented. The theoretical as well as experimental methods of evaluating coupling loss factor are considered for point and line connections of plates. Damping loss factor estimation methods are also discussed for plate structures. Modal density of rectangular plates with different boundary conditions is presented.

## 3.2 Thermal Analogy of SEA

Since the concept of the flow of energy is fundamental to the study of SEA, the thermal analogy can give a better understanding of the basic concepts of SEA [25]. There is a very good analogy between statistical energy analysis and flow of heat between two bodies. The flow of heat is very easy for conceptual visualization, and therefore the concepts involved in SEA can be better understood with such an analogy. Therefore, before going to further details of SEA, the thermal analogy of SEA is presented here. Figure 3.1 shows two bodies connected to each other. One of the bodies, *body 1* is given heat energy due to which its temperature increases. Some of the heat energy dissipated through radiation to the surroundings and some of the heat energy is transferred to *body 2*. The temperatures of both the bodies are governed by the amount of heat energy radiated to the surroundings and the amount of heat energy transferred between them.

The amount of heat energy transferred between them is quantified by the strength of coupling. That means if there is a greater flow of heat energy between them, they are strongly coupled; if the flow of heat energy between them is less, then they are said to be weakly coupled. The amount of heat energy transferred depends on the material connecting the two bodies which determines the amount of coupling. A good conductor of heat attached between the bodies provides strong coupling and an insulator provides weak coupling. Similarly other parameters of each of the body and surroundings influence the amount of heat radiated to outside.

Depending on the type of material used to connect the two bodies and the extent of radiation loss from each of the bodies, temperatures of each of the bodies show a definite pattern as follows,

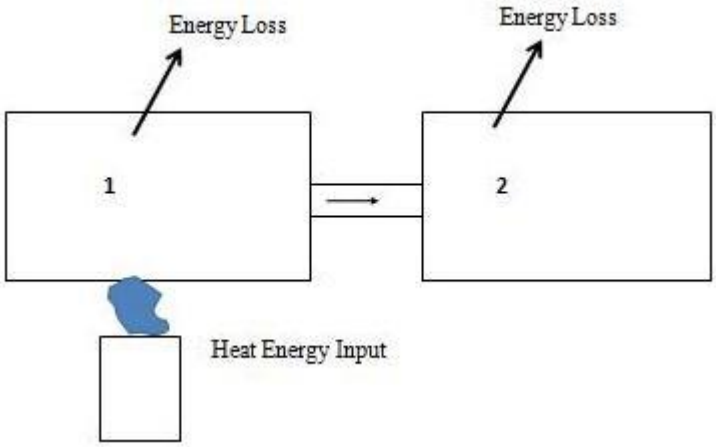


Figure 3.1 Heat flow between two bodies

The temperature of the bodies when there is high radiation loss in addition to strong coupling is shown in figure 3.2(a). Heat from body 1 is lost as radiated heat and the rest flows to body 2 where it is further radiated in to the surroundings. Due to high radiation and strong coupling temperature of both the bodies remain low as shown in the figure 3.2 (a).

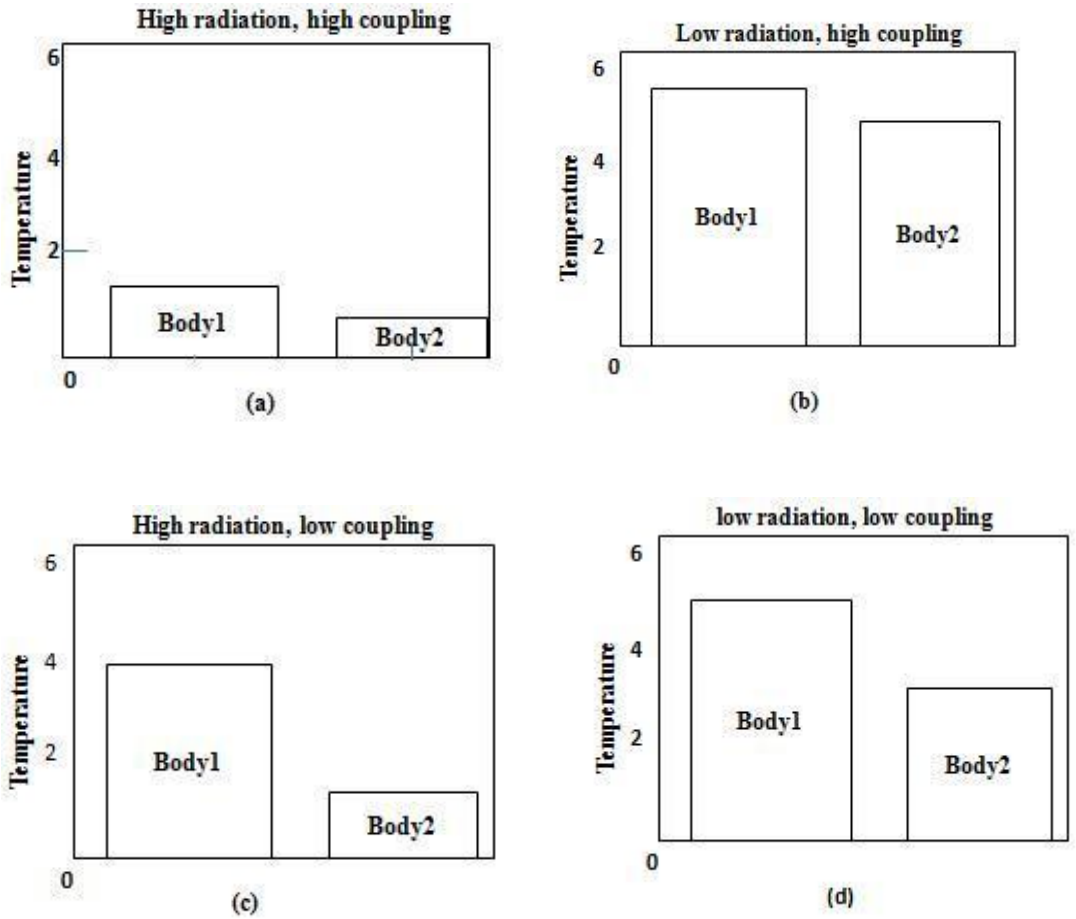


Figure 3.2: Temperature of two bodies shown in Figure 3.1

The temperature of the bodies when there is low radiation from both of them but are strongly coupled is as shown in Figure 3.2(b). There is no significant loss of heat from body 1 due to radiation and most of the heat flow in to body 2. Similarly, there is no significant loss of heat from body 2. Due to very low radiation and strong coupling there is enough heat conserved within each of the bodies which raises their temperature as shown in the above Figure 3.2(b).

The temperature of the bodies when there is high radiation loss from both of them but are weakly coupled is shown in Figure 3.2(c). Heat from body 1 is lost as radiated heat; due to weak coupling very little heat flows in to body 2 where it is further radiated in to the surroundings. Body 1 still has enough heat to increase its temperature. Due to the above

reasons, the temperature of body 1 is far greater than the temperature of body 2 as shown in the Figure 3.2(c).

The temperature of the bodies when there is low radiation and low coupling is as shown in Figure 3.2(d). There is no significant loss of heat due to radiation from both the bodies. In addition, very little heat flows from body 1 to body 2. Due to very low radiation loss temperatures of both the bodies increase as shown in the Figure 3.2(d). However, the temperature of body 2 is definitely less than the case in which there was strong coupling between the bodies.

The thermal model can be easily related to structural vibration. Let us consider two coupled plates connected by welding in complex structure. If one of the subsystem getting vibration energy through force excitation, some of the vibration energy is damped out in the first subsystem and the rest flows in to the second subsystem depending upon the properties of interconnecting elements. The exchange of energy between the two subsystems depends on the modes of vibration in the given frequency range in each of the system. Detailed mathematical models will follow in later sections, but here an attempt is made to relate the thermal model with a vibrating structure.

The temperature of the thermal system can be compared to the modal energy of a vibrating system. The amounts of energy that is present in the system after dissipation through damping and transferred to the neighbouring substructure represent the energy associated with vibration modes. This energy is popularly referred as the modal energy which will actually indicate the vibration level of the system.

The radiative loss of the thermal model can be compared to dissipation through damping of the vibratory system. Energy is lost from a vibratory system due to damping and

the total loss of energy can be computed if the frequency of vibration and damping factor of the material are known.

Strength of coupling of the thermal model can be compared to the mechanical coupling. Some materials allow vibration to be easily transmitted and some materials almost prevent the transmission of vibration. The amount by which they allow or disallow vibration depends primarily on the frequency of vibration. The strength of the mechanical coupling is quantified by coupling loss factor which is one of the most significant parameters used in SEA.

The thermal capacity of a thermal model can be compared with the modal density of a vibratory model. Since each mode of vibration has definite energy stored in it, modal density, which is a measure of the number of modes in a frequency band, is related to the amount of energy stored in each system.

The above parameters of the vibratory model which are analogous to the thermal model are summarized in Table 3.1.

Table 3.1: Analogy between Thermal Energy and SEA

| **Thermal Energy Model** | **Vibratory Structure Model** |
|---|---|
| Temperature | Modal Energy |
| Radiative Loss | Damping |
| Conductivity | Mechanical Coupling |
| Thermal Capacity | Modal Density |

Now it can be seen from Figure 3.2(a) to 3.2(d) how the vibration level of two connected substructures depends on the strength of damping and coupling loss factors. The source of heat in Figure 3.1 becomes a source of vibration from a machine attached to one of the systems. The four cases discussed in the above cases form a prototype for a vibration control problem. It is imperative that for any vibration control problem the case presented in

Figure 3.2(a) is the ideal situation. To reduce vibration, vibration has to be damped out in both the substructures and both the substructures must be completely isolated. Obviously, vibration of the source must be reduced in the first place, which is not always easy.

### 3.3 Power flow between systems

The SEA method consists of first dividing a structure along its natural boundaries to form a set of 'n' structural elements. The important equation used in the statistical energy analysis is the power balance equation between different coupled subsystems. For a subsystem 'p' connected to many subsystems 's', with 's' varying, as shown in Figure 3.3,the power balance equation can be written as,

$$\prod_{in}^{p} = \prod_{diss}^{p} + \sum_{s \neq p} \prod_{coup}^{ps} \tag{1}$$

The structure is considered under steady-state conditions and all the power components stated are time-averaged quantities. The transmitted power and internal dissipated power are usually calculated as

$$\prod_{diss}^{p} = \omega \eta_{p} E_{p}$$

$$\prod_{coup}^{p} = \omega \eta_{ps} E_{p} \tag{2}$$

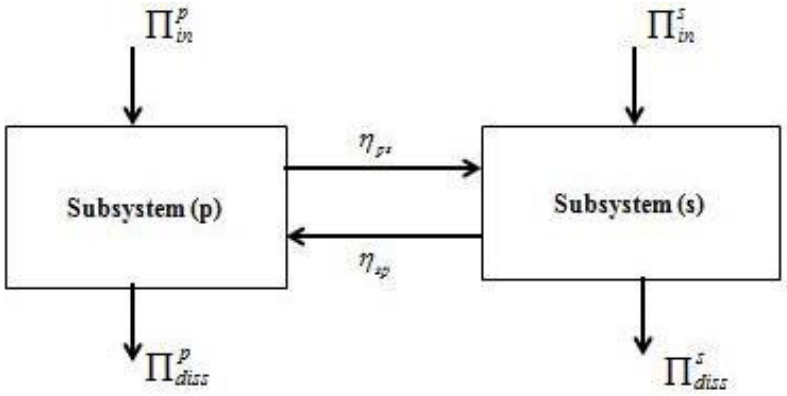


Figure 3.3: Power flow between two systems

The power balance equations can be rearranged as

$$\Pi_{in}^{p} = \omega\eta_{p}E_{p} + \omega\sum_{s\neq p}\eta_{ps}E_{p} - \omega\sum_{s\neq p}\eta_{sp}E_{s} \qquad (3)$$

$where,\ p = 1,2,3...n$

When the numbers of systems are connected to each other then the equations are written in matrix form and the total loss factor appears on the diagonal elements,

$$\begin{bmatrix} \eta_{11} & \cdots & -\eta_{n1} \\ \vdots & \ddots & \vdots \\ -\eta_{1n} & \cdots & \eta_{nn} \end{bmatrix} \begin{Bmatrix} \omega E_1 \\ \vdots \\ \omega E_n \end{Bmatrix} = \begin{Bmatrix} \Pi_{in}^{1} \\ \vdots \\ \Pi_{in}^{n} \end{Bmatrix} \qquad (4)$$

If the loss factors and power inputs are known as a function of frequency, one can solve for the steady-state energies by standard matrix techniques. Usually only one of the $\Pi_{in}^{p}$ is nonzero. Also many of the $\eta_{ps}$ are zero because element 'p' is not directly coupled to all other SEA elements. To produce frequency response curves for the various energies $E_p$, equation (4) must be solved over and over again for each frequency band in the range of frequencies under consideration.

### 3.4 Analytical methods for coupling loss factor estimation

Coupling loss factor can be obtained by modal approach and wave approach. Both approaches are useful and interrelated to each other. A wave can be denoted by a sum of modes or a mode can be denoted by a wave superposition. Although the basic formulation of statistical energy analysis is in terms of coupled modes, the direct evaluation of coupling loss factor from this approach is difficult because it comprises the estimation of complicated integrals to average on frequency and space. On the other hand, there is an important source of theoretical work in the literature on wave transmission across junctions in semi-infinite systems that can be used to indirectly estimate the coupling loss factor.

#### 3.4.1 Modal approach

For the evaluation of the CLF by the modal approach a pair of arbitrary subsystems joined at a point is considered. Two reciprocal situations are considered for the system. By considering sinusoidal force of rms amplitude '$l_p$' at frequency 'f' applied to an arbitrary point 'A' in subsystem 'p' as shown in figure 3.4.

The power balance equation for subsystem 'p' is

$$\Pi_{p,in} = \Pi_{p,diss} + \Pi_{ps}$$

*or* (5)

$$l_p^2 G_{pA} = 2\pi f \eta_p E_p + v_j^2 R_{sj}$$

Where,

$G_{pA}$ - Input conductance of subsystem 'p'

$\eta_p$ - Damping Loss Factor of subsystem 'p'

$v_j$ - The rms velocity at the junction

$R_{sj}$ - Input resistance of subsystem's' at the junction

$\Pi_{p,in}$ - Power input to subsystem 'p'

$\Pi_{p,diss}$ - Power dissipated from subsystem ‘p’

$\Pi_{ps}$ - Power transmitted from subsystem ‘p’ to subsystem‘s’

E-Vibration Energy

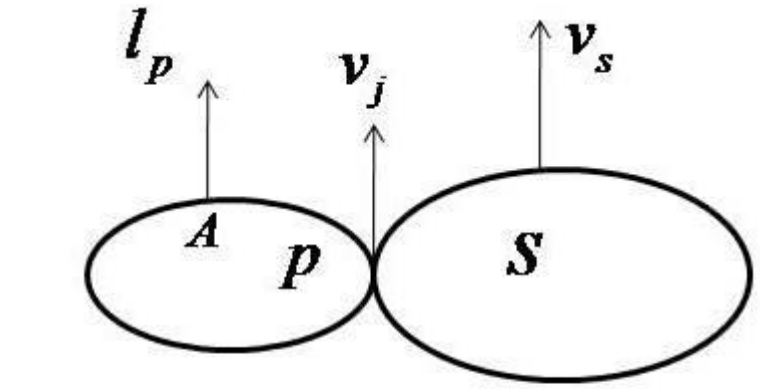


a. Initial situation

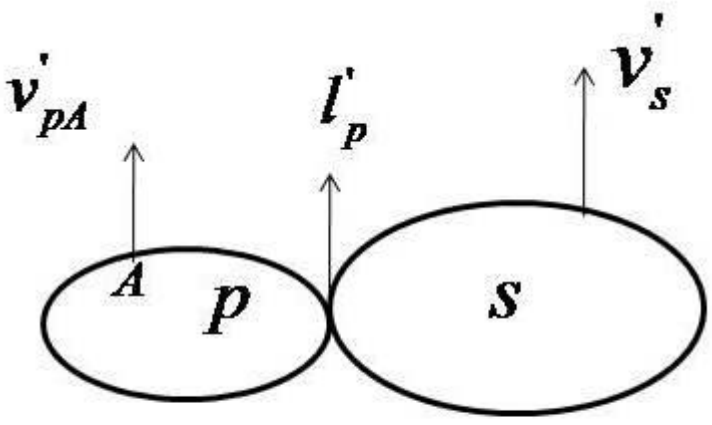


b.Reciprocal situation

Figure 3.4: Illustration of the modal approach

The power balance equation for subsystem‘s’ is

$$\Pi_{ps} = \Pi_{s,diss}$$
$$or \qquad (6)$$
$$v_j^2 R_{sj} = 2\pi f \eta_s E_s$$

Adding equation (5) and (6),

$$l_p^2 G_{pA} = 2\pi f \left(\eta_p E_p + \eta_s E_s\right) \qquad (7)$$

Subtracting equation (6) from equation (5)

$$l_p^2 G_{pA} = 2v_j^2 R_{sj} + 2\pi f \left(\eta_p E_p - \eta_s E_s\right) \qquad (8)$$

From equation (7) and (8), the velocity at junction can be correlated to the force,

$$l_p^2 G_{pA} = 2v_j^2 R_{sj} + \frac{l_p^2 G_{pA}}{\left(\eta_p E_p + \eta_s E_s\right)}\left(\eta_p E_p - \eta_s E_s\right) \qquad (9)$$

$$\frac{v_j^2}{l_p^2} = \frac{G_{pA}}{R_{sj}} \frac{\eta_s E_s}{(\eta_p E_p + \eta_s E_s)} \qquad (10)$$

Consider a sinusoidal force of rms amplitude $l_j'$ at frequency f applied to the junction in the reciprocal situation. The velocity at the junction is given by

$$v_j'^2 = \frac{l_j'^2}{\left|Z_{pj} + Z_{sj}\right|^2} \qquad (11)$$

Where,

$Z_{pj} + Z_{sj}$ - is the total impedance of the junction.

The power balance equation for subsystem ‘p’ with mass $M_p$ is

$$\Pi'_{p,in} = \Pi'_{p,diss}$$

*or*

$$v_j'^2 R_{pj} = 2\pi f \eta_p E_p = 2\pi f \eta_p M_p \left\langle v_{pA}'^2 \right\rangle \tag{12}$$

The velocity at point "A" can be found by means of the reciprocal relation,

$$\frac{v_j}{l_p} = \frac{v'_{pA}}{l'_j} \tag{13}$$

From equation (11) and (12)

$$\frac{\left\langle v_{pA}'^2 \right\rangle}{l_j'^2} = \frac{R_{pj}}{2\pi f \eta_p M_p \left| Z_{pj} + Z_{sj} \right|^2} \tag{14}$$

Squaring equation (13) and averaging point "A" over the subsystem while keeping the force constant, gives

$$\frac{\left\langle v_j^2 \right\rangle}{l_p^2} = \frac{\left\langle v_{pA}'^2 \right\rangle}{l_j'^2} \tag{15}$$

$$\frac{R_{pj}}{2\pi f \eta_p M_p \left| Z_{pj} + Z_{sj} \right|^2} = \frac{G_{pA}}{R_{sj}} \frac{\eta_s E_s}{(\eta_p E_p + \eta_s E_s)} \tag{16}$$

$$\frac{4(2\pi f)\eta_p M_p G_{pA}}{\left(1 + \frac{\eta_p E_p}{\eta_s E_s}\right)} = \frac{4 R_{pj} R_{sj}}{\left| Z_{pj} + Z_{sj} \right|^2} = \tau(f)_{ps} \tag{17}$$

Where,

$\tau(f)_{ps}$ - The transmission coefficient as a function of frequency f.

The value of input conductance can be written in terms of mass and average frequency spacing,

$$G_{pA} = \frac{\pi n(\omega)}{2M_p} \tag{18}$$

$$n(\omega) = \frac{1}{2\pi\overline{\delta f}} \tag{19}$$

Using the equation (17), (18) and (19)

$$\tau(f)_{ps} = \frac{4(2\pi f)\eta_p M_p G_{pA}}{\left(1+\frac{\eta_p E_p}{\eta_s E_s}\right)} \tag{20}$$

$$\tau(f)_{ps} = \frac{4(2\pi f)\eta_p M_p \left(1 \Big/ 4M_p \overline{\delta f}\right)}{\left(1+\frac{\eta_p}{\eta_s}\left(\frac{\eta_s+\eta_{sp}}{\eta_{ps}}\right)\right)} \tag{21}$$

Solving for $\eta_{ps}$ and using equation

$$\eta_{sp} = \eta_{ps}\left(\overline{\delta f_s} \Big/ \overline{\delta f_p}\right) \tag{22}$$

$$\eta_{ps} = \frac{\overline{\delta f}_p \tau_{ps}}{2\pi f - \tau_{ps}\left(\frac{\overline{\delta f_p}}{\eta_p}+\frac{\overline{\delta f_s}}{\eta_s}\right)} \tag{23}$$

The modal overlap factor can be given as,

$$\beta_p = \frac{f\eta_p}{\overline{\delta f_p}} \tag{24}$$

The coupling loss factor relation in terms of modal overlap factor can be given as,

$$\eta_{ps} = \frac{\overline{\delta f_p}}{\pi f}\frac{\tau_{ps}}{2-\tau_{ps}\left(\frac{1}{\pi\beta_p}+\frac{1}{\pi\beta_s}\right)} \tag{25}$$

Where,

$\eta_{ps}$ -Coupling Loss Factor

$\delta f$ - Average Frequency Spacing

$\beta$ -Modal overlap Factor

A general expression for coupling loss factor for point connected system in terms of infinite system transmission coefficient can be written as

$$\eta_{ps} = \frac{\overline{\delta f_p}}{\pi f} \beta_{corr} \frac{\tau_{ps,\infty}}{2 - \tau_{ps,\infty}} \tag{26}$$

Where,

$$\beta_{corr} = \frac{1}{\left(1 + \left(\frac{1}{2\pi\left(\beta_{p,net} + \beta_{s,net}\right)}\right)^8\right)^{1/4}}$$

The coupling loss factor for two line connected subsystems by assuming comparable damping for all modes in a given frequency range is,

$$\eta_{ps} \cong \frac{\overline{\delta f}_p}{\pi f} \beta_{corr} I_{ps}^{line}(k_p, k_s) \frac{\tau_{ps}}{2 - \tau_{ps}} \tag{27}$$

Where,

$$I_{ps}^{line} = \frac{L_j}{4}\left(\frac{k_p^4 k_s^4}{k_p^4 + k_s^4}\right)^{1/4}$$

$$\tau_{ps} = \frac{4R'_{p\infty}R'_{s\infty}}{\left|Z'_{p\infty} + Z'_{s\infty}\right|^2}$$

k- Bending wave number

$L_j$ –Junction length

$Z'$ –Line impedance of a subsystem for a uniform line connection

### 3.4.2 Effect of material properties on coupling loss factor

Today an amazing variety of materials are available in market for different applications. Combinations of ceramics, metals and polymer composites are used in racing cars and other automotive parts. Selection of appropriate material for particular application which gives better vibro-acoustic performance is very important. Some of the materials from metal, polymers and composites were selected for evaluating coupling loss factors.

Coupling loss factors were estimated by equations (26) and (27) for point and line connected plates. The programmes are made in MATLAB for estimating coupling loss factors by changing input parameters such as density and modulus of elasticity for different materials. The material properties are given in Table 3.4.2.1.

Table 3.4.2.1 Properties of materials

| Sr.No. | Materials | Density($Kg/m^3$) | Modulus of Elasticity (GPa) |
|---|---|---|---|
| 1 | Steel | 7800 | 200 |
| 2 | Acrylic | 1200 | 3.2 |
| 3 | Copper | 8940 | 125 |
| 4 | Composite -carbon/epoxy sheet with volume fraction of fibres-50% | 1600 | 210 |
| 5 | Glass | 2500 | 70 |
| 6 | Rubber | 1200 | 0.02 |

The results of coupling loss factors for line connected plates for different materials are shown in Figure 3.5. It has been observed from Figure 3.5 that at lower frequencies the values of CLF for all materials are nearer to each other, while at higher frequencies they remain fairly constant. CLF values are less for Elastomer-Rubbers, Thermoplastic-Acrylics, Non-ferrous metal-Copper as compared to composite-carbon/epoxy sheet for line connected plates. Increase in frequency of every material decreases the values of coupling loss factor.

In Figure 3.6, coupling loss factors result for point connected plate is shown. The two plates connected to each other are in same plane. It has been observed from Figure 3.6 that coupling loss factor values are more for composite plates as compared to elastomer, thermoplastic and non-ferrous metals.

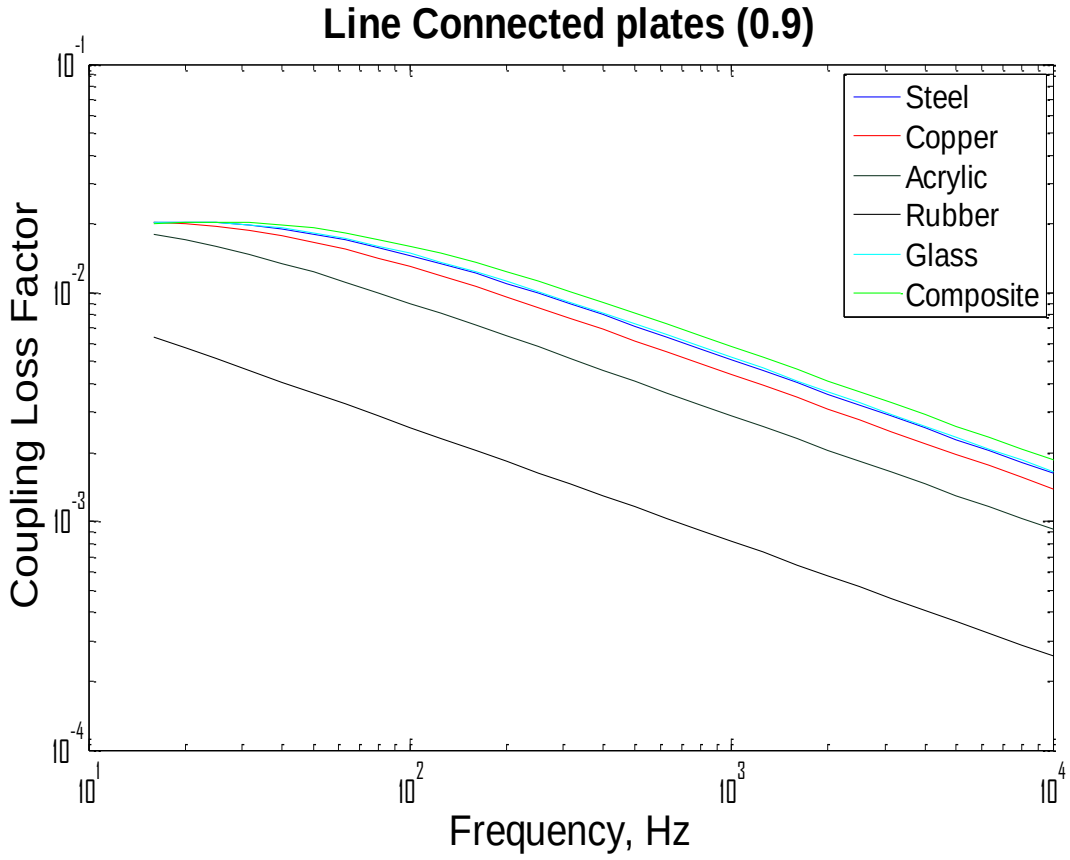


Figure 3.5 Coupling loss factor for line connected plates (0.9m) with different materials.

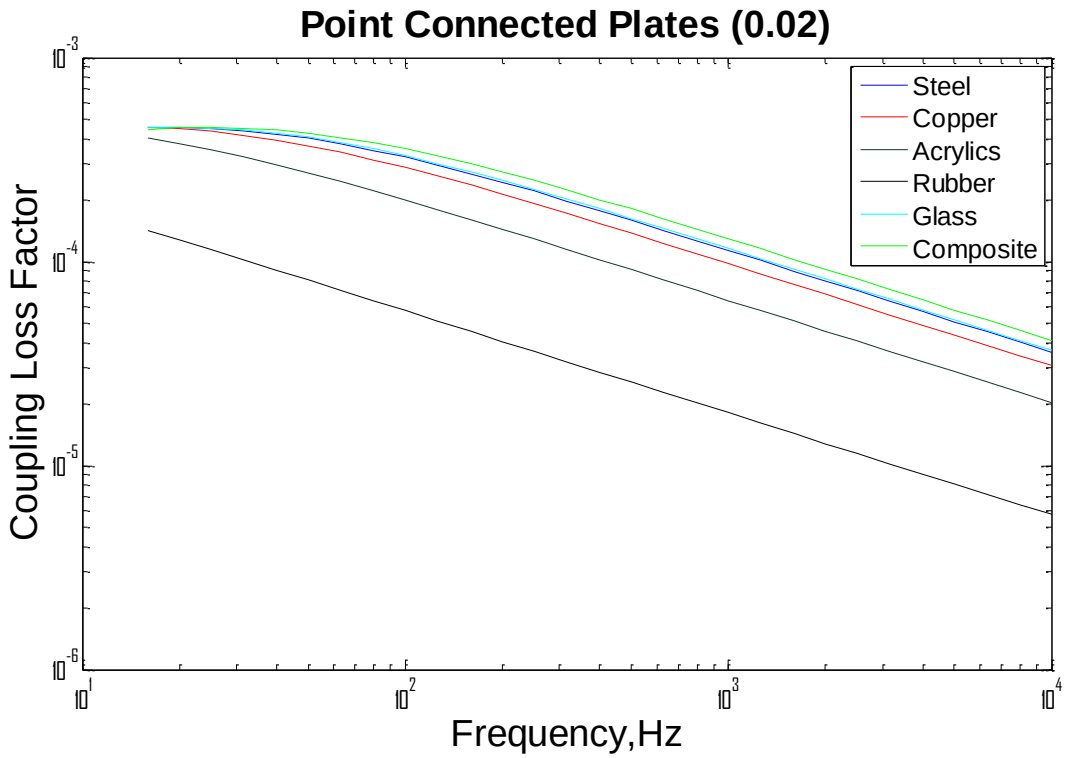


Figure 3.6 Coupling Loss Factor for point connected plates (0.02 m) with different materials

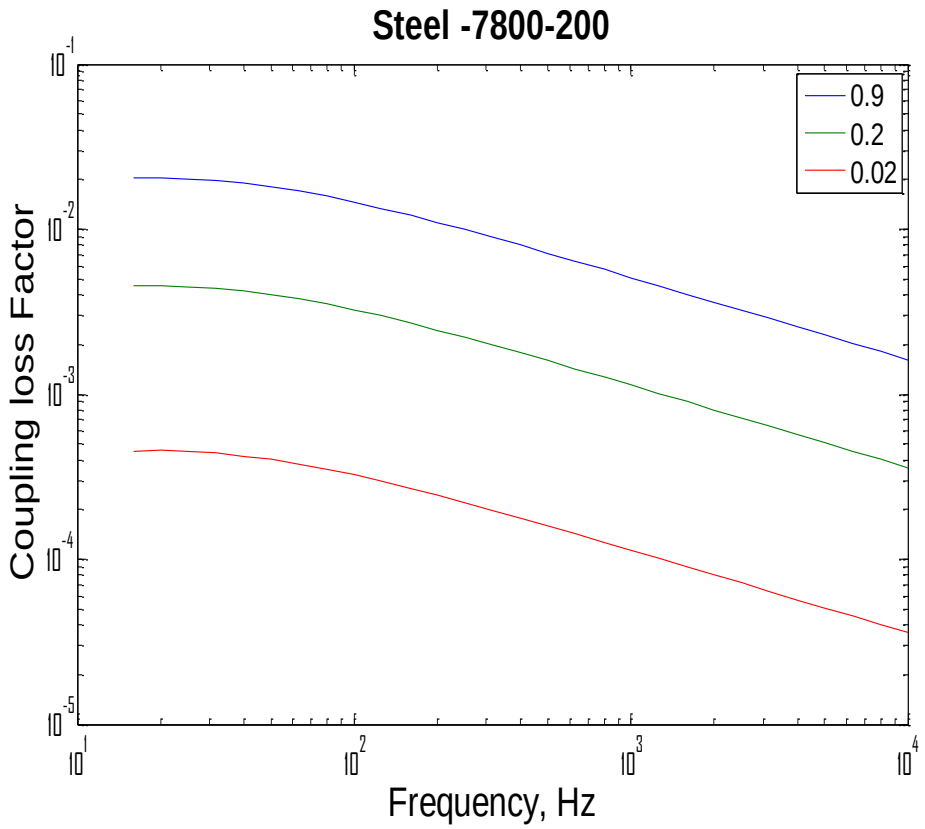


Figure 3.7 Coupling loss factor for point and line connected plates

Coupling loss factor values for two connected plates of steel in same plane is shown in Figure 3.7. The joining lengths of two steel plates are 0.02 m, 0.2 m and 0.9 m. It has been observed from Figure 3.7 that coupling loss factors are more for 0.9 m than 0.2 m and 0.02 m. Also with increase in frequency coupling loss factor values decreases for all joining lengths (0.02 m, 0.2 m and 0.9 m) of two steel plates having same dimensions.

### 3.4.3 Wave approach

One-dimensional subsystems as shown in Figure 3.8., connected to each other at their ends are used to explain the wave approach [01]. The reverberant energy in subsystem ‘p’ is denoted by a reflected and an incident wave at the junction. A wave is also transmitted in the subsystem, but this does not essentially constitute the reverberant energy because the size and the damping level of the subsystem "s" are not suggested. Somewhat, the formulation of Eq. [$\prod_{ps} = 2\pi f\left(\eta_{ps}E_p - \eta_{sp}E_s\right)$] is used to find the power transmitted from the reverberant energy in subsystem ‘p’ to subsystem ‘s’.

$$\prod_{p\to s} = 2\pi f \eta_{ps} E_p \tag{28}$$

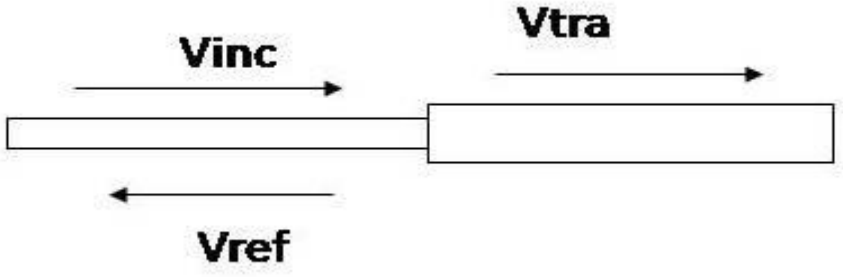


Figure 3.8 Illustration of the wave approach

Assuming the amount of power transmitted from subsystem ‘s’ back into subsystem ‘p’ is incoherent. The total power transmitted is $\prod_{ps} = \prod_{p\to s} - \prod_{s\to p}$. This assumption is valid if there is a modal overlap in the system.

The transmitted power in the wave transmission model is given by,

$$\prod_{tra} = \tau_{ps,\infty} \prod_{inc} \tag{29}$$

Where $\tau_{ps,\infty}$ is the infinite system transmission coefficient and estimated by,

$$\tau_{ps,\infty} = \frac{4R_{p\infty}R_{s\infty}}{\left|Z_{p\infty} + Z_{s\infty}\right|}$$

Where $Z_{p\infty}$ and $Z_{s\infty}$ are the semi-infinite input impedances of the coupled subsystems and R denotes the real part of the impedance. In the estimation of $\tau_{ps,\infty}$ the correct subsystem junction impedances must be used.

The reflected power is given by,

$$\prod_{ref} = \left|r^2\right| \prod_{inc} \tag{30}$$

Where r is the amplitude reflection coefficient at the interface, $\left|r^2\right| = \tau_{ps,\infty}$

The energy of subsystem ‘p’ is represented by

$$E_p = \frac{L_p}{C_{gl}}\left(\prod_{inc} + \prod_{ref}\right) = \frac{1}{2\overline{\delta f}_p}\left(\prod_{inc} + \prod_{ref}\right) \tag{31}$$

Using $\delta f_p = \frac{C_{gl}}{2L_p}$ for a one-dimensional subsystem with length $L_p$ and group speed $C_{gl}$

$$\eta_{ps} = \frac{\overline{\delta f_p}}{\pi f}\frac{\tau_{ps,\infty}}{2 - \tau_{ps,\infty}} \tag{32}$$

From above equation it is being clear that, the coupling loss factor is in terms of transmission coefficient and it can be determined by impedance of structure.

### 3.5 Experimental methods for determining coupling loss factors

Coupling loss factors are essential to calculate noise and vibration levels of an present system or a system at the design phase. For some simple cases comprising conservative coupling, coupling loss factors can be theoretically calculated. However, in most practical situations, particularly those involving non-conservative coupling such as a bearing-shaft interface, they cannot be calculated theoretically and must be obtained from experimental measurements. Several methods are available to measure CLFs such as the power injection method [04], the structural intensity technique [43], the energy level difference method [11] and power coefficient method [52].

#### 3.5.1 Power injection method (PIM)

According to SEA theory, it is not possible to predict the response for a single frequency at a single point on a structure, like the deterministic methods. Instead, SEA predicts averaged and lumped energetic quantities, and for this reason SEA makes use of two main types of averaging.

- Frequency averaging is done over a frequency band of one-third octave band or octave band. Other types of frequency bands are also in use.
- In spatial averaging, energy density of subsystem represents global vibration energy obtained by integrating throughout the subsystem.

The PIM is based on the measurement of the power input into the substructures introduced by a random excitation and of the vibrational kinetic energy as an estimate of the total vibrational energy. The PIM technique allows the identification of the SEA parameters

through the response measurement that are the power input and the energy. The PIM technique consist, to inject power into subsystem ‘p’, then the power input and the energy level of each subsystem are measured.

Suppose we have a system comprising just two subsystems. The SEA equations are

$$\Pi_p = \omega\eta_p E_p + \omega\eta_{ps} E_p - \omega\eta_{sp} E_s \tag{33}$$

$$\Pi_s = \omega\eta_s E_s + \omega\eta_{sp} E_s - \omega\eta_{ps} E_p \tag{34}$$

Equations (33) and (34) can be written in matrix form as,

$$\begin{Bmatrix} \Pi_p \\ \Pi_s \end{Bmatrix} = \omega \begin{bmatrix} \eta_p + \eta_{ps} & -\eta_{sp} \\ -\eta_{ps} & \eta_s + \eta_{sp} \end{bmatrix} \begin{Bmatrix} E_p \\ E_s \end{Bmatrix} \tag{35}$$

Now excite only subsystem ‘p’ over some frequency band. The measured input power is $\Pi_p^{(1)}$ while $\Pi_s = 0$ .

Thus,

$$\begin{Bmatrix} \Pi_p^{(1)} \\ 0 \end{Bmatrix} = \omega \begin{bmatrix} \eta_p + \eta_{ps} & -\eta_{sp} \\ -\eta_{ps} & \eta_s + \eta_{sp} \end{bmatrix} \begin{Bmatrix} E_p^{(1)} \\ E_s^{(1)} \end{Bmatrix} \tag{36}$$

Where $E_p^{(1)}$ and $E_s^{(1)}$ are the measured subsystem energies. Now excite only subsystem ‘s’ over the same band:

$$\begin{Bmatrix} 0 \\ \Pi_s^{(2)} \end{Bmatrix} = \omega \begin{bmatrix} \eta_p + \eta_{ps} & -\eta_{sp} \\ -\eta_{ps} & \eta_s + \eta_{sp} \end{bmatrix} \begin{Bmatrix} E_p^{(2)} \\ E_s^{(2)} \end{Bmatrix} \tag{37}$$

Putting equation (36) and (37) together in matrix form gives,

$$\begin{bmatrix} \Pi_p^{(1)} & 0 \\ 0 & \Pi_s^{(2)} \end{bmatrix} = \omega \begin{bmatrix} \eta_p + \eta_{ps} & -\eta_{sp} \\ -\eta_{ps} & \eta_s + \eta_{sp} \end{bmatrix} \begin{bmatrix} E_p^{(1)} & E_p^{(2)} \\ E_s^{(1)} & E_s^{(2)} \end{bmatrix} \tag{38}$$

and therefore

$$\begin{bmatrix} \eta_p + \eta_{ps} & -\eta_{sp} \\ -\eta_{ps} & \eta_s + \eta_{sp} \end{bmatrix} = \frac{1}{\omega} \begin{bmatrix} \prod_p^{(1)} & 0 \\ 0 & \prod_s^2 \end{bmatrix} \begin{bmatrix} E_p^{(1)} & E_p^{(2)} \\ E_s^{(1)} & E_s^{(2)} \end{bmatrix}^{-1} \tag{39}$$

The coupling loss factors and damping loss factors are obtained by solving above relation.

This approach has the following limitations:-

i)It is generally accepted that experimental estimates of the input power are subject to various, sometimes important, and still unknown errors.

ii) The power injection technique relies on the generation of a subsystem energy matrix but the energy cannot be measured directly and must be deduced from a set of kinetic or dynamic variable discrete points distributed over a subsystem.

iii) For systems divided into several subsystems, the power injection method is time consuming.

iv) The matrix inversion involved in the calculation of coupling loss factors poses some numerical problems due to the poorly conditioned matrix used for inversion. Sometimes the coupling loss factors prove to be negative, which is incoherent

v) To avoid numerical problems when inverting the matrix, it is required to assume that the subsystems are weakly coupled; this limits the possibility of using statistical energy analysis for a general structural model, which has strong coupling.

### 3.5.2 Energy level difference method

In the present work, energy level difference method has been used for estimation of CLFs of Plates with screw and bolted junctions, which was developed by Craik [11]. Assuming that subsystem 1 is directly excited from structure in which N subsystems are available. Subsystem 1 is directly connected to receiving subsystem and other non-source subsystems. Coupling loss factor from the source to receiving subsystem can be expressed as

$$\eta_{12} = \left[ \left( \eta_{22} + \eta_{21} + \ldots\ldots + \eta_{2N} \right) - \eta_{32} \frac{E_3}{E_2} - \eta_{42} \frac{E_4}{E_2} \ldots\ldots - \eta_{N2} \frac{E_N}{E_2} \right] \frac{E_2}{E_1} \tag{40}$$

$$\eta_{12} = \left[ \eta_2 - \eta_{32} \frac{E_3}{E_2} - \eta_{42} \frac{E_4}{E_2} \ldots\ldots - \eta_{N2} \frac{E_N}{E_2} \right] \frac{E_2}{E_1} \tag{41}$$

Where $\eta_{12}$ is the coupling loss factor from subsystem 1 to 2 , $E_1$ is the vibrational energy of subsystem 1 and $\eta_2$ is the DLF of subsystem 2.When the effect of non-source subsystems on $\eta_{12}$ is neglected. The above equation becomes,

$$\eta_{12} = \eta_2 \frac{E_2}{E_1} \tag{42}$$

### 3.5.3 Structural intensity technique

The estimation of the CLF involves the measurement of the power flow across the joint and the energy stored at the source subsystem. The net power flow can be measured using the structural intensity technique. Therefore it is of practical interest to employ the structural intensity technique to measure CLFs. There are several structural intensity techniques. By comparison, the biaxial accelerometer technique and the two-accelerometer array technique are easy to implement in practice. If two subsystems are coupled through a structural joint, the net power flow from subsystem ‘p’ into the subsystem ‘s’ across the joint can be expressed as

$$\eta_{ps} = \frac{LI_n}{\omega E_p} \tag{43}$$

Where,

$I_n$ .-Intensity component

E-Vibrational Energy

This method has two main disadvantages if the number of subsystems is large. Those are as follows,

i) It is very time consuming, especially in the cases where only a few of the CLFs need to be determined.

ii) The energy coefficient matrix may be ill-conditioned since most of the elements in the coefficient matrix are zero.

In comparison with other power flow measurement techniques, the structural intensity technique offers two advantages:

i) The net power flows associated with different structural wave types can be distinguished.

ii) The net power flow across a structural joint can be directly measured on the receiving structure.

### 3.5.4 Power coefficient method

Fahy (1998) suggested the power coefficient measurement method to measure dissipation coefficients and power transfer. These have been given as

Power transfer coefficient ($M_{ps}$) = $\eta_{ps} n_p \omega = \eta_{sp} n_s \omega = M_{sp}$ (44)

Power dissipation coefficient ($M_p$) = $\eta_p n_p \omega$ (45)

Where,

$n$ - denotes the modal density.

The advantages of this method are as follows,

i) This method is easier to implement for complex structures.

ii) It does not involve in any input power measurement because of this measurement errors are less.

iii) It depends on the linear dimensions of the interface between the 'p' and 's' subsystems, while the coupling loss factor also depends on the other subsystem dimensions.

The limitations of this method are as follows,

i) This method gives results similar to the power injection method at frequencies where the modal overlap factor is greater than 1. The approximation error of this method is important when modal overlap factor is less than 1 for selected frequencies.

ii) This method requires many measurements of velocity.

### 3.6 Methods for estimation of damping loss factors

The damping loss factor is important parameter in all types of dynamical analysis, including statistical energy analysis. For various subsystems, the overall response level is inversely proportional to the level of damping.This is denoted in a power balance equation for an isolated subsystem by

$$\prod_{in} = \prod_{diss} = 2\pi f \eta E_{tot} \tag{46}$$

Where,

$\prod_{in}$ - The input power,

$\prod_{diss}$ -The dissipated power,

$E_{tot}$ - The total energy of the dynamical response in the subsystem at frequency $f$ (Hz). The quantity $\eta$ is the ratio of energy dissipated per oscillation cycle to the total energy in the subsystem. Three methods are most commonly used methods to estimate damping loss factor. Those are decay rate method, half power bandwidth method and power injection method.

The decay rate method for measuring damping is based on the transient response of resonant mode to linear damping. After the end of an initial excitation, the energy E of the mode at its resonance frequency $f$ decreases with time. Define the decay rate as the slope of the decay in units of dB / s. The decay rate method can be applied to the measurement of the single resonant mode damping.

Power injection method for measuring damping loss factor is based on the basic power balance equation. In this method a constant excitation source must be used and must be equipped with power measuring transducers. The damping value of the single mode can be measured using sinusoidal excitation as long as the response of the subsystem is dominated by this mode. The average damping of a group of modes can be measured using broadband excitation. In this case, the damping value must be set on a number of excitation points in order to ensure a correct balance of the modal responses.

### 3.6.1 Half power bandwidth method

The most common method for determining damping is to measure the frequency bandwidth between the points of the response curve as shown in Figure 3.9.The usual convention is to consider points $Z_1$ and $Z_2$ , to be located at frequencies on the response curve where the amplitude of response of these points is $\frac{1}{\sqrt{2}}$ times the maximum amplitude. The bandwidth at these points is normally referred as 'half-power bandwidth'. The frequency interval between these two half-power points is $\Delta\omega = \omega_2 - \omega_1$. Damping loss factor of this method is defined as,

$$\eta = \frac{\Delta\omega}{\omega_n} \tag{47}$$

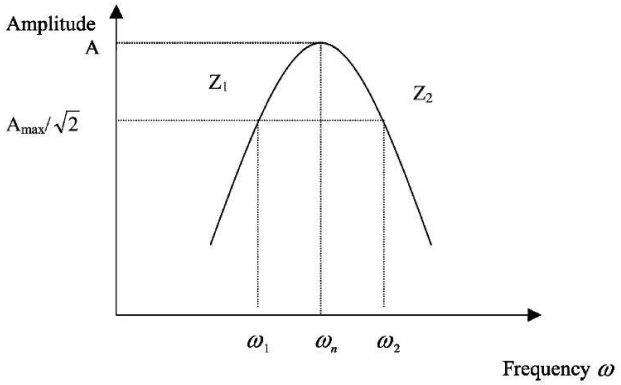


Figure 3.9 Half power bandwidth method

### 3.7 Modal density determination for plate structure

Modal density expression is explained for the free vibration of rectangular plate [72]. A rectangular plate with simply supported, free-free and clamped-free is considered.

The modal density of a simply supported plate can be given by

$$n(\omega) = \frac{S}{4\pi}\sqrt{\frac{m''}{B}} - \frac{1}{4}\left(\frac{m''}{B}\right)^{1/4}\left(\frac{L_1 + L_2}{\pi}\right)\omega^{-1/2} \tag{48}$$

The modal density of a free plate can be given by

$$n(\omega) = \frac{S}{4\pi}\sqrt{\frac{m''}{B}} + \frac{1}{2}\left(\frac{m''}{B}\right)^{1/4}\left(\frac{L_1 + L_2}{\pi}\right)\omega^{-1/2} \tag{49}$$

and the modal density of a clamped-free plate can be given by

$$n(\omega) = \frac{S}{4\pi}\sqrt{\frac{m''}{B}} - \frac{1}{2}\left(\frac{m''}{B}\right)^{1/4}\left(\frac{L_1 + L_2}{\pi}\right)\omega^{-1/2} \tag{50}$$

Where,

$n(\omega)$ -modal density

B- The flexural rigidity

$$B = \frac{Eh^3}{12(1-\upsilon^2)}$$

E-Modulus of elasticity

h- Thickness of plate

υ- Poisson's ratio

ρ- Density of material

$$m'' = \rho h$$

$L_1$ and $L_2$ - Dimensions of rectangular plate

S –Surface area of plate.

### 3.8 Closer

The different methods of estimating coupling loss factor, modal density and damping loss factor for plates are documented in the current chapter. The input power given to the subsystem is not required to measure in energy level difference method for estimation of coupling loss factors whereas it is required in all other methods. The ensuing chapter (**Chapter 4**) attempts experimental arrangement for determining statistical energy analysis parameters for plates.

# Chapter 4

# EXPERIMENTAL SETUP FOR THE ESTIMATION OF STATISTICAL ENERGY ANALYSIS PARAMETERS

## 4.1 Introduction:

Objective of this chapter is to present constructional details of test setup for conducting the experiment and to measure the statistical energy analysis parameters for selected structures. FFT analyzer, impact hammer, accelerometers, vibration exciter and pulse software have been employed for the measurements. The experimental arrangements for estimating statistical energy analysis parameters and details of the instruments used for experimentation have been explained.

## 4.2 Experimental arrangement for estimating statistical energy analysis parameters

The experimental setup for estimating statistical energy analysis parameters is shown in figure 4.1. The test structure had excited using impact hammer to induce transient signals. Impact testing had performed by fixed hammer metod. In this method, hammer was applied at a single point and response was measured at various locations on structure. The impact hammer had directly connected to data acquisition systems. Piezoelectric accelerometer had mounted on structure as the standard IS 14883:2000/ISO 5348:1998 to measure the acceleration of that structure. The mounting position of piezoelectric accelerometer on structure had changed. At nine locations on structure, piezoelectric accelerometer had mounted. The electrical signal from piezoelectric accelerometer is passed to data acquisition system. B and K data acquisition system had used to collect, record, and analyze the data. The windows based computer with pulse software had connected to data acquisition system. Pulse

is a useful task-oriented vibration and sound analysis system. It offers the platform for a range of PC-based measurement solutions from Bruel and Kjaer. Pulse Type 3560-B compact data acquisition unit upto 4 input channels had used. Data acquisition system with pulse software had used to post-process the measured data for estimating statistical energy analysis parameters.

To induce steady state conditions, the vibration exciter had used for some test structures. The experimental setup is as shown in figure 4.2. The signal had passed through oscillator for enhancing the signal and exciting the structure at all required frequencies.

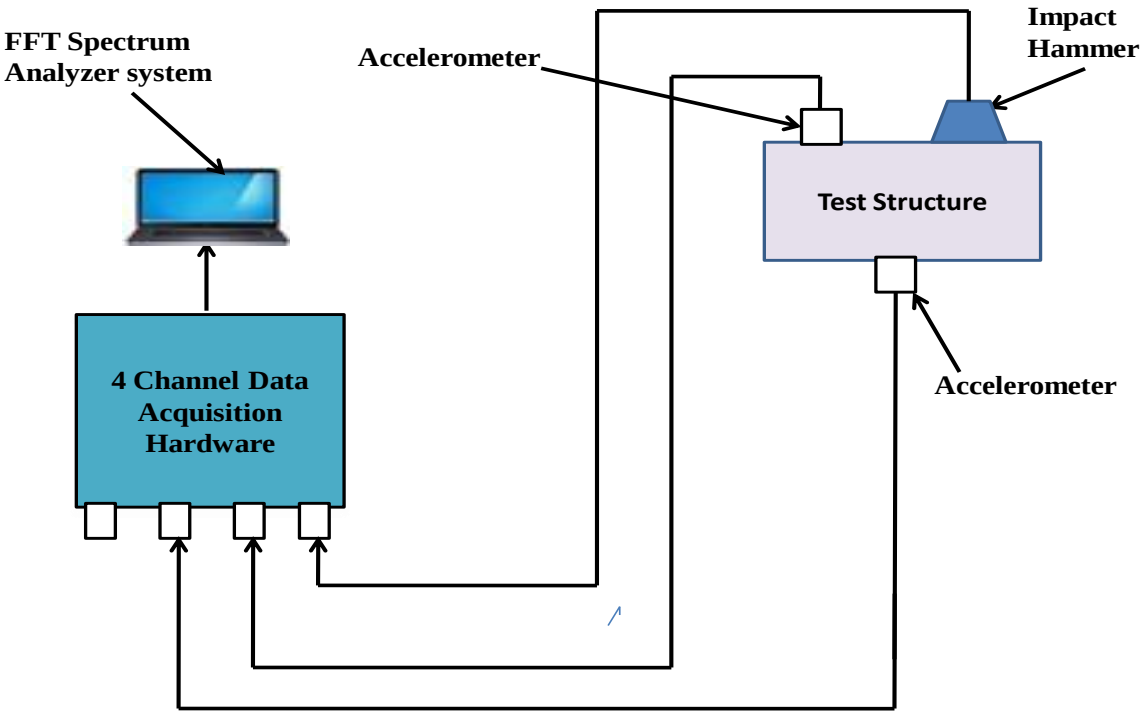


Figure 4.1 Experimental setup for statistical energy analysis parameter estimation-Transient excitation

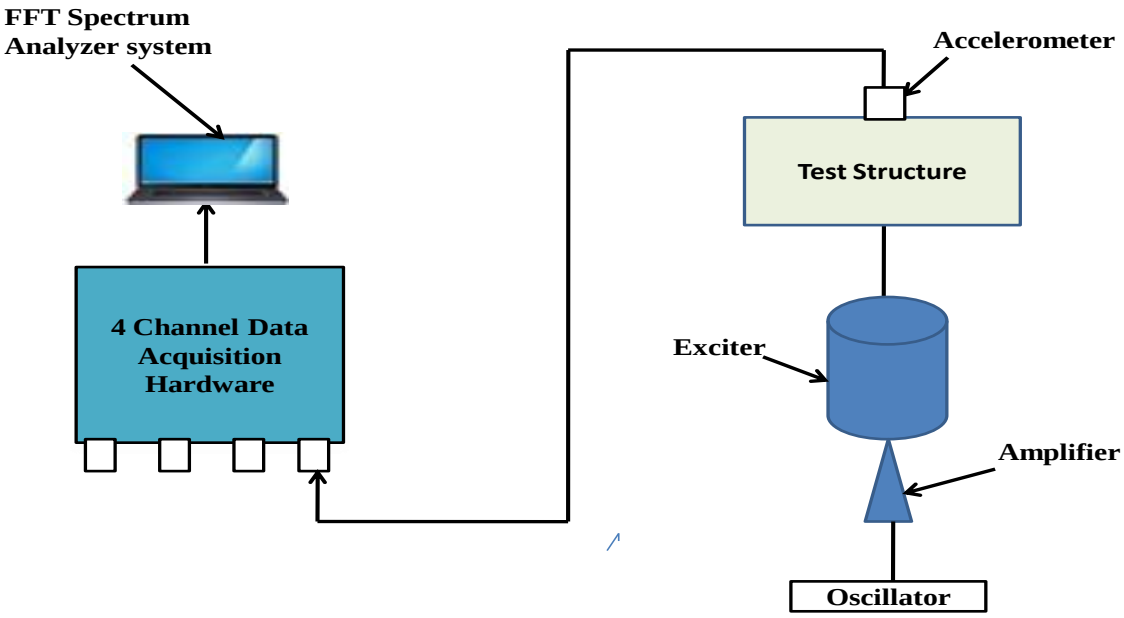


Figure 4.2 Experimental setup for statistical energy analysis parameter estimation-Persistent excitation

## 4.3 FFT Analyzer

Fast Fourier Transform analyzers, which are known as FFT analyzers for short, are the most important instrumentation for the analysis of vibration signals. They derive the name FFT from the name of the algorithm, which is used for converting the time domain information into frequency domain information. The basic operation of an FFT analyzer can be explained as follows,

Consider the analog signal of as shown in Figure 4.3 which may be a typical vibration signal. This signal when fed into a FFT analyzer is first sampled to convert into a discrete or digital signal. Although there is a small difference between a digital signal and discrete signal, we shall use both of them without distinguishing between them. Digital signal is continuous in time but discrete in amplitude. Discrete signal is discrete in time but continuous in amplitude. A discrete or digital signal is defined only at discrete intervals of time.

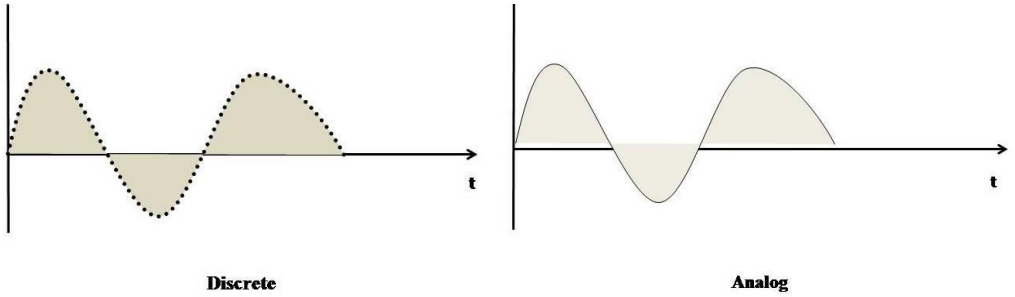


Figure 4.3 Sampling of an analog signal

Now the signal, which is in the form of discrete numbers, has to be suitably manipulated to obtain the frequency domain information. There are several algorithms, which are available to carry out this task. The FFT algorithm is the most popular one, which is used in these analyzers. The FFT algorithm is applied on a block of data and therefore the number of points in each block must be first decided. Since the signal from the transducers is continuously transmitted, the corresponding digitized signal is continuously available. The specifications of FFT analyzer is given in Table 4.3.1.

Table 4.3.1 Specifications of 4 channel FFT Analyzer

| | |
|---|---|
| Make | Bruel and Kjaer |
| Frequency Range | 1Hz to 26.5kHZ |
| Frequency Accuracy | 0.00025% |
| Frequency resolution | 1 mHz |
| Phase resolution | 100 m degrees |
| Ambient operating temperature | 10 to $55^0$c |
| Storage temperature | 25 to $70^0$c |
| Humidity | 93% RH |
| Operating peak values | 12.7 mm, 15m/$s^2$ |

## 4.4 Impact Hammer

An impact hammer is used to excite and measure the impact forces on small and medium structures.The duration of impact time is directly linked to the frequency content of the force applied**.** The impact hammer is used as part of a dynamic structural testing system for modal analysis and structural response prediction. The specifications of impact hammer are given in Table 4.4.1.The photograph of impact hammer is shown in figure 4.4


Figure 4.4 Photograph of Impact Hammer

Table 4.4.1 Specifications of Impact Hammer

| | |
|---|---|
| Impact Hammer | Type 8206, Serial No.55940 |
| Range full scale | 222 N |
| Maximum force | 4448 N |
| Maximum compression | 222 N |
| Frequency range | 5 kHz |
| Head Mass | 100/ 140 grams |
| Sensitivity | 22.5 mV/N |
| Operating temperature range | -73° to 60° C |
| Overall length | 221.5 mm |
| Handle material | Anodized Al |
| Case material | Stainless steel |
| Accessories included | Head extender, cable, tips |

## 4.5 Accelerometers

The optimum choice of vibration transducer is the piezoelectric accelerometer. It is possible to utilize the wide frequency range offered by this type of accelerometers. For the absolute measurement of vibration, the piezoelectric accelerometer is extensively accepted as the best accessible transducer. Titanium ASTM Grade 5 is used as crystal in piezoelectric transducer. This crystal is placed in casing and spring force is applied on it through a block of mass. The piezoelectric crystal is subjected to variable force from block mass and spring because whole assembly vibrates with certain amplitudes which results in voltage change across piezoelectric crystal faces. The specifications of the accelerometer are given in Table 4.5.1. The piezoelectric accelerometers have the following advantages,

1. Useful on very wide frequency ranges. The linearity over a very wide dynamic range is excellent.

2. The acceleration signal can be electronically integrated to make available velocity and displacement data. It is possible to measure acceleration in different environmental conditions

3. External power supply is not required. It is extremely durable because moving parts are not used.

Figure 4.5 Photograph of Accelerometer

Table 4.5.1 Specifications of Accelerometer

| | |
|---|---|
| Accelerometer | Type 4514, Serial No.57125 |
| Case Material | Titanium |
| Sensing Element | Ceramic |
| Sealing | Hermetic |
| Weight | 8.7 gram |
| Mounting surface flatness | 25μm |
| Mounting Torque | Max.2.3 Nm |
| Temperature Range | -51 to $+121^0$c |
| Mounted Resonance Frequency | 32kHz |

## 4.6 Vibration exciter

Vibration exciter SI-220 is an electrodynamics type of device. It consists of a powerful magnet placed centrally surrounding which is suspended the exciter coil. This set is surrounded by a magnetic circuit with high permeability for optimal performance. Special attention has been paid to the design to minimize the leakage magnetic flux at the top of the vibration table. When an electric current passes through the excitation coil, a magnetic field is created around the coil. This field interacts with the field due to the central permanent magnet and results in an upward or downward movement of the suspended coil depending on the direction of the current flow in the coil. If an alternating current is injected into the coil, it goes up and down continuously. Thus, by controlling the frequency of the current of the coil, the vibration frequency is controlled.By controlling the amount of current, the amplitude of vibration is controlled. The specifications of vibration exciter are given in Table 4.6.1.

Table 4.6.1 Specifications of vibration Exciter

| | |
|---|---|
| Peak sine force | 100 N |
| Peak velocity at resonance | 1 m/sec |
| Max. Displacement | 8 mm peak to peak |
| Bare table acceleration | 200m/sec$^2$ |
| Max. Allowable payload | 750 gm |
| Power requirement | 150 VA |
| Weight | 20 kg |

## 4.7 Closure

Experimental arrangement for estimating statistical energy analysis parameters has been presented. The detail specifications of each instrument used for experimentation have been given. Experimental readings of statistical energy analysis parameters are presented in Chapter 5.

# Chapter 5

# ESTIMATION OF DAMPING LOSS FACTOR AND MODAL DENSITY FOR PLATES

## 5.1 Introduction

In this chapter experimental results for free-free, simply supported and clamped-free boundary condition plates are presented. The parameters of statistical energy analysis of the plate viz. modal densities and damping loss factors have been evaluated. Theoretical and experimental results of modal densities of plates with different boundary conditions have been compared.

## 5.2 Experimental procedure for estimation of modal density and damping loss factors for free-free boundary condition plates

The experimental set-up for measuring damping loss factor and modal density is shown in Figure 5.1. The experimental set-up consisted of four channel data acquisition hardware, FFT Analysis software, accelerometers and impact hammer. Plates of different materials like mild steel, aluminium and stainles steel had taken as test specimens. The plate structures had suspended by nylon threads from rigid frame. This plate structure had excited by impact hammer to produce transient conditions. Accelerometer had mounted on plate structure and measurements had taken by varying positions of accelerometer and impact hammer. The signal from impact hammer and accelerometer had passed to FFT analysis software through data acquisition hardware. Autospectrum from FFT analysis software with different accessories are shown in Figure 5.2. In autospectrum, frequency is on x-axis and vibration level is on y-axis. Experiments were conducted in the frequency range of 0-5000Hz. Modal density had estimated by counting number of natural frequencies from selected frequency bands. For this autospectrums from FFT analysis software had used. For the evaluation of damping loss factor, half-power bandwidth method is used. Root mean square

values of amplitude had plotted on Figure 5.3 and corresponding frequencies have used for estimating damping loss factor. The results of damping loss factor and modal densities for free-free boundary condition plate are given in Table 5.2.1 and Table 5.2.2.

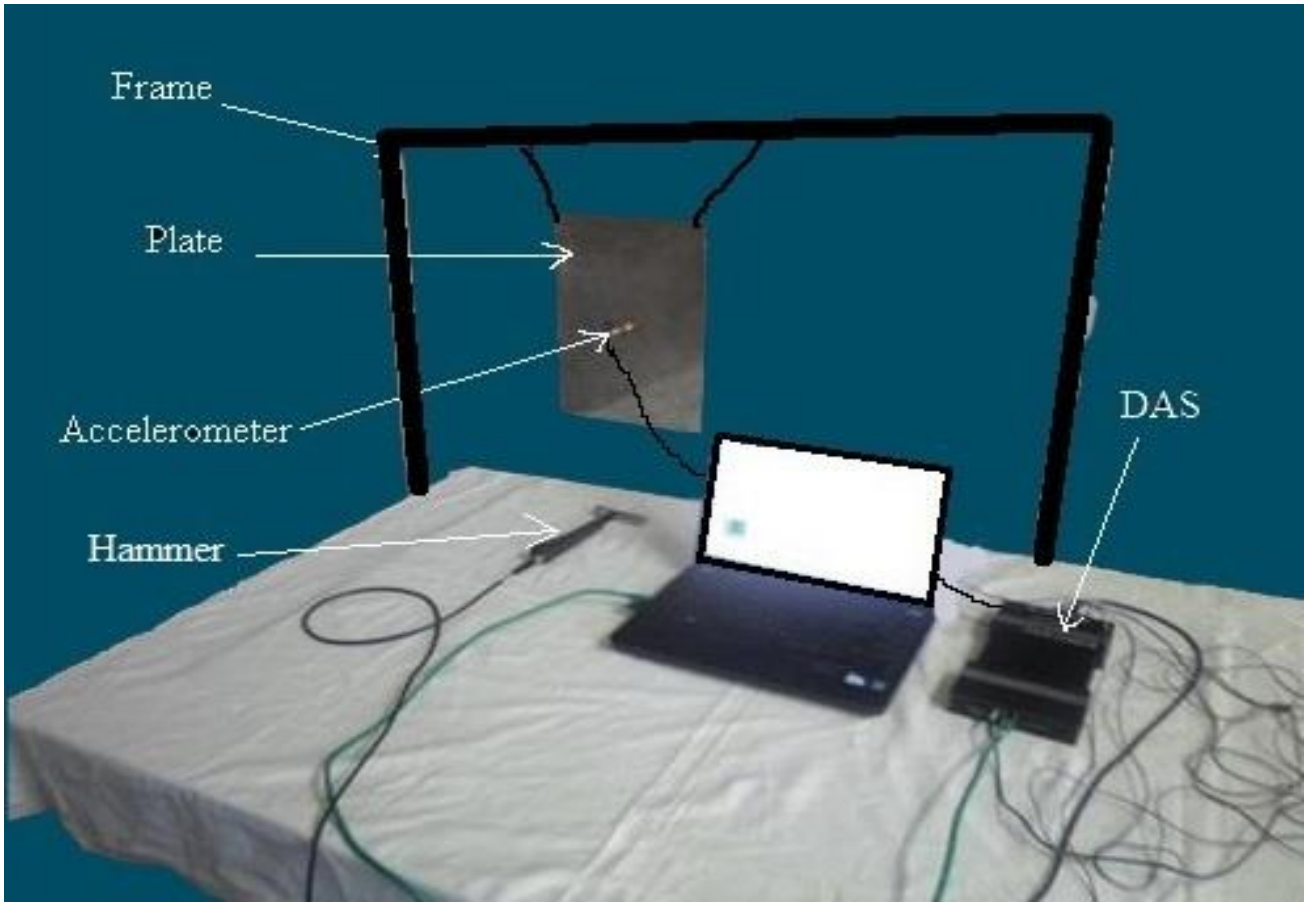


Figure 5.1 Experimental set up for free –free boundary condition plate

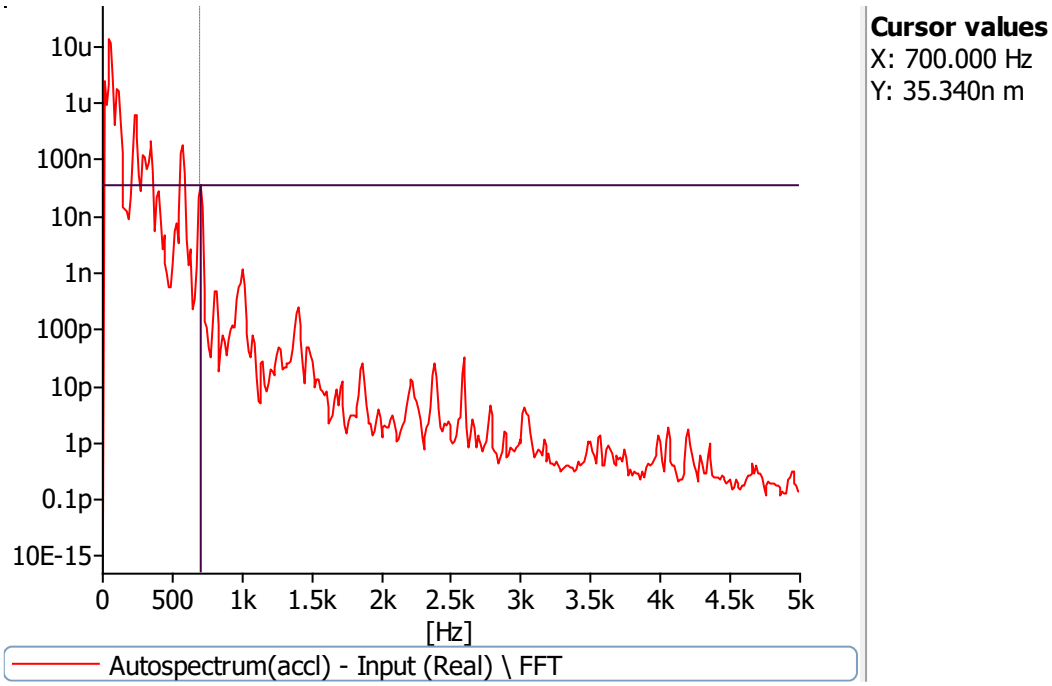


Figure 5.2 Amplitude Vs Frequency for Stainless steel free-free boundary condition plate

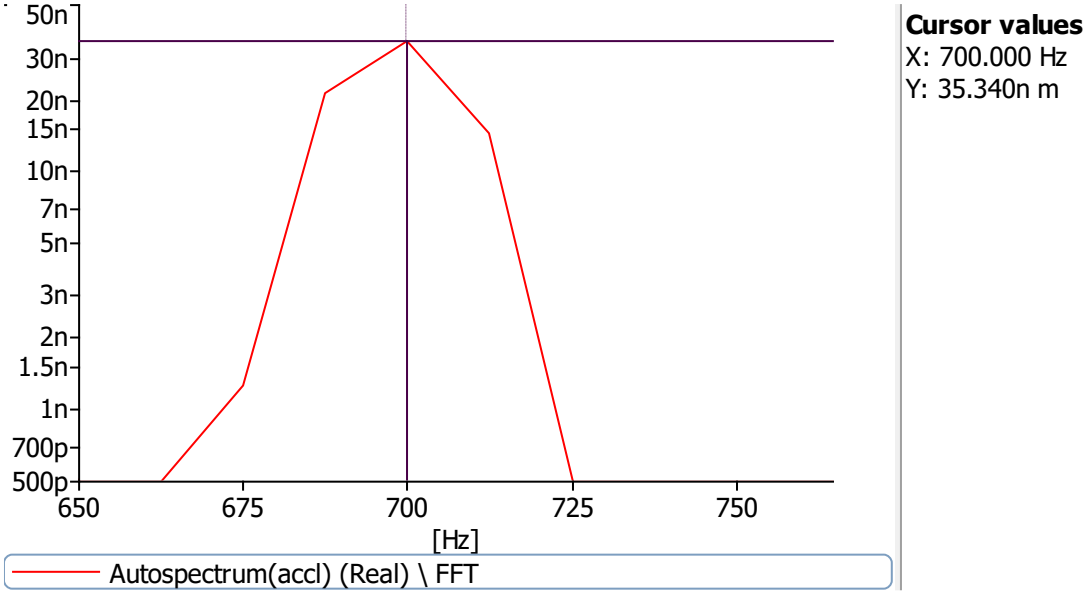


Figure 5.3 Peak at 700 Hz frequency

Maximum amplitude (A) = 35.340 nm

$$\frac{A}{\sqrt{2}} = \frac{35.340}{\sqrt{2}} = 24.989nm$$

$f_1$= 690.7276 Hz  $f_2$= 706.203 Hz  f = 700 Hz

$$\eta = \frac{f_2 - f_1}{f} = 0.0221$$

Table 5.2.1 DLFs of mild steel, aluminium and stainless steel for free-free boundary condition plate

| | Mild Steel | | Aluminium | | Stainless Steel | |
|---|---|---|---|---|---|---|
| Sr No. | Frequency (Hz) | DLF | Frequency (Hz) | DLF | Frequency (Hz) | DLF |
| 1 | 290 | 0.025502 | 350 | 0.0462546 | 350 | 0.039434 |
| 2 | 465 | 0.013623 | 537.5 | 0.0390992 | 575 | 0.03232 |
| 3 | 630 | 0.0100924 | 650 | 0.034796 | 700 | 0.02211 |
| 4 | 935 | 0.0103174 | 800 | 0.027147 | 1000 | 0.01654 |
| 5 | 1270 | 0.0048843 | 1050 | 0.019023 | 1400 | 0.01439 |
| 6 | 1675 | 0.0051236 | 1350 | 0.0149074 | 1675 | 0.01352 |
| 7 | 1940 | 0.0050928 | 1575 | 0.016646 | 1712 | 0.0114883 |
| 8 | 2575 | 0.00806 | 1962 | 0.01531 | 1975 | 0.011243 |
| 9 | 3250 | 0.007587 | 3650 | 0.006567 | 2775 | 0.00618 |
| 10 | 4138 | 0.005912 | 4388 | 0.006505 | 4200 | 0.004905 |
| 11 | 4862 | 0.00536 | 4925 | 0.005738 | 4950 | 0.005288 |

Table 5.2.2 Modal densities of mild steel, aluminium and stainless steel for free-free boundary condition plate

| Sr.No. | Frequency (Hz) | Modal Densities | | |
|---|---|---|---|---|
| | | Mild steel | Aluminium | Stainless steel |
| 1 | 125 | 0.04 | 0.04 | 0.04 |
| 2 | 250 | 0.032 | 0.032 | 0.032 |
| 3 | 500 | 0.028 | 0.028 | 0.028 |
| 4 | 1000 | 0.026 | 0.026 | 0.026 |
| 5 | 2000 | 0.024 | 0.024 | 0.022 |
| 6 | 4000 | 0.022 | 0.022 | 0.021 |

## 5.3 Results and discussion

Modal densities and damping loss factors of free-free boundary condition plates are compared .The materials used for plate were mild steel, aluminium and stainless steel.

### 5.3.1 Modal density of free-free boundary condition plates

The results of theoretical and experimental of free-free boundary condition plates made of mild steel, stainless steel and aluminium are shown in Figure 5.4, Figure 5.5 and Figure 5.6. Experimental values of modal density are in close to theoretical values of modal density for all plates under free-free boundary condition.

In free-free boundary condition of plate, the movement of plate are not constrained in any direction. Because of which plate can move in any direction. Due to this, the numbers of resonance modes present at lower frequency range are more which results in higher modal density of free-free boundary condition plate.

As expected the modal density decreases with increase in frequency. Within lower frequency range, decrease in modal density is stiff, whereas it converges to constant value in higher frequency region. This can be explained based on the fact that in higher frequency

range, the numbers of resonance modes present are comparatively less compared to low frequency band.

In higher frequency range, failure chances of structure due to external excitation are less because of less modal density. It is possible to excite the structure in wide range of frequency at higher frequency range.

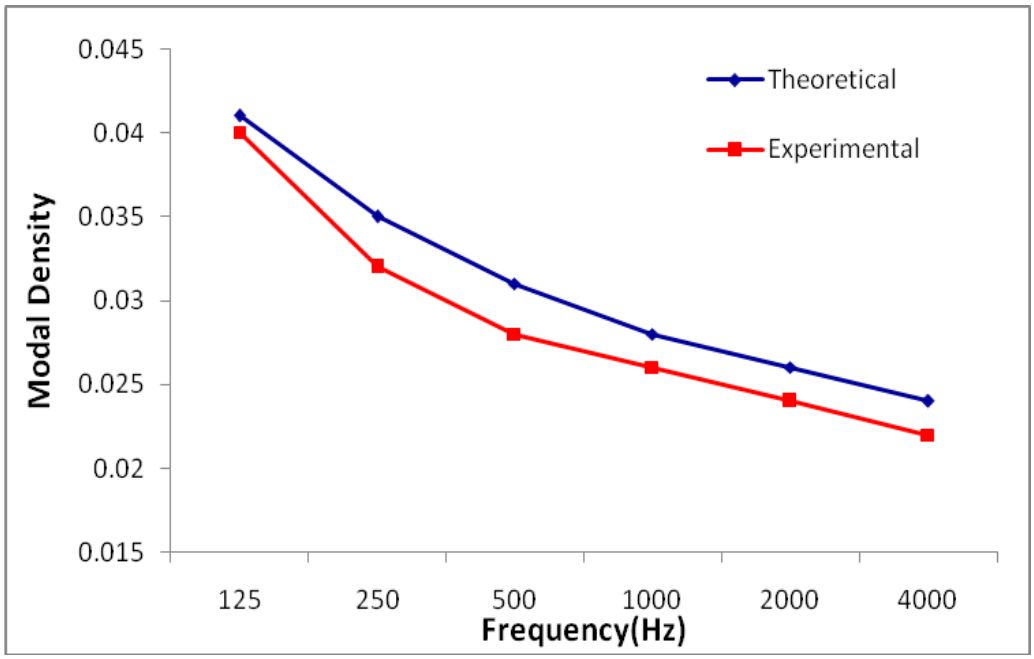


Figure 5.4 Modal densities for free-free boundary condition mild steel plate

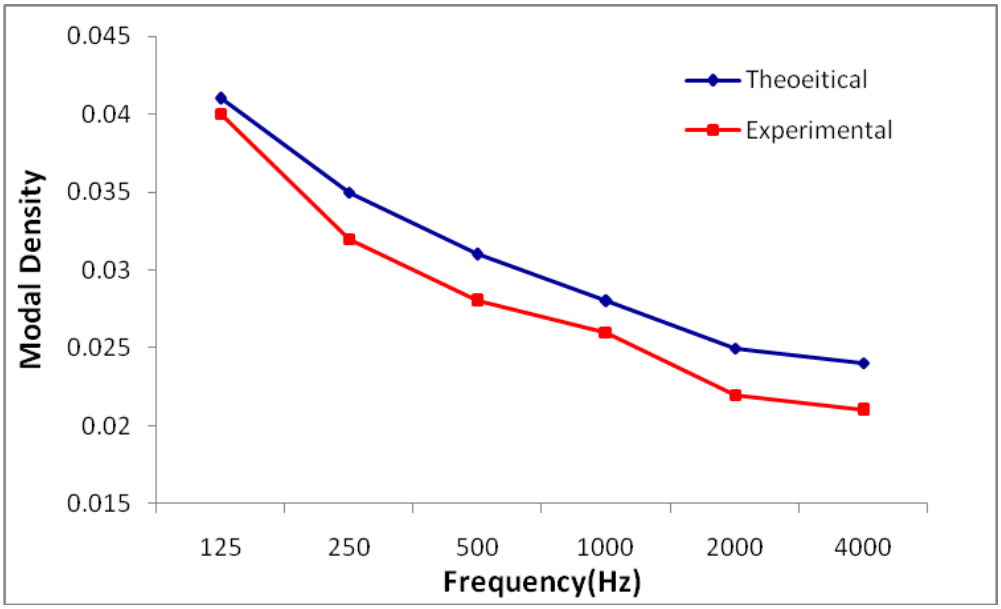


Figure 5.5 Modal densities for free-free boundary condition stainless steel plate

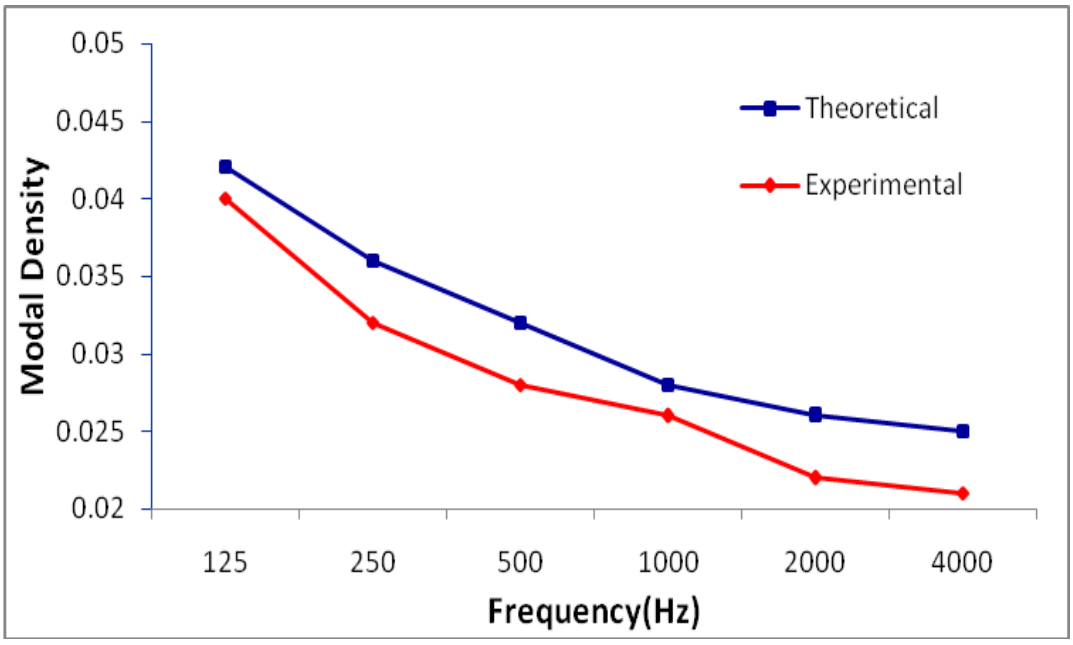


Figure 5.6 Modal densities for free-free boundary condition aluminium plate

### 5.3.2 Damping loss factors of free-free boundary condition plates

Damping loss factor for plates of mild steel, aluminium and stainless steel under free-free boundary condition has been estimated by half power bandwidth method. The results of damping loss factors are presented for mild steel, aluminium and stainless steel plates. In Figure 5.7, it can be observed by comparing the results at lower frequencies the value of damping loss factor falls steeply while at higher frequencies it remains fairly constant. It can be further observed that damping loss factor have significant values at lower modes and very less values at higher modes. Based on this one can conclude that the damping effect at higher modes have insignificant effect.

The values of damping loss factor for aluminium is more as compared to mild steel and stainless steel. So it is possible to use aluminium rather than mild steel and stainless steel for more dissipation of energy.

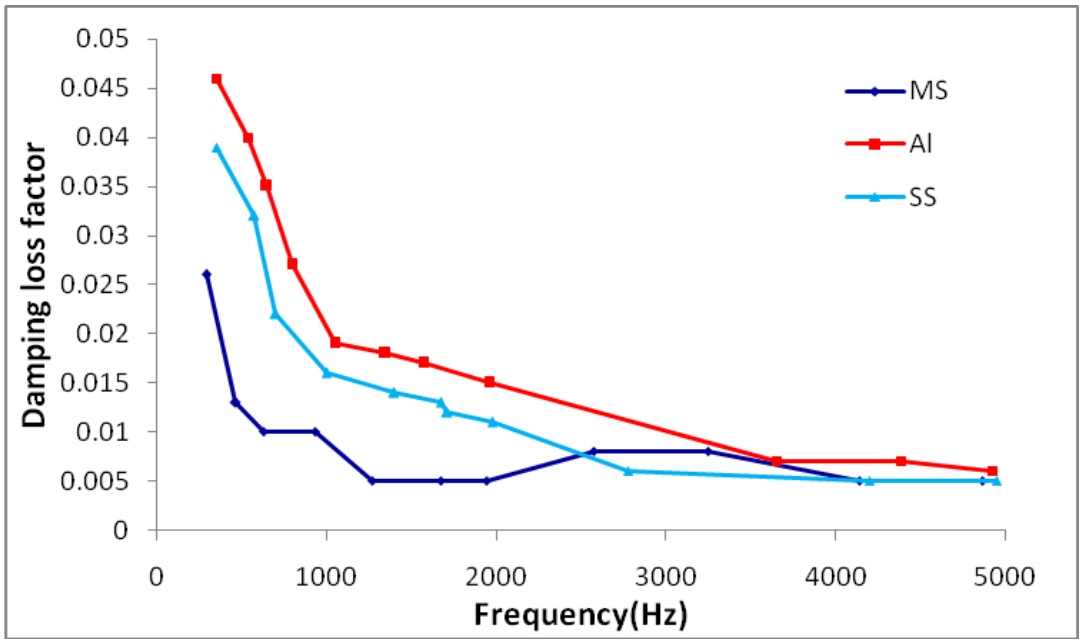


Figure 5.7 Damping loss factors for free-free boundary condition plates

## 5.4 Modal density and damping loss factors for free-free boundary condition plates of composite materials

Fiber reinforced composites are widely used in applications that exploit their high strength / weight and modulus / weight ratios. These advantages have made composite materials, the material of choice in many critical applications such as the aeronautical, marine and space industries. In some applications, structures constructed from fiber-reinforced composites may be subjected to random excitation covering a large portion of, or in some cases even the entire range of audible frequencies. The result is that many modes are excited, making deterministic methods impractical. Probabilistic technique, the statistical analysis of energy , is the tool most commonly used to model the dynamics of high frequencies. So, SEA parameters like modal density and damping loss factor have been determined for composite plates. Composite plates have prepared by hand layup technique. These plates made up of different ply orientation have been taken for investigation. Material properties of composite plates are given in Table 5.4.4. The elastic constants of fibre reinforced composite plates have been estimated experimentally according to ASTM-D-3039 standard. The properties of composite elements are given in Table 5.4.1, Table 5.4.2 and Table 5.4.3.

Table 5.4.1 Properties of E-glass fiber

| | |
|---|---|
| Tensile strength | 3445 MPa |
| Compressive strength | 1080 MPa |
| Density | 2.54 g/cm$^3$ |
| Thermal expansion | 5.4 μm/m$^0$c |

Table 5.4.2 Properties of LY-556

| | |
|---|---|
| Tensile strength | 35-37 MPa |
| Ultimate elongation | 12-24 % |
| Tensile modulus | 1500-1700 MPa |
| Chemical formula | $C_{18}H_{21}ClO_3$ |

Table 5.4.3 Properties of Graphene

| | |
|---|---|
| Tensile modulus | >1000 GPa |
| Tensile strength | > 5GPa |
| Bulk modulus | 0.241 g/cc |
| Dia. average X & Y dimensions | 5- 10 micron |
| Thickness avg. Z dimension | 3-6 nm |
| Number of layer | Avg. number of layer 3-6 |
| Purity | 96-99% |
| Surface Area | 210- 300 m^2/g |

Table 5.4.4 Material properties of composite plates (Dimensions-400*300*2 mm)

| Sr. No | Composition of Material | Fiber Orientation |
|---|---|---|
| 1 | 10%E-glass fiber, 90% LY-556 epoxy resin | $[0]_{12}$ Unidirectional |
| 2 | 10%E-glass fiber, 90% LY-556 epoxy resin) | $[0_3,+/-45,90]s$ Quasi isotropic |
| 3 | 10%E-glass fiber, 90% LY-556 epoxy resin) | $[(0,90)_2,0,90]s$ Cross-ply |
| 4 | 10%E-glass fiber, 90% LY-556 epoxy resin and 0.83 % filler | $[0]_{12}$ Unidirectional |
| 5 | 10%E-glass fiber, 90% LY-556 epoxy resin and 0.83 % filler | $[0_3,+/-45,90]s$ Quasi isotropic |

The experimental procedure for estimating modal density and damping loss factors for plates of composite materials are similar to aluminium, mild steel and stainless steel plates. The results of modal density and damping loss factors are shown in Table 5.4.5, Table 5.4.6 and Table 5.4.7.

Table 5.4.5 Modal densities of free-free boundary condition composite plate

| Sr. No. | Frequency (Hz) | E-1 Unidirectional orientation | E-2 Quasi isotropic orientation | E-3 Cross-ply orientation | G-1 Unidirectional orientation | G-2 Quasi isotropic orientation |
|---|---|---|---|---|---|---|
| 1 | 500 | 0.036 | 0.034 | 0.036 | 0.034 | 0.036 |
| 2 | 1000 | 0.034 | 0.036 | 0.034 | 0.034 | 0.036 |
| 3 | 1500 | 0.034 | 0.03 | 0.034 | 0.032 | 0.036 |
| 4 | 2000 | 0.034 | 0.03 | 0.034 | 0.034 | 0.034 |
| 5 | 2500 | 0.03 | 0.03 | 0.034 | 0.034 | 0.034 |
| 6 | 3000 | 0.03 | 0.028 | 0.03 | 0.03 | 0.034 |
| 7 | 3500 | 0.03 | 0.028 | 0.03 | 0.03 | 0.032 |
| 8 | 4000 | 0.028 | 0.028 | 0.032 | 0.03 | 0.03 |
| 9 | 4500 | 0.028 | 0.028 | 0.03 | 0.03 | 0.03 |
| 10 | 5000 | 0.028 | 0.028 | 0.03 | 0.03 | 0.03 |

Table 5.4.6 Damping loss factors of free-free boundary condition composite plate

| Sr.No. | E-1 Unidirectional orientation | | E-2 Quasi isotropic orientation | | E-3 Cross-ply orientation | |
|---|---|---|---|---|---|---|
| | Frequency (Hz) | DLF | Frequency (Hz) | DLF | Frequency (Hz) | DLF |
| 1 | 16 | 0.635 | 16 | 0.622 | 16 | 0.648 |
| 2 | 128 | 0.394 | 160 | 0.354 | 160 | 0.392 |
| 3 | 912 | 0.098 | 640 | 0.189 | 880 | 0.222 |
| 4 | 1024 | 0.0556 | 720 | 0.141 | 1136 | 0.15 |
| 5 | 1376 | 0.0444 | 816 | 0.149 | 1360 | 0.135 |
| 6 | 1440 | 0.031 | 1088 | 0.0404 | 1472 | 0.057 |
| 7 | 1888 | 0.0297 | 1456 | 0.033 | 1632 | 0.051 |
| 8 | 2432 | 0.0234 | 1616 | 0.035 | 2096 | 0.027 |
| 9 | 3184 | 0.0162 | 2064 | 0.0196 | 3536 | 0.0163 |
| 10 | 4592 | 0.01 | 4592 | 0.017 | 4640 | 0.0084 |

Table 5.4.7 Damping loss factors of free-free boundary condition composite plate with graphene

| Sr.No. | G-1 Unidirectional orientation | | G-2 Quasi isotropic orientation | |
|---|---|---|---|---|
| | Frequency (Hz) | DLF | Frequency (Hz) | DLF |
| 1 | 16 | 0.6 | 16 | 0.613 |
| 2 | 160 | 0.262 | 288 | 0.359 |
| 3 | 272 | 0.114 | 336 | 0.1241 |
| 4 | 384 | 0.097 | 688 | 0.0797 |
| 5 | 512 | 0.088 | 1120 | 0.078 |
| 6 | 752 | 0.0605 | 1856 | 0.0484 |
| 7 | 1104 | 0.0447 | 2576 | 0.0313 |
| 8 | 2688 | 0.03177 | 3600 | 0.0304 |
| 9 | 2944 | 0.0454 | 3904 | 0.0262 |
| 10 | 4752 | 0.026 | 4896 | 0.0247 |

## 5.5 Results and discussion

Five composite specimens have been tested to evaluate modal density and damping loss factor with free-free boundary condition plates. The effect of fibre orientation of composite plates on modal density and damping loss factors are compared.

### 5.5.1 Effect of fibre orientation on modal density

The experimental and theoretical modal densities are compared for composite plates in free- free boundary condition. There is variation in experimental and theoretical values of modal density because of modal overlap. Modal density depends on flexural rigidity of composite plates. The elastic constants such as modulus of elasticity, poisons ratio along x and y direction were tested by universal testing machine according to ASTM D-3039 for composite plates with different fiber orientation. The flexural rigidity for all composite plates were estimated by the elastic constants. The flexural rigidity of cross-ply plate is less as compared to unidirectional plate. Therefore modal density of cross-ply plate is comparatively

more than unidirectional plate. The modal densities for unidirectional (E-1), quasi-isotropic (E-2) and cross-ply (E-3) plates are shown in Figure 5.8, Figure 5.9 and Figure 5.10. The reason in variation of modal density may also be because of orientation angle of plies.

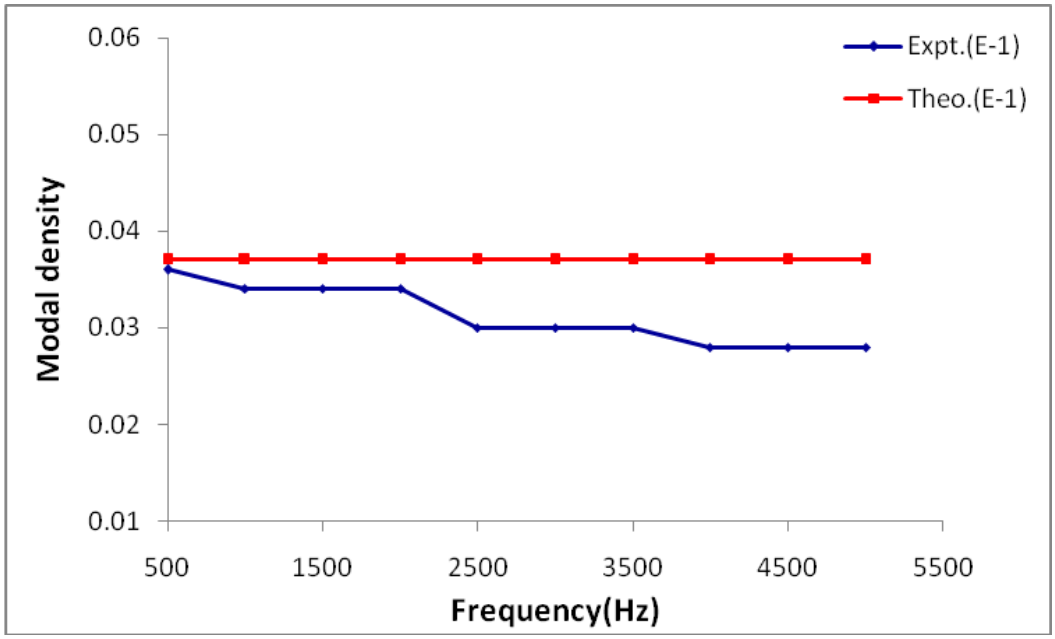


Figure 5.8 Modal density of unidirectional orientation composite plate

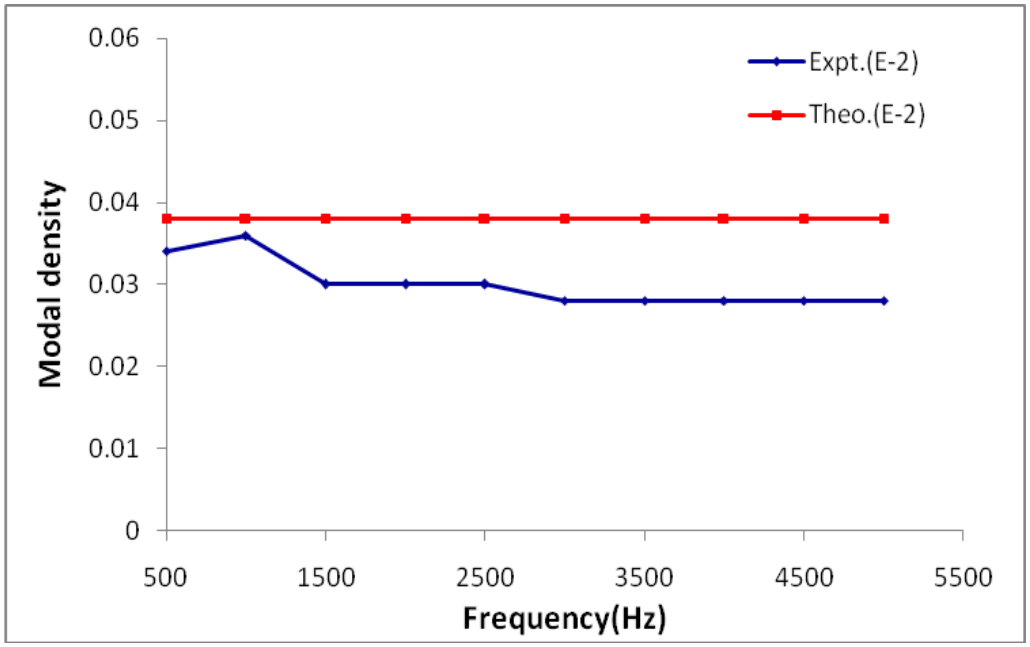


Figure 5.9 Modal density of quasi isotropic orientation composite plate

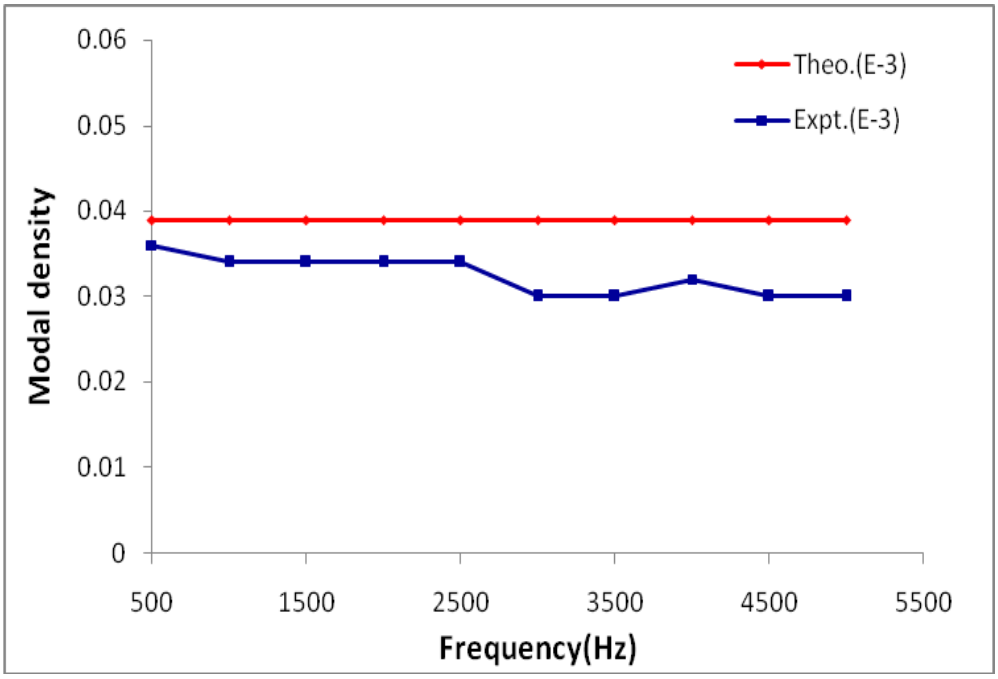


Figure 5.10 Modal density of cross-ply orientation composite plate

### 5.5.2 Effect of graphene in composite plate on modal density

It is clearly observed in Figure 5.8 and Figure 5.11, that the values of modal density for rectangular plate made up of unidirectional orientation without graphene (E1) are more than unidirectional orientation with graphene (G1). There is small variation in experimental and theoretical values of modal density because of modal overlap. Due to addition of doping material, there is variation in shrinkage and warpage of resin. Doping material changes the modulus of elasticity and Poisson's ratio values in x and y direction for composite plates. The values of modulus of elasticity in x and y direction increases due to addition of graphene in resin. Because of this, modal density of unidirectional plate with graphene is less.Decrease in modal density because of graphene addition, will help to excite that structure at more number of excitation frequencies in selected frequency range. Also from Figure 5.11 and Figure 5.12, it has been observed that modal densities of quasi-isotropic plate are more than unidirectional plate. The variation of the modal density with fiber orientation, gives designers additional flexibility when incorporating composite plates in design.

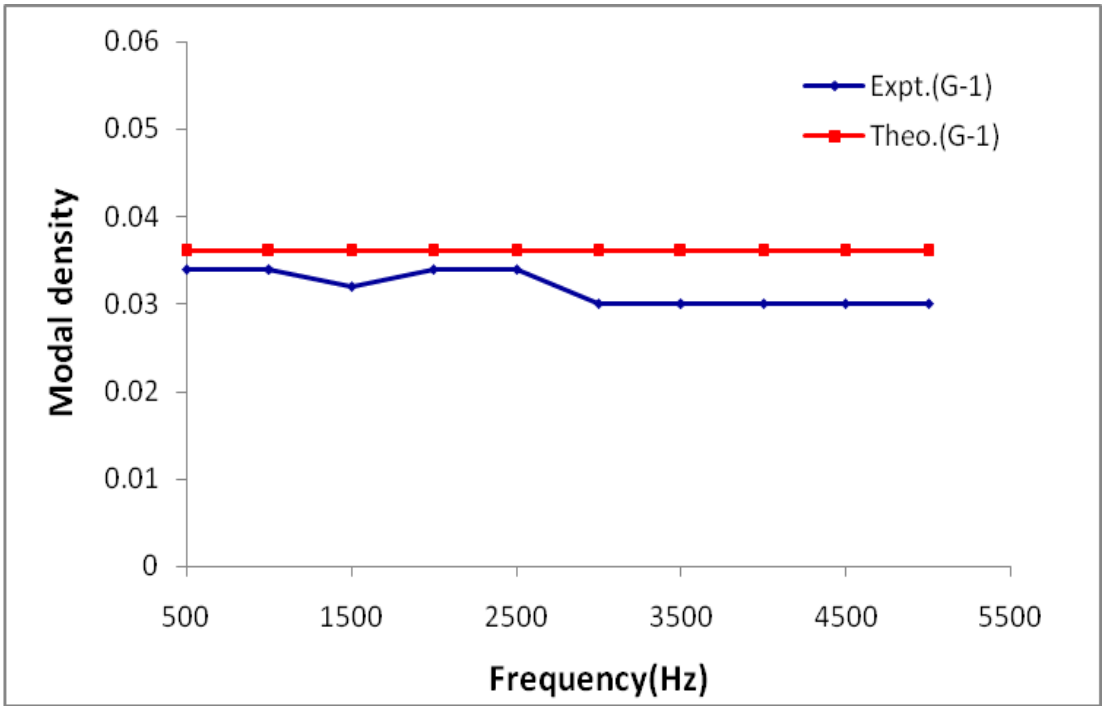


Figure 5.11 Modal density of unidirectional orientation composite plate with graphene

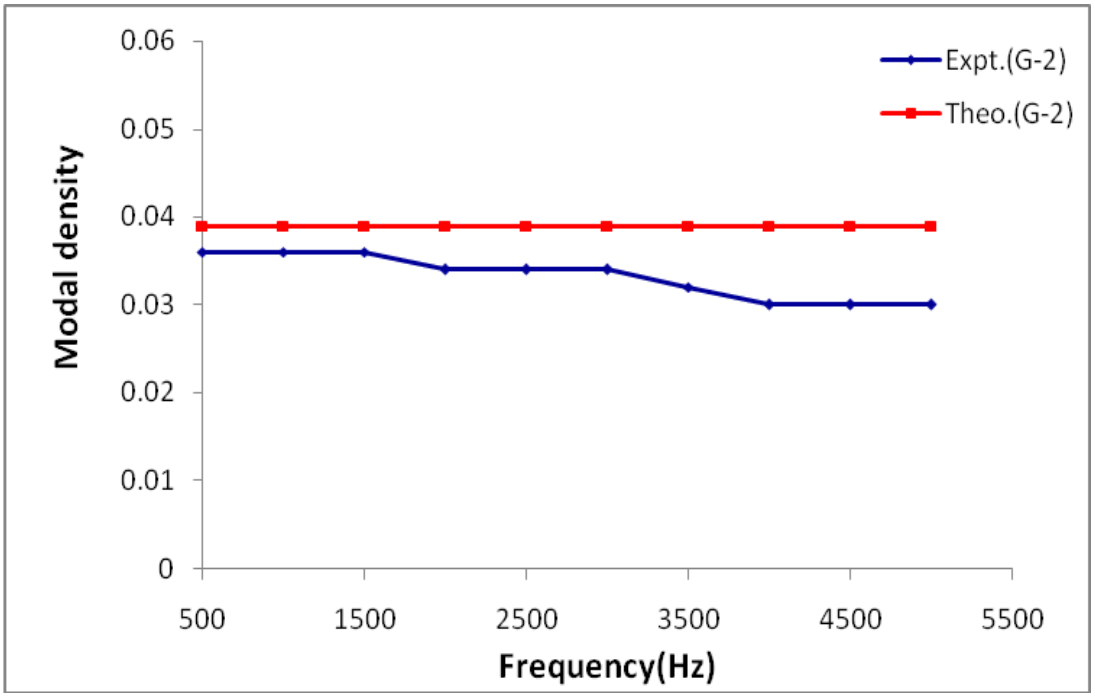


Figure 5.12 Modal density of quasi isotropic orientation composite plate with graphene

### 5.5.3 Damping loss factors for composite plates

It has been observed that at low frequencies there is drastic change between damping loss factor values whereas these values are comparatively constant at a higher frequency range. The values of damping loss factor for composite plates are considerably greater than plates made up with conventional materials. In comparison among the composite plates with different fiber orientations, the damping loss factor values of plate with unidirectional fiber orientation is lower than the plates with cross ply and quasi isotropic orientations as shown in Figure 5.13 and Figure 5.14. Due to addition of graphene, damping loss factors are relatively more at higher frequency, but at lower frequency those values are less as shown in Figure 5.15.

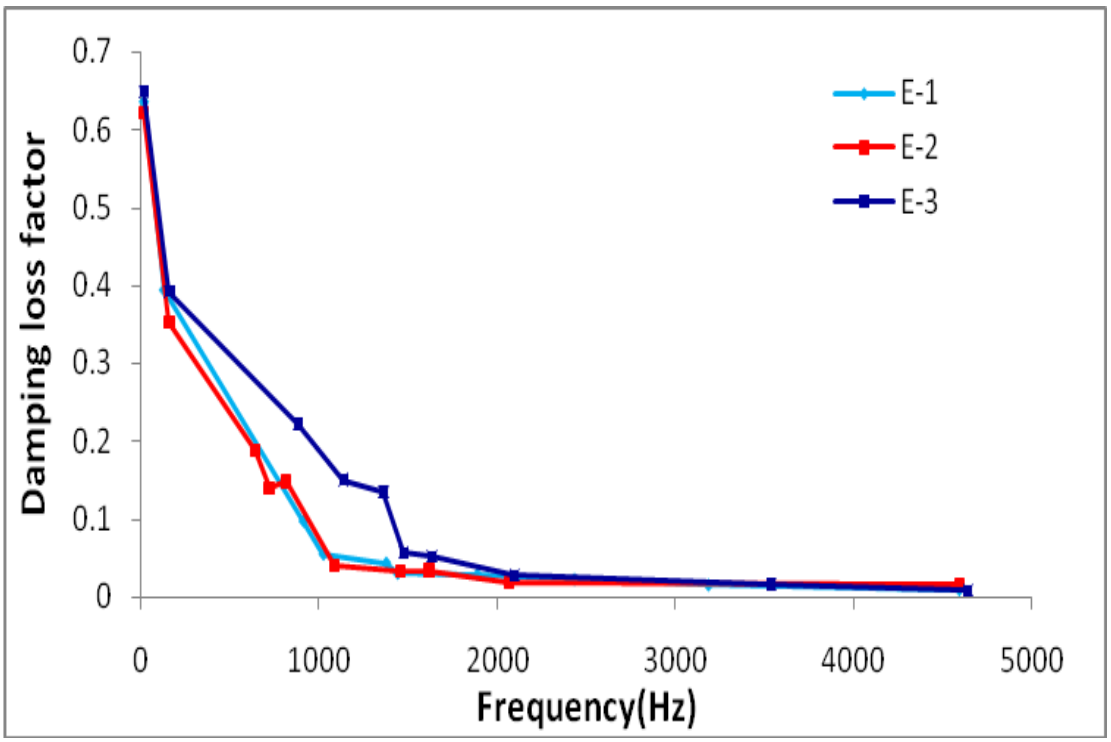


Figure 5.13 Damping loss factors for unidirectional(E-1), quasi isotropic (E-2) and cross ply (E-3) composite plates of free-free boundary condition.

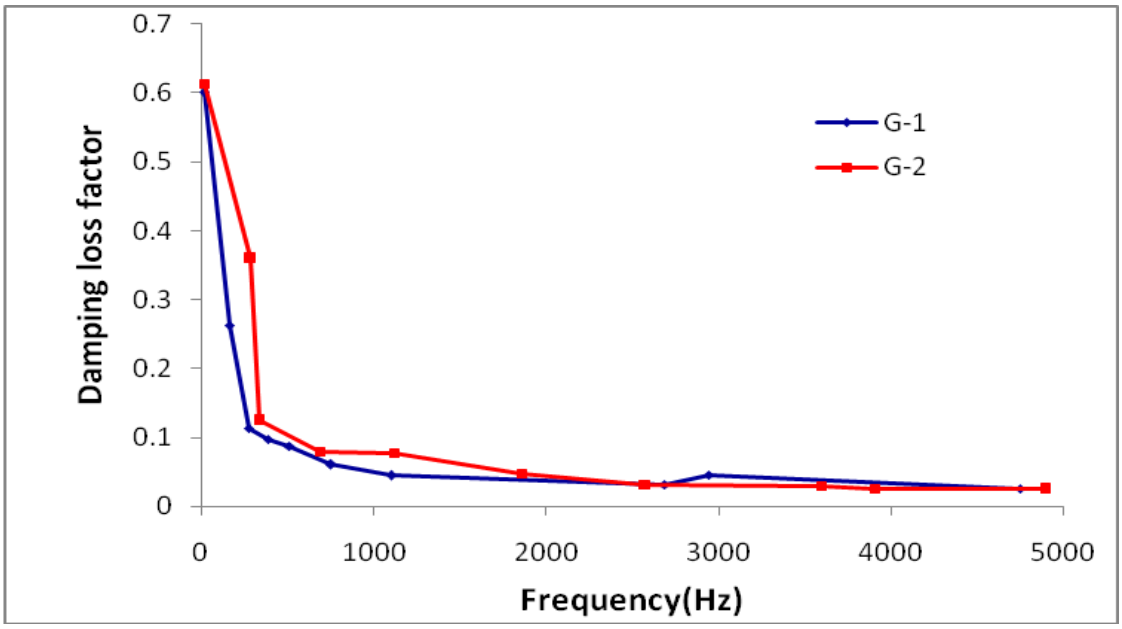


Figure 5.14 Damping loss factors for unidirectional(G-1) and quasi isotropic (G-2) composite plates of free-free boundary condition.

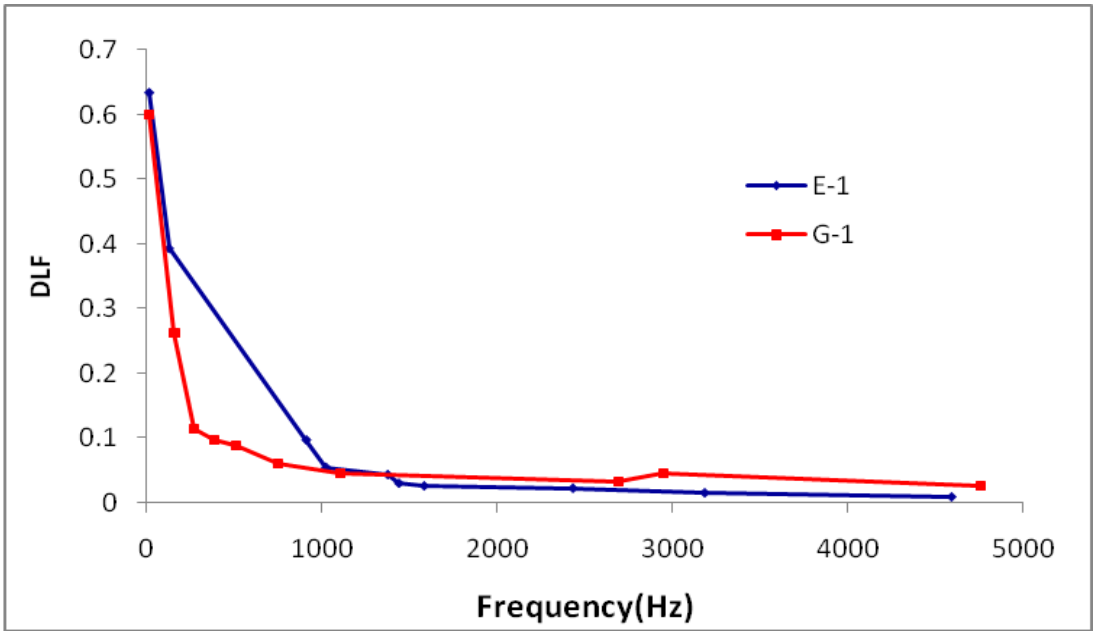


Figure 5.15 Damping loss factors for unirectional composite plates of free-free boundary condition with and without graphene.

### 5.6 Experimental set up for simply supported and clamped-free plates

Simply supported condition of plate had achieved by using the metal frame having bolts for tightning purpose as shown in Figure 5.16. The plate had placed in that frame and accelerometer had mounted on the plate. The excitation to that plate had given by impact hammer and by using the FFT analyzer the data had recorded.

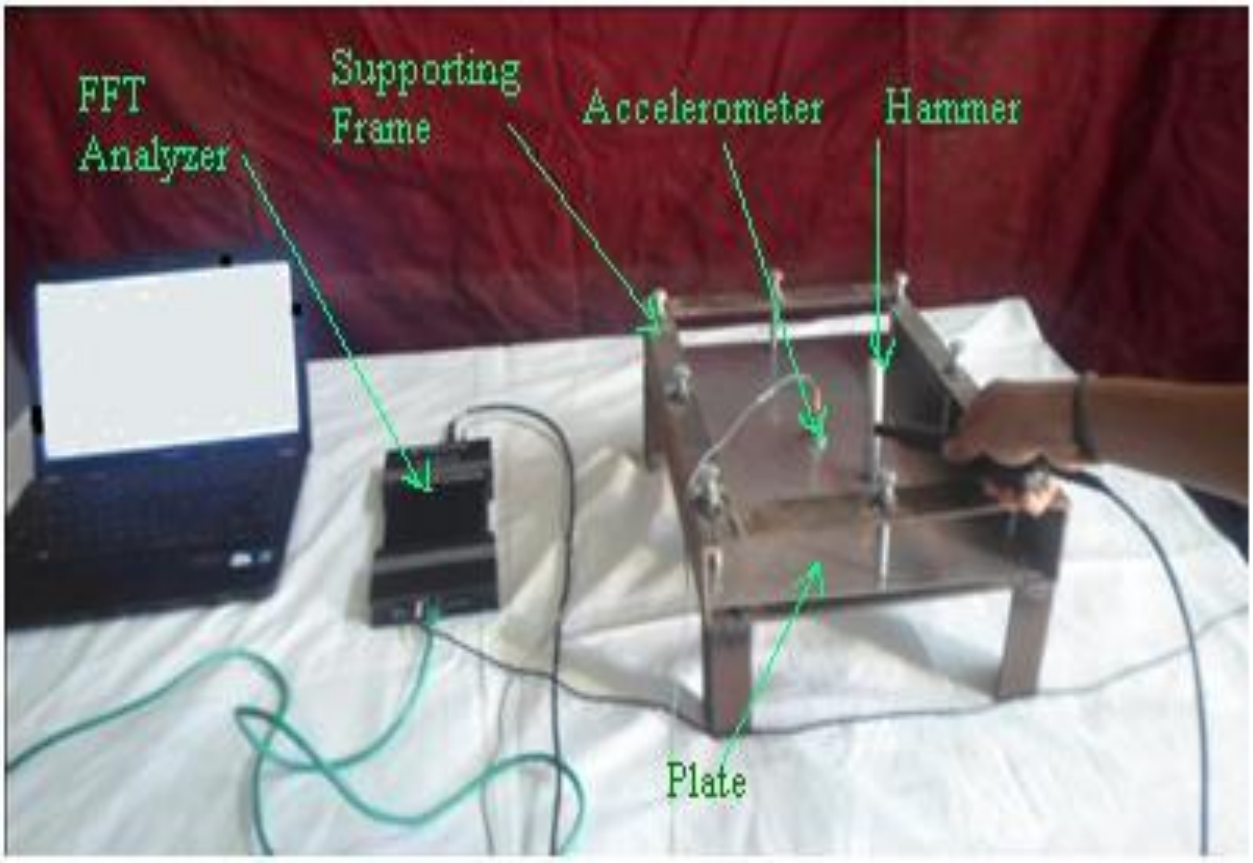


Figure 5.16 Experimental set up for simply supported plate

The results of damping loss factor and modal densities for simply supported plate are given in Table 5.6.1 and Table 5.6.2.

Table 5.6.1 DLFs of mild steel, aluminium and stainless steel for simply supported plate

| | Mild Steel | | Aluminium | | Stainless Steel | |
|---|---|---|---|---|---|---|
| Sr No. | Frequency (Hz) | Damping Loss Factor | Frequency (Hz) | Damping Loss Factor | Frequency (Hz) | Damping Loss Factor |
| 1 | 312.5 | 0.0284126 | 350 | 0.0462531 | 336 | 0.03689 |
| 2 | 550 | 0.0275644 | 650 | 0.034795 | 752 | 0.026554 |
| 3 | 1000 | 0.0261851 | 800 | 0.027147 | 1296 | 0.023781 |
| 4 | 1225 | 0.01852 | 1050 | 0.0290229 | 1776 | 0.016198 |
| 5 | 1938 | 0.013477 | 1575 | 0.026287 | 2912 | 0.007861 |
| 6 | 3400 | 0.007202 | 2800 | 0.008993 | 3600 | 0.006439 |
| 7 | 4013 | 0.006884 | 4112 | 0.006484 | 4288 | 0.007763 |
| 8 | 4875 | 0.005451 | 4838 | 0.007631 | 4992 | 0.005889 |

Table 5.6.2 Modal densities of mild steel, aluminium and stainless steel simply supported plate

| Sr.No. | Frequency (Hz) | Modal Densities | | |
|---|---|---|---|---|
| | | Mild steel | Aluminium | Stainless steel |
| 1 | 125 | 0 | 0 | 0 |
| 2 | 250 | 0.008 | 0.008 | 0.008 |
| 3 | 500 | 0.016 | 0.016 | 0.012 |
| 4 | 1000 | 0.014 | 0.018 | 0.014 |
| 5 | 2000 | 0.016 | 0.02 | 0.014 |
| 6 | 4000 | 0.014 | 0.018 | 0.016 |

Only one edge of the plate had fixed with the help of fixture for clamped-free plate. The same test specimens had used for this condition. The excitation to that plate had given by impact hammer and by using the FFT analyzer the data had recorded. The results of damping loss factor and modal densities for clamped-free plate are given in Table 5.6.3 and Table 5.6.4.

Table 5.6.3 DLFs of mild steel, aluminium and stainless steel clamped-free plate

| | Mild Steel | | Aluminium | | Stainless Steel | |
|---|---|---|---|---|---|---|
| Sr No. | Frequency (Hz) | Damping Loss Factor | Frequency (Hz) | Damping Loss Factor | Frequency (Hz) | Damping Loss Factor |
| 1 | 275 | 0.051221 | 312.5 | 0.075103 | 312.5 | 0.050459 |
| 2 | 575 | 0.02575 | 525 | 0.045477 | 1038 | 0.017367 |
| 3 | 850 | 0.023801 | 1100 | 0.030259 | 1500 | 0.016572 |
| 4 | 1300 | 0.013205 | 1775 | 0.023317 | 2288 | 0.01112 |
| 5 | 2163 | 0.019993 | 3250 | 0.01138 | 3025 | 0.009566 |
| 6 | 3625 | 0.009105 | 3913 | 0.006815 | 3825 | 0.007182 |
| 7 | 4438 | 0.006055 | 4537 | 0.006839 | 4125 | 0.006415 |
| 8 | 4763 | 0.004942 | 4763 | 0.005128 | 4650 | 0.00392 |

Table 5.6.4 Modal densities of mild steel, aluminium and stainless steel clamped-free plate

| Sr.No. | Frequency (Hz) | Modal Densities | | |
|---|---|---|---|---|
| | | Mild steel | Aluminium | Stainless steel |
| 1 | 125 | 0.024 | 0.024 | 0.024 |
| 2 | 250 | 0.024 | 0.024 | 0.024 |
| 3 | 500 | 0.016 | 0.016 | 0.012 |
| 4 | 1000 | 0.016 | 0.016 | 0.014 |
| 5 | 2000 | 0.014 | 0.016 | 0.014 |
| 6 | 4000 | 0.014 | 0.016 | 0.012 |

## 5.7 Results and discussion

Modal densities and damping loss factors of simply supported and clamped-free plates are compared for different materials. The materials used for plate are mild steel, aluminium and stainless steel.

### 5.7.1 Modal density of plates with different materials

For simply supported plates, experimental values of modal density are close to theoretical values of modal density for mild steel, stainless steel, aluminium as shown in Figure 5.17, Figure 5.18 and Figure 5.19. In simply supported boundary condition, all four edges of plates are clamped by tightening screw. So, all the six degree of freedom of composite plate are constrained. Due to this, first, six natural frequencies are zero. Therefore modal density at initial frequency range for simply supported plate is zero.

In cantilever boundary condition, one side of the plate is clamped. Due to this, first three natural frequencies of the cantilever plates are zero. So, the first mode occurs at little bit higher frequency than the free-free plate and modal density remains low and constant upto certain frequencies at initial frequency range.

At low frequencies, excitation of plate depends on the boundary condition of the plates. When the plates are excited at very high frequencies, the connection between plate and tightening element becomes flexible. Due to this, effect of boundary condition becomes negligible as the excitation frequency increases. Therefore the modal density of all types of boundary condition plates converges to a constant value.

When structure is having simply supported boundary condition, it should be excited in low-frequency range. The values of modal density are comparatively less in low-frequency range.

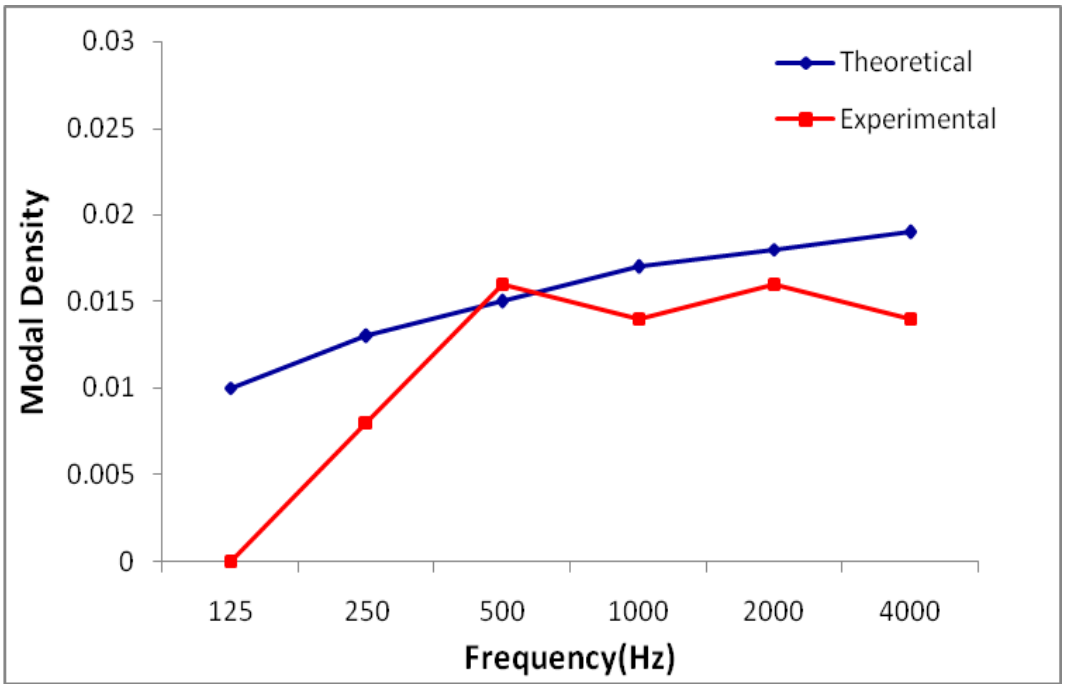


Figure 5.17 Modal density for simply supported mild steel plate

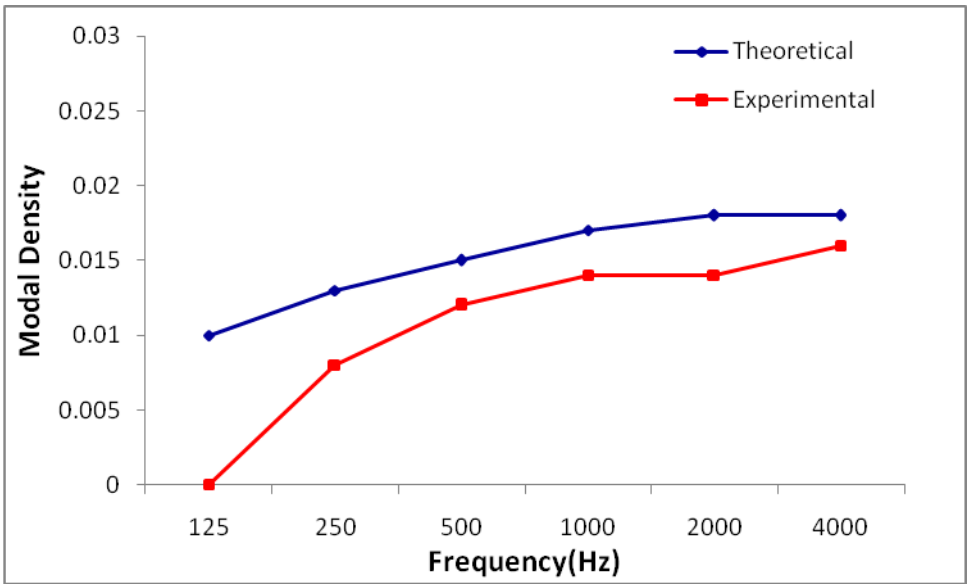


Figure 5.18 Modal density for simply supported stainless steel plate

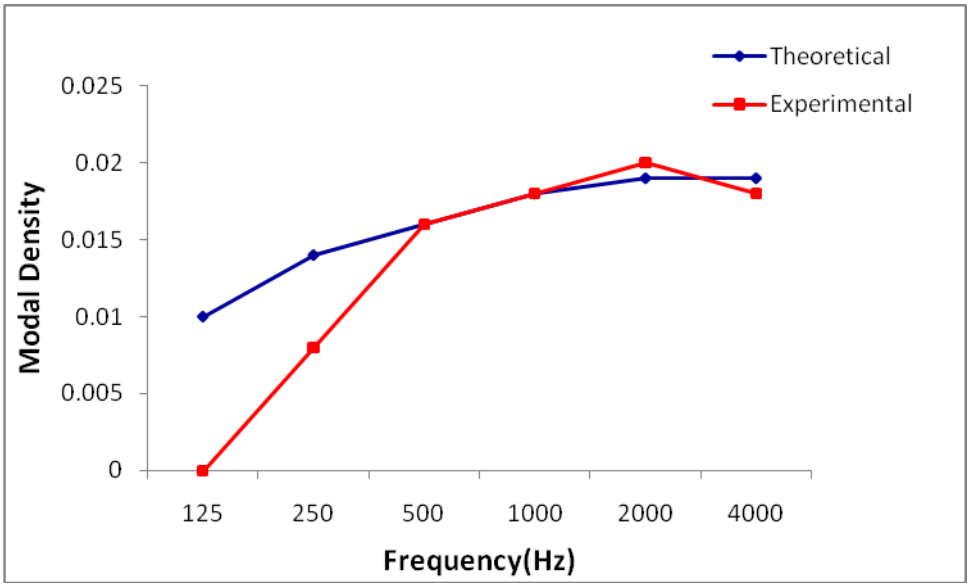


Figure 5.19 Modal density for simply supported aluminium plate

It has been observed from Figure 5.20 and Figure 5.21 that at lower frequency there is variation in modal densities for free-free, simply supported and clamped-free plates, but it converges to a constant value in mid and high frequency range. The values of modal density for free-free boundary condition are more than other boundary condition of plates. Instead of free-free boundary conditions of plate, it is better to use other boundary conditions of plate in practical situations because of lower values of modal densities.

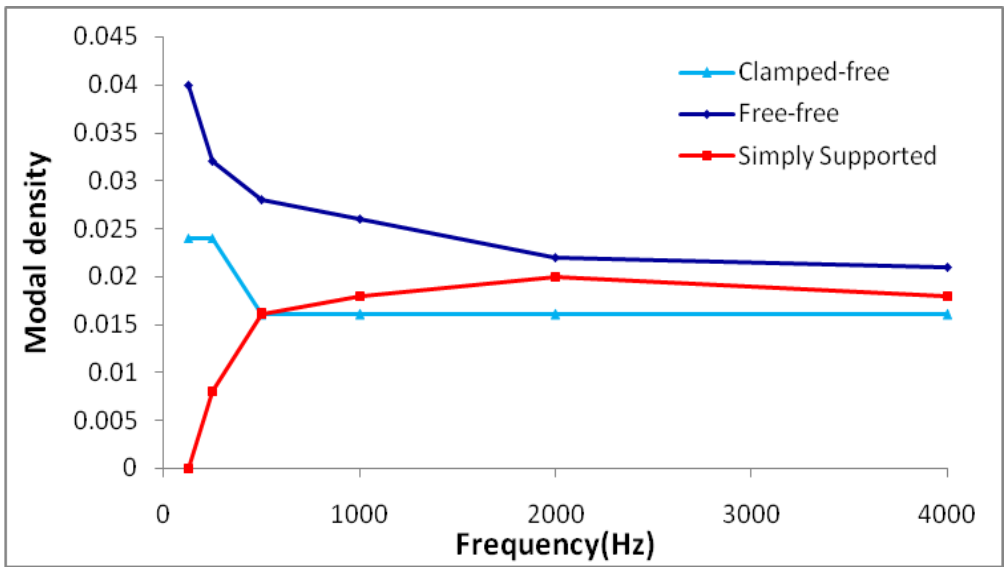


Figure 5.20 Experimental modal density of aluminium plate

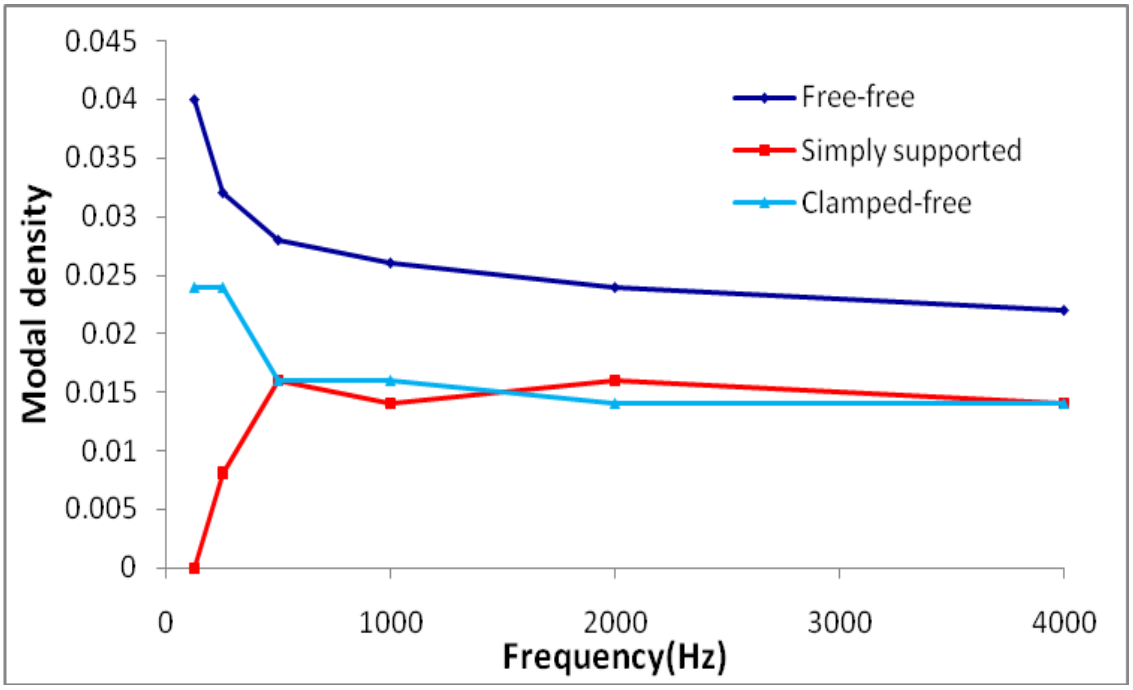


Figure 5.21 Experimental modal density of mild steel plate

### 5.7.2 Damping loss factor of plates with different materials

The results of damping loss factors are compared for mild steel, aluminium and stainless steel plates. The results are shown in Figure 5.22 and Figure 5.23. It has been observed that at lower frequencies the value of the damping loss factor drops significantly, while at higher frequencies it remains constant. Damping loss factor is less of mild steel plate as compared to aluminium and stainless steel plates for simply supported and clamped-free plates. Aluminium plate damps more vibration and acoustics energy in simply supported and clamped-free boundary condition. Damping loss factors are more for simply supported and clamped-free boundary condition than free-free boundary condition of plates.

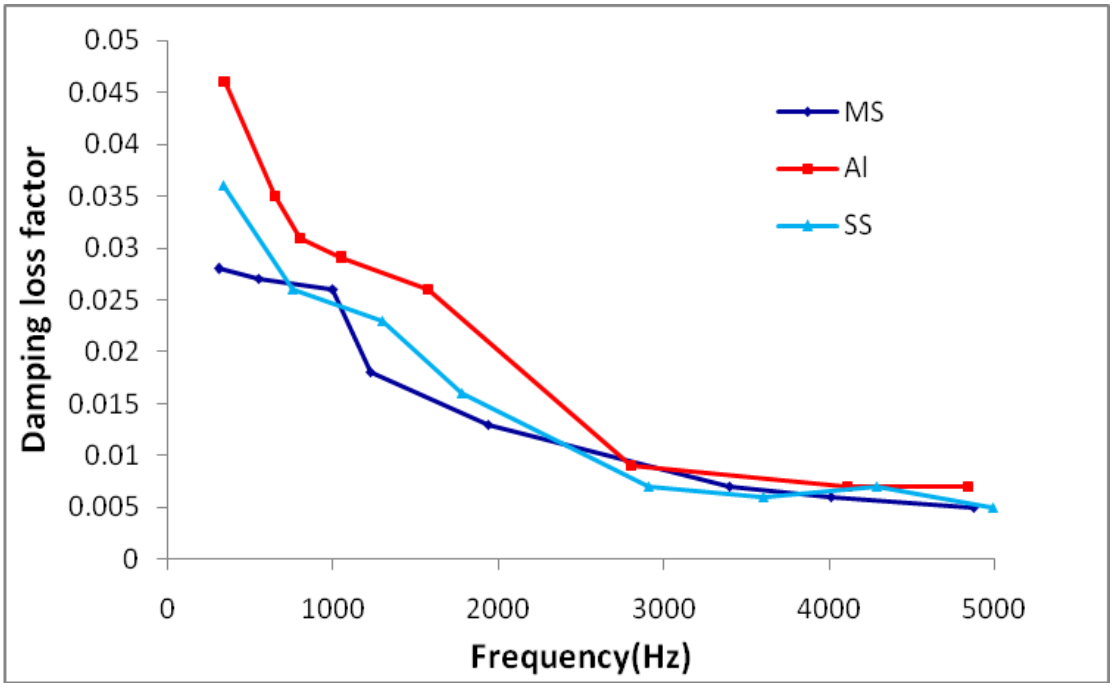


Figure 5.22 Damping loss factors for simply supported plates

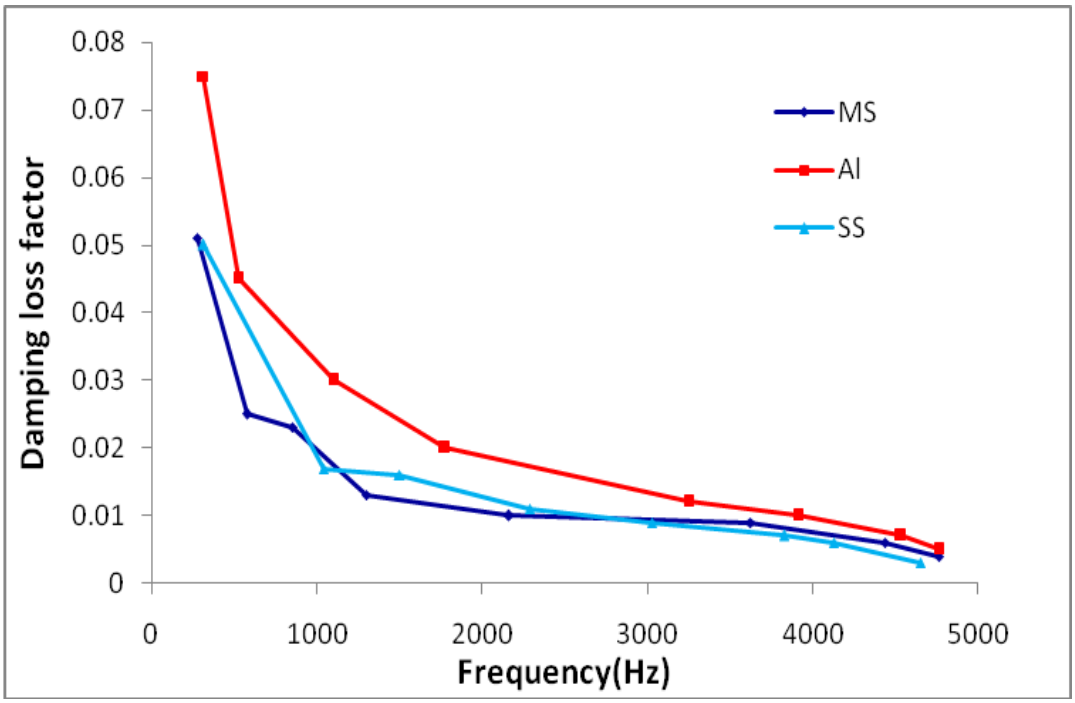


Figure 5.23 Damping loss factors for clamped-free plates

## 5.8 Closure

Experimental readings of damping loss factors and modal density have been taken for plate structure. It has been observed that the experimental readings have been recorded quite accurately and can be used for the further study. Discussions on experimental and theoretical outcomes have been presented.

# Chapter 6

# COUPLING LOSS FACTOR ESTIMATION FOR DIFFERENT STRUCTURAL JUNCTIONS OF IDEALIZED SUBSYSTEMS

## 6.1 Introduction

In this chapter, experimental procedure of estimating coupling loss factors for joined plates in same and perpendicular to each other have been explained. The experimental results of coupling loss factor for screwed and bolted junctions of aluminium plates are presented. Also the experimental values of coupling loss factors for riveted and bolted junctions of composite plates with different fibre orientation are presented. Hinge and line junctions for perpendicular beams have been experimentally tested for coupling loss factor and the results are compared with modal and wave approach. Effect of tightening torque on coupling loss factors for structural junctions of aluminium and composite plates have been presented.

## 6.2 Experimental procedure of estimating coupling loss factors for aluminium plates in same plane

Thin rectangular plates made up of aluminium with similar dimensions had joined with bolted junctions. These plates had connected to each other in same plane. The arrangement of instrumentation for determining coupling loss factor is shown in Figure 6.1. Joined plates had hung by nylon threads. A rigid frame had used for connecting one end of nylon thread. The impact hammer had used to apply the force on one of the plate. The accelerometers had mounted on the plates to capture the vibration signals of plates. Measurements had taken by changing the position of the accelerometers on the plates. The accelerometers had connected to data acquisition hardware. The data had processed by FFT analysis software and spectrums had observed in frequency domain and time domain. The torque range had used to apply the tightening torque at junction of the plates. Autospectrums

from four channels FFT Analyzer for 0.3 kgf-m tightening torque of two aluminium plates are shown in Figure 6.2 and Figure 6.3. Autospectrums for screwed junction of aluminium plates are shown Figure 6.4 and Figure 6.5.

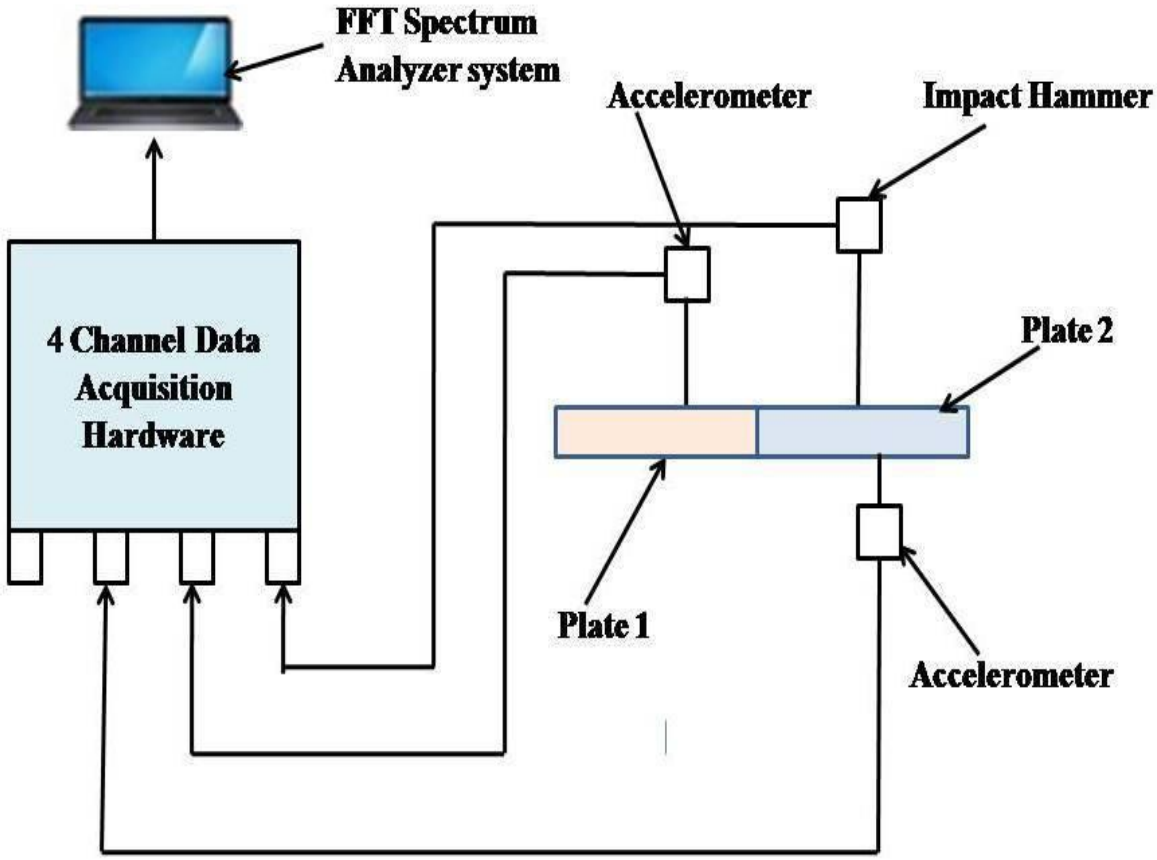


Figure 6.1 Arrangement of instrumentation for plates in same plane

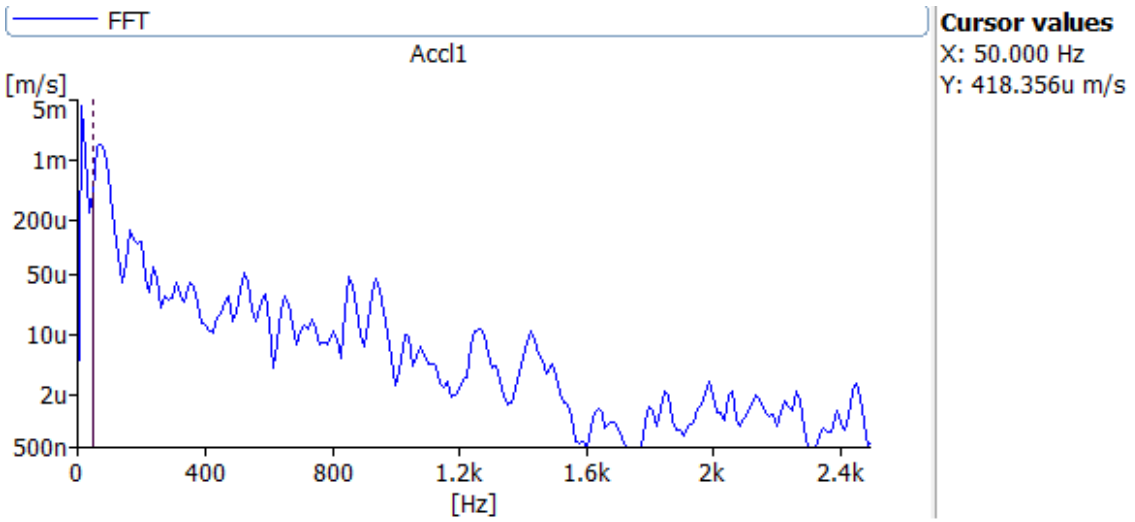


Figure 6.2 Autospectrum of screwed junction for plate 1

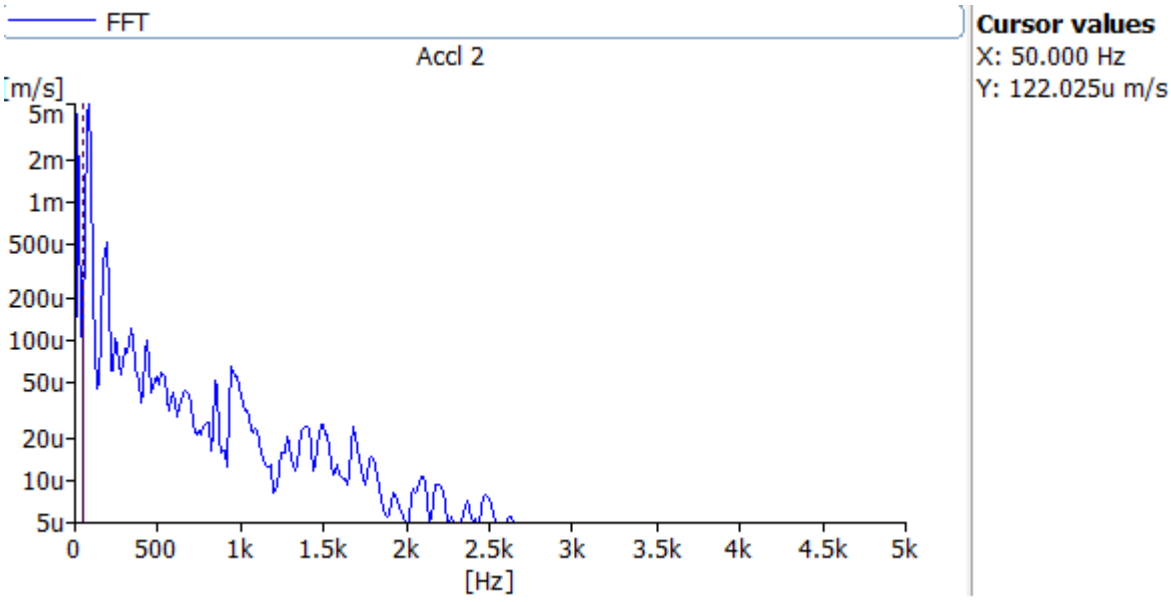


Figure 6.3 Autospectrum of screwed junction for plate 2

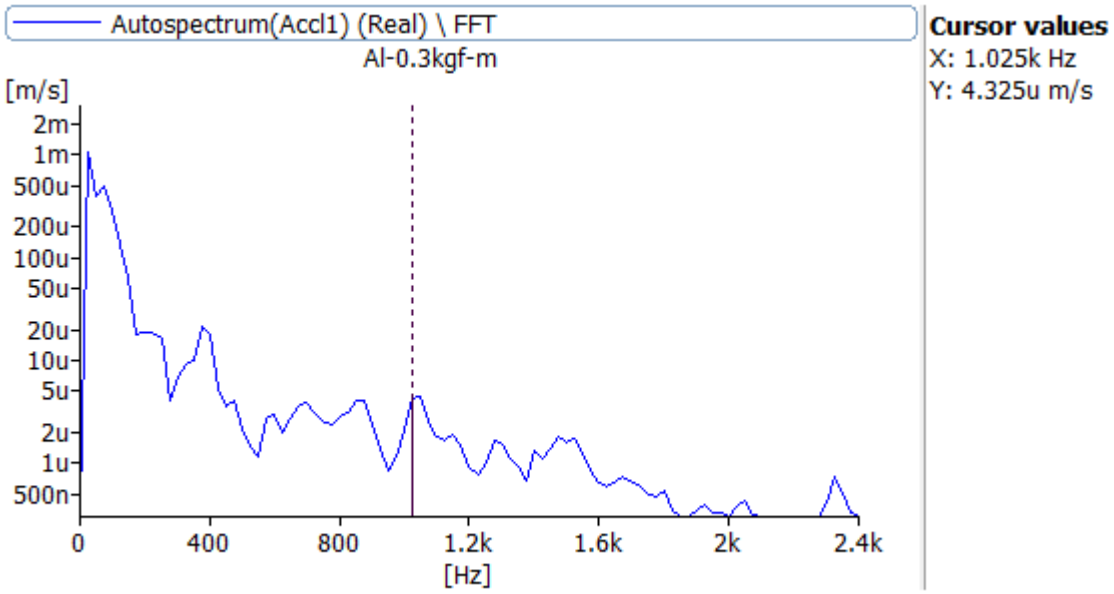


Figure 6.4 Autospectrum of bolted junction for plate 1

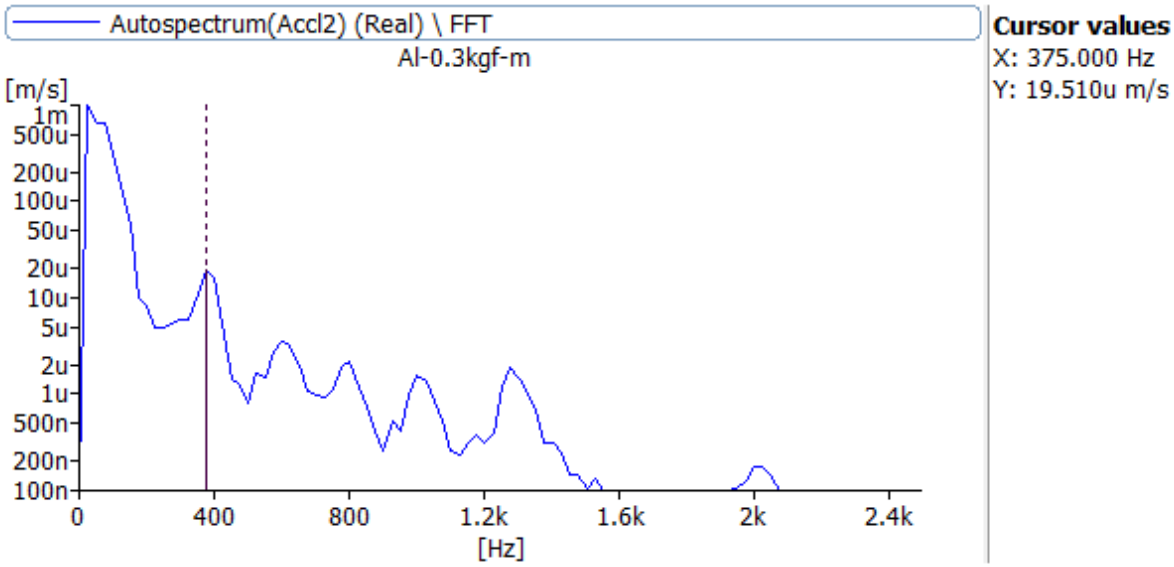


Figure 6.5 Autospectrum of bolted junction for plate 2

For estimating coupling loss factors of plates in same plane the energy level difference method is used. The vibration energy (E) is calculated corresponding to 50 Hz frequency. The values of velocity are taken from autospectrum of accelerometer 1 and 2 corresponding to 50 Hz frequency. The damping loss factor is estimated by half power bandwidth method. The values of coupling loss factors for aluminium plates connected by screwed and bolted junctions with different torque are presented in Table 6.2.1 and Table 6.2.2. The sample calculations for the value of coupling loss factor is given as,

$$E_2 = M\left\langle V^2 \right\rangle$$
$$E_2 = (0.648)\left(1.2203\times10^{-4}\right)^2$$
$$E_2 = 9.6496\times10^{-9}\,J$$
$$E_1 = 1.1342\times10^{-7}\,J$$
$$\eta_{12} = \eta_2 \frac{E_2}{E_1}$$
$$\eta_{12} = 0.5759\left(\frac{9.6496\times10^{-9}}{1.1342\times10^{-7}}\right)$$
$$\eta_{12} = 0.049$$

Table 6.2.1 Coupling loss factors for aluminium plates in same plane for screwed and bolted junctions

| Sr.No. | Frequency(Hz) | Expt.values of coupling loss factor | |
|---|---|---|---|
| | | Screwed junction | Bolted junction |
| 1 | 50 | 0.049 | 0.065 |
| 2 | 300 | 0.032 | 0.04 |
| 3 | 537.5 | 0.021 | 0.036 |
| 4 | 650 | 0.01 | 0.018 |
| 5 | 1325 | 0.001 | 0.001 |

Table 6.2.2 Coupling loss factors for aluminium plates in same plane for bolted junctions with different tightening torque

| Sr. No. | Frequency (Hz) | Expt.values of CLF for 0.9 Kgf-m tightening torque | Expt.values of CLF for 0.3 Kgf-m tightening torque |
|---|---|---|---|
| 1 | 350 | 0.009 | 0.008 |
| 2 | 900 | 0.0015 | 0.001 |
| 3 | 1075 | 0.0014 | 0.001 |
| 4 | 1475 | 0.0009 | 0.00033 |
| 5 | 2100 | 0.0009 | 0.0003 |

## 6.3 Experimental procedure of estimating coupling loss factors for composite plates in same plane

Thin composite rectangular plates had joined with different types of junctions in same plane. To determine coupling loss factors, arrangement for experimentation is shown in Figure 6.6. The structural junctions of composite plates are shown in Figure 6.7. Bolted and riveted junctions of composite plates in same plane had tested. Joined plates had hung by nylon threads. The tightening torques applied at bolted junctions of each composite plate had 0.3 kgf-m and 0.7 kgf-m. Impact hammer had used to apply the force on one plate. The responses of the plates had measured by accelerometers. For evaluating the vibration energy stored in each plate, measurements had taken at different locations of each composite plate. For frequency spectrums, the data had transferred from accelerometer to FFT analysis software. Autospectrums for bolted junctions with 0.3 kgf-m tightening torque of composite plates are shown in Figure 6.8 and Figure 6.9. The coupling loss factors are estimated using the equation (42) for composite plates in same plane. The results of coupling loss factors for composite plates are presented in Table 6.3.1, Table 6.3.2 and Table 6.3.3.

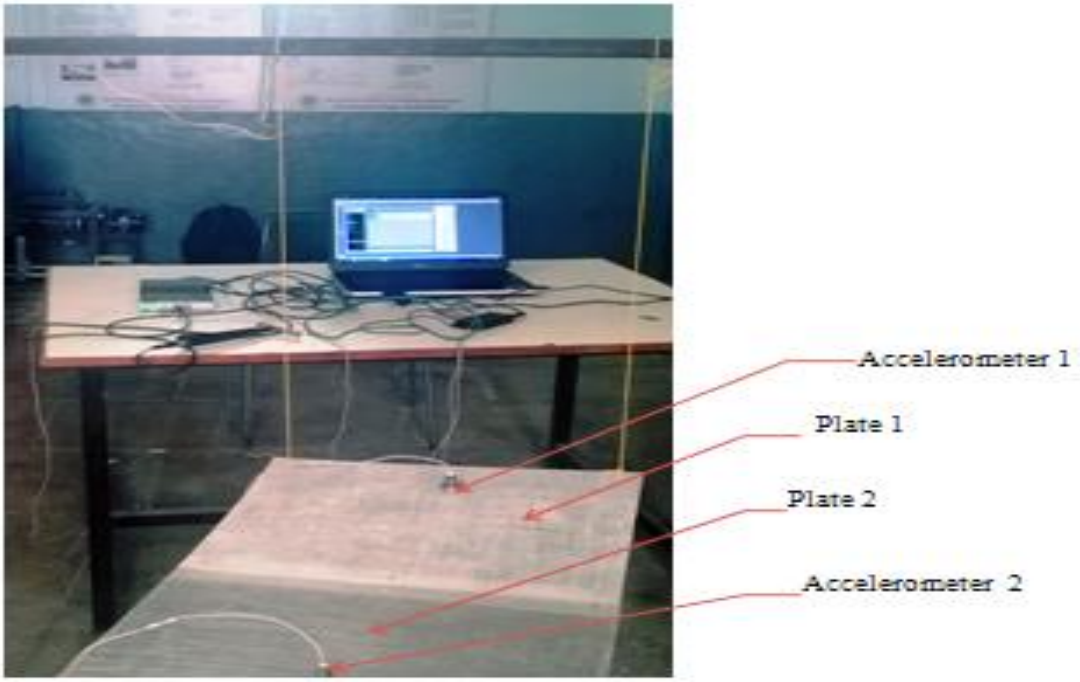


Figure 6.6 Experimental set up of composite plates in same plane

Table 6.3.1 Coupling loss factors for composite plates of bolted and riveted junctions in same plane

| Sr. No. | Freq. (Hz) | Theoretical values of CLF for composite plates | Freq. (Hz) | Expt.values of CLFs for E-1 (Unidirectional) Bolted junction | Freq. (Hz) | Expt.values of CLFs for E-1 (Unidirectional) Riveted junction |
|---|---|---|---|---|---|---|
| 1 | 240 | 0.05139 | 200 | 0.03596 | 176 | 0.01632 |
| 2 | 500 | 0.02467 | 925 | 0.01145 | 672 | 0.001421 |
| 3 | 1000 | 0.012333 | 1550 | 0.010363 | 1456 | 0.000472 |
| 4 | 3000 | 0.004111 | 2800 | 0.001 | 2912 | 0.000129 |

Table 6.3.2 Coupling loss factors for composite plates of different fiber orientations in same plane connected by bolted junction

| Sr.No. | Freq. (Hz) | Expt.values of CLFs for E-1 (Unidirectional) Bolted junction | Freq. (Hz) | Expt.values of CLFs for E-2 (Quasi isotropic) Bolted junction | Freq. (Hz) | Expt.values of CLFs for E-3 (Cross ply) Bolted junction |
|---|---|---|---|---|---|---|
| 1 | 25 | 0.0902 | 25 | 0.0597 | 25 | 0.13157 |
| 2 | 200 | 0.03596 | 400 | 0.001956 | 350 | 0.04119 |
| 3 | 925 | 0.01145 | 1150 | 0.001391 | 650 | 0.0115 |
| 4 | 1550 | 0.010363 | 1625 | 0.0057786 | 1575 | 0.00274 |
| 5 | 2800 | 0.001 | 2800 | 0.00032157 | 2850 | 0.001268 |

Table 6.3.3 Coupling loss factors for unidirectional composite plates in same plane with different tightening torque.

| Sr.No. | Freq. (Hz) | Expt.values of CLFs for E-1 Bolted junction (0.7 Kgf-m) | Freq. (Hz) | Expt.values of CLFs for G-1 Bolted junction (0.7Kgf-m) | Freq. (Hz) | Expt.values of CLFs for E-1 Bolted junction (0.3Kgf-m) |
|---|---|---|---|---|---|---|
| 1 | 25 | 0.0902 | 25 | 0.02046 | 25 | 0.0321 |
| 2 | 200 | 0.03596 | 350 | 0.00104 | 250 | 0.012857 |
| 3 | 925 | 0.01145 | 875 | 0.001544 | 950 | 0.000161 |
| 4 | 1550 | 0.010363 | 1525 | 0.00152 | 1575 | 0.000197 |
| 5 | 2800 | 0.001 | 2650 | 0.0014 | 2675 | 0.002896 |

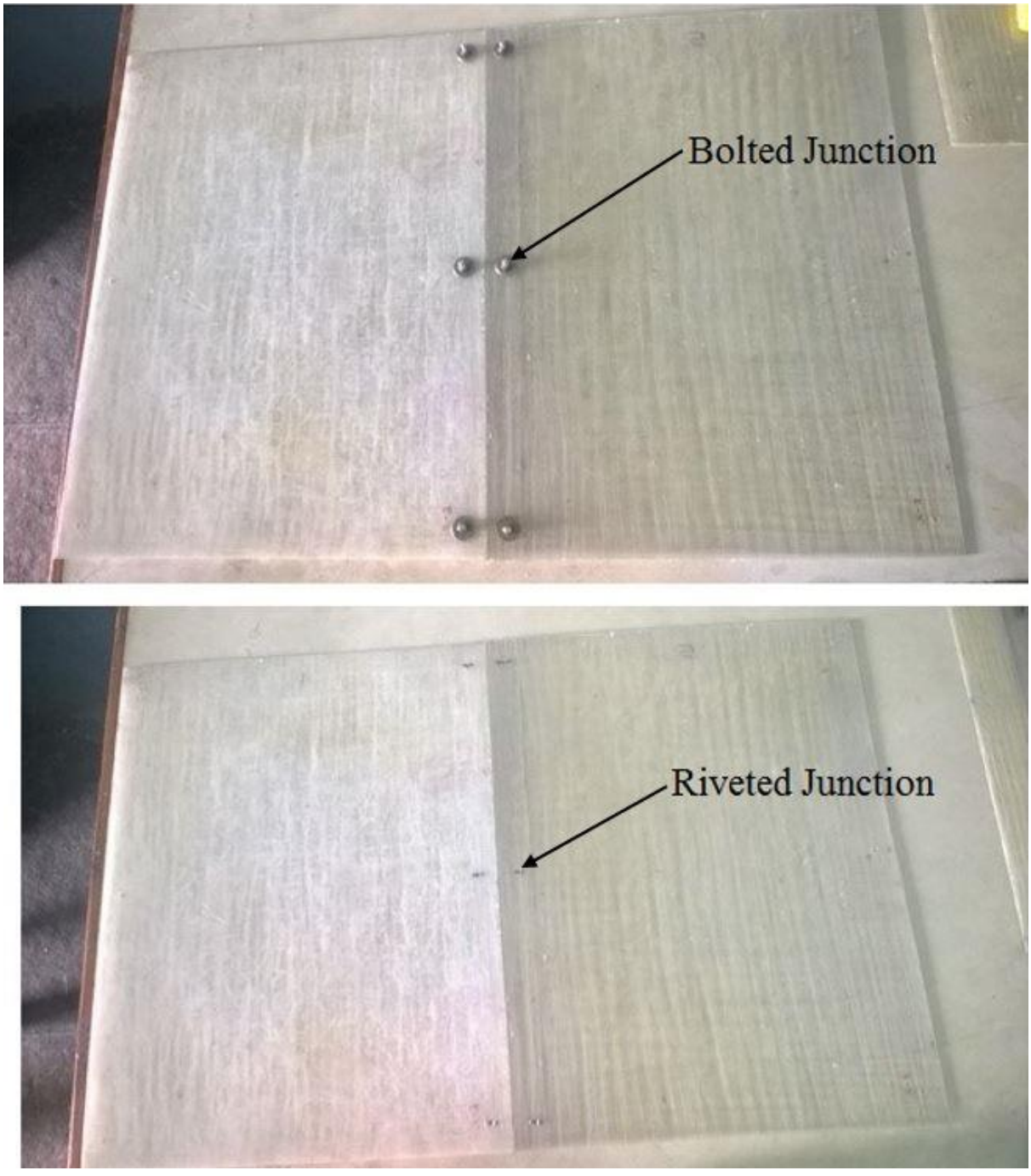


Figure 6.7 Bolted and Riveted junctions for composite plates

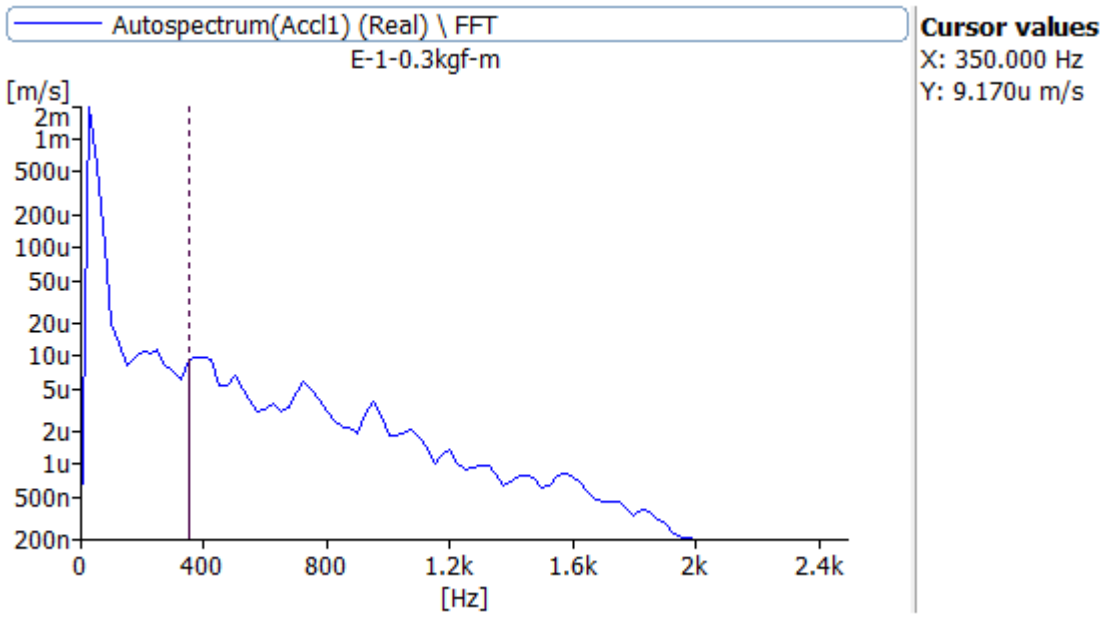


Figure 6.8 Autospectrum of unidirectional composite plates with 0.3 kgf-m tightening torque for plate 1

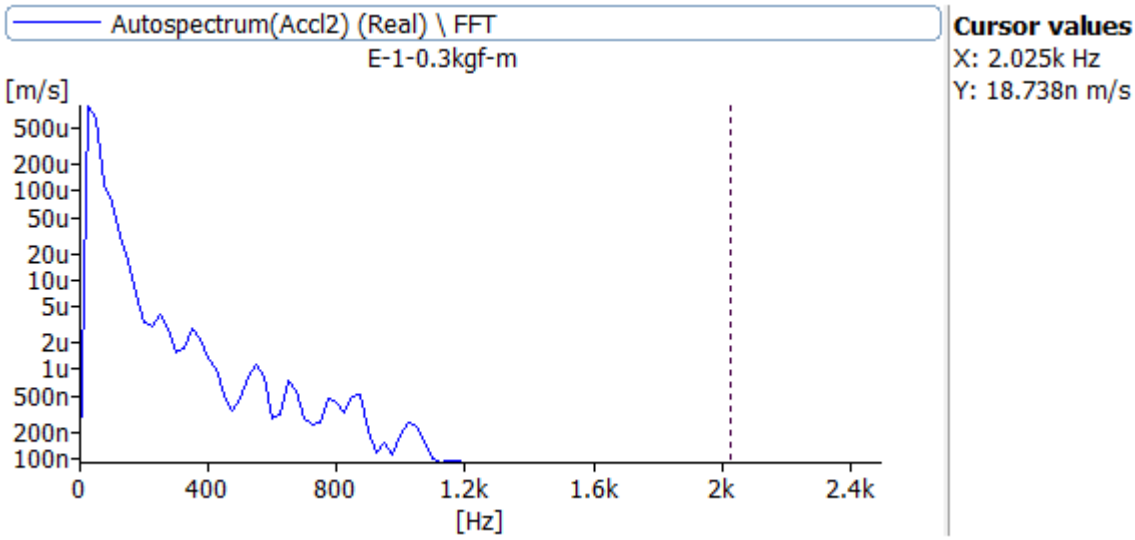


Figure 6.9 Autospectrum of unidirectional composite plates with 0.3 kgf-m tightening torque for plate 2

### 6.4 Results and discussion

Reliability of statistical energy analysis models depends on good estimate of coupling loss factors. In statistical energy analysis, subsystems coupling between them are represented by coupling loss factors. Coupling loss factor is a unique parameter at statistical energy analysis and is connected with a central statistical energy analysis result; the average power flow between the groups of coupled modes is proportional to the difference of the average modal energies of the groups of modes. To predict noise and vibration levels of a product at the design phase, CLF plays an important role. For some simple cases, coupling loss factor can be theoretically calculated. However, for most practical situations, mainly for those including different structural junctions such as screwed, bolted, riveted etc., they cannot be calculated theoretically and must be obtained from experimental measurements.

#### 6.4.1 Screwed and bolted junctions of aluminium plates

It has been observed that for line connected plates coupling loss factors are more than for point connected plates. But for point connections, there is use of bolts, screws, rivets, hinges and spot welding. It is difficult to predict coupling loss factors of structures joined with different point connections. Two aluminium plates connected by screw and bolt joints have been experimentally tested.

Results shown in Figure 6.10 reveal that the theoretically estimated values of CLF for point junctions are closer to the experimental values of both screw and bolt junctions. Whenever there is increase in connecting points either by screw or bolt, the values of CLF increased. It means that point connections are tending towards the line connections.

Two plates connected in same plane shows that screwed junction have lower values of coupling loss factor for screwed junction than bolted junction. A reason for this difference is the tightening force effect in between two plates at junctions.

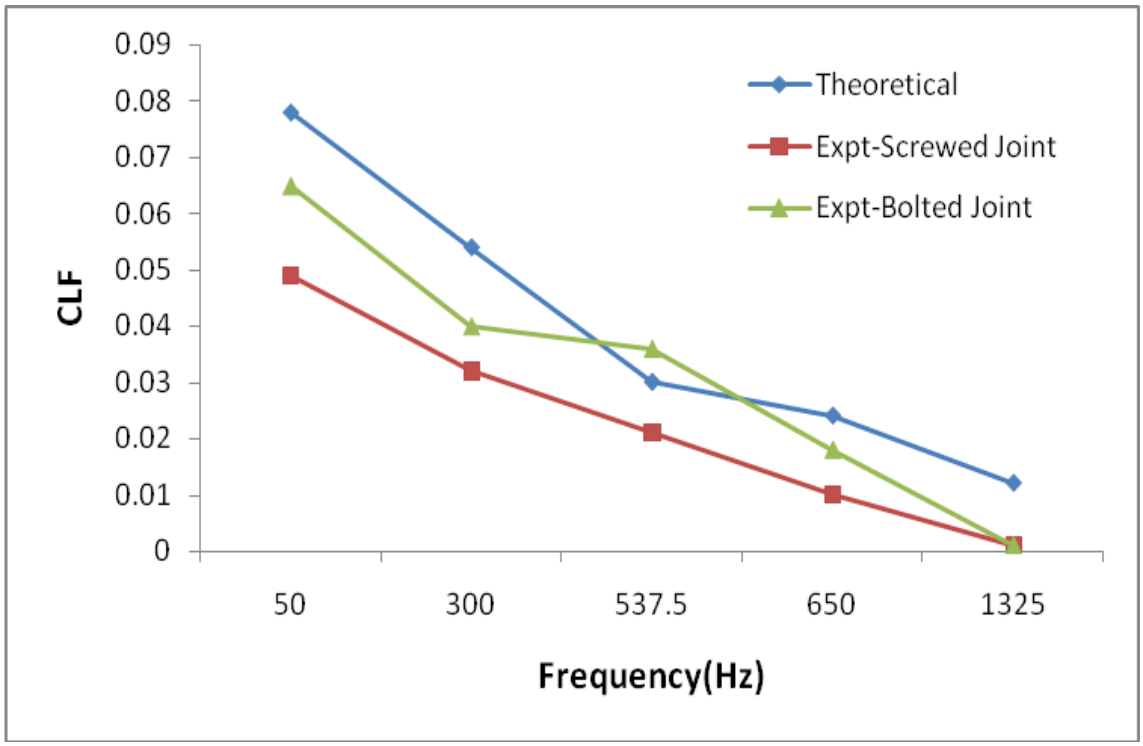


Figure 6.10 Comparison of theoretical and experimental results of CLFs for Aluminium plates in same plane

### 6.4.2 Effect of tightening torque on bolted junction of aluminium plates

The plates of aluminium have been joined with bolted junctions in same plane. Experimentally estimated coupling loss factors for bolted junctions with different torque are shown in Figure 6.11. The values of coupling loss factor for 0.9 kgf-m torque are relatively high than 0.3 kgf-m torque for bolted junction of plates. This is because of the stiff connection between two plates.

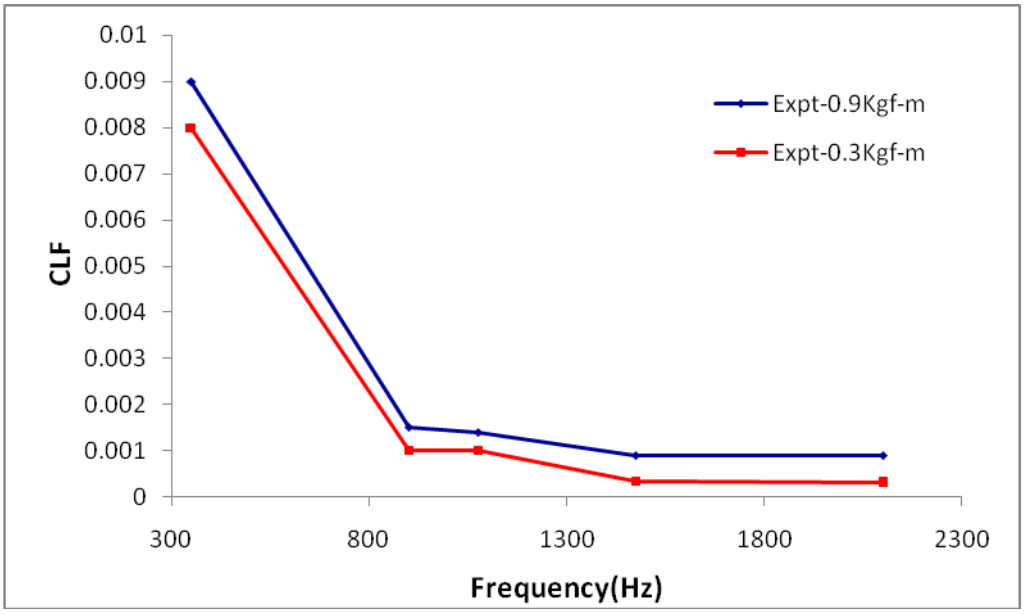

Figure 6.11 Comparison of experimental results of CLFs for different torque at junction of Aluminium plates

### 6.4.3 Bolted and riveted junctions composite plates

Plates made up of composite materials with different fibre orientation have been experimentally tested. Results shown in Figure 6.12, reveal that the values of coupling loss factor for bolted junction (E-1B) are more than riveted junction (E-1R). The coupling loss factors of composite plates with different fibre orientation are compared in Figure 6.13. It is found that the tightening torque applied at structural junctions affects the values of coupling loss factor. It increases with increase in tightening torque applied at bolted junction for plates connected in same plane. It has been observed from Figure 6.14 that at higher tightening torque (0.7 Kgf-m}, the values of coupling loss factor are more than lower torque (0.3 Kgf-m) . Also because of graphene addition in plate material, coupling loss factors are relatively decreases as shown in Figure 6.15. The examined connection shows lower values of coupling loss factor for riveted junction as compared to bolted junction.

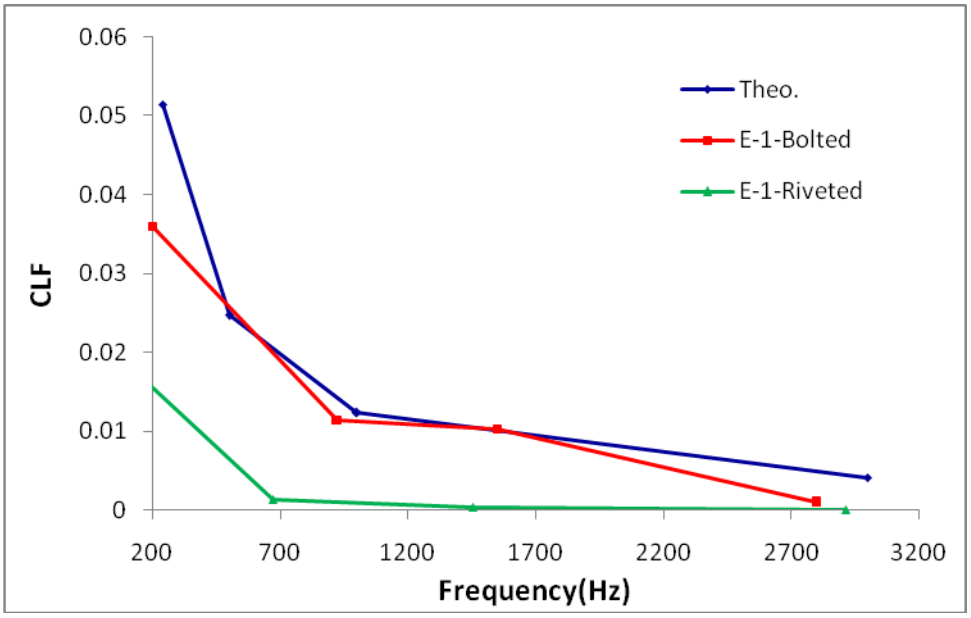


Figure 6.12 Coupling loss factors for bolted (E-1B) and riveted (E-1R) junction of composite plate.

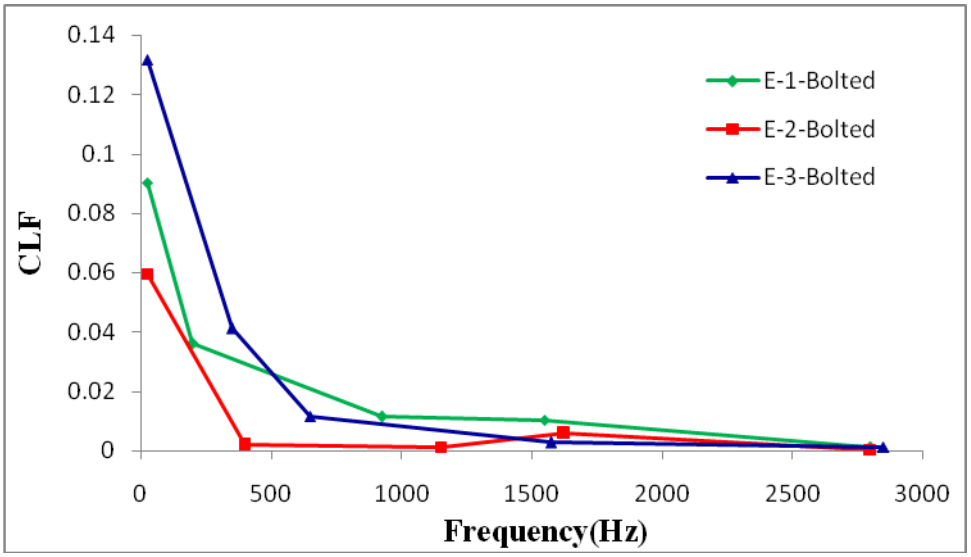


Figure 6.13 Coupling loss factors for different fibre orientation of composite plates with bolted junction

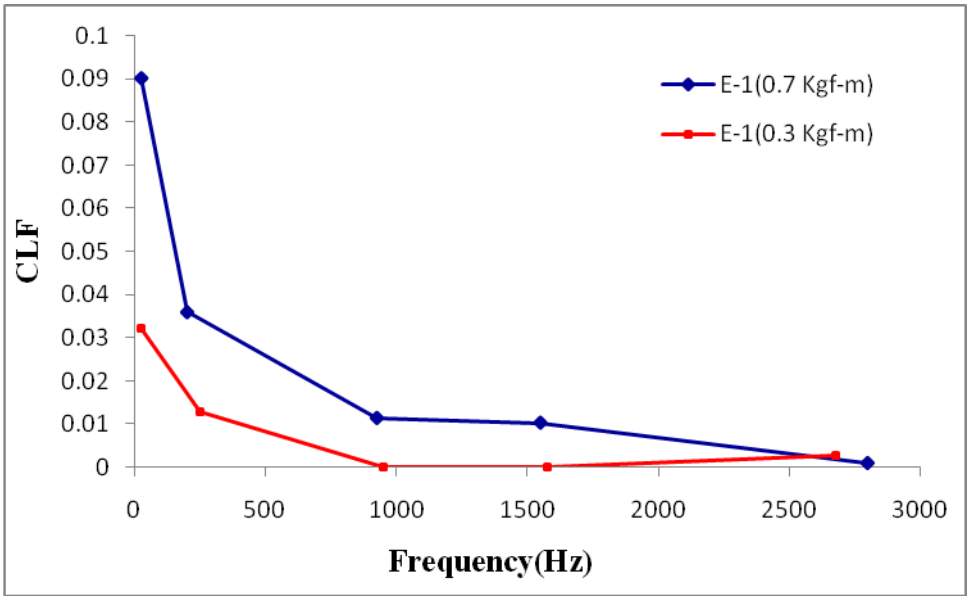


Figure 6.14 Effect of tightening torque on coupling loss factors for unidirectional composite plates

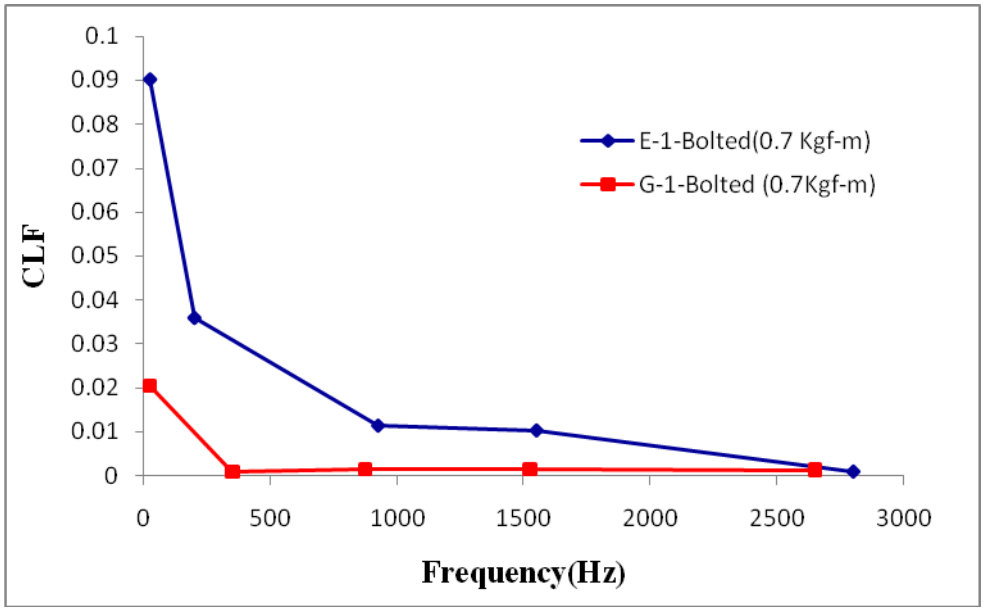


Figure 6.15 Effect of graphene on coupling loss factors for unidirectional composite plates

## 6.5 Experimental procedure of estimating coupling loss factors for aluminium plates in perpendicular plane

Thin aluminium rectangular plates had joined with different types of junctions and they had perpendicular to each other as shown in Figure 6.16. Two important types of junctions i.e. screwed and bolted had tested. Arrangements of instrumentation for perpendicular aluminium plates are shown in Figure 6.17.These joined plates had hung by nylon threads. One end of nylon thread had connected to a frame. About 150 kg weight had kept at each bottom end of frame, because of this frame becomes more rigid. The force had applied to one of the plate by impact hammer. The responses of the plates had measured by accelerometers. Both signals from accelerometers had connected to an FFT Analyzer. Systematic measurements had carried out at different locations for evaluating the vibration energy stored in each plate by using RMS amplitudes of velocities. To process the data, it had transferred from data acquisition hardware to FFT analysis software. The dimensions of aluminium plates were (400mm x 300mm x 2mm).The modulus of elasticity and density of chosen materials had 69 GPa and 2700 $Kg/m^3$. The bolted joints of aluminium plates are shown in Figure 6.18. The values of coupling loss factors of aluminium plates in perpendicular plane are presented in Table 6.5.1.

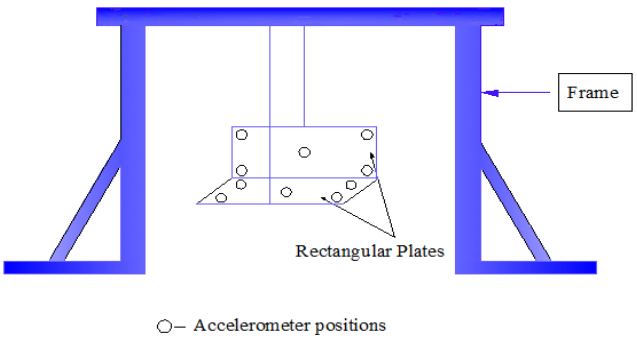


Figure 6.16 Experimental arrangements for perpendicular plates

Table 6.5.1 Coupling loss factors for aluminium plates in perpendicular plane with bolted and screwed junctions.

| Sr.No. | Frequency (Hz) | Theoretical values of CLF for Aluminium plates | Experimental values of CLF for Aluminium plates | |
|---|---|---|---|---|
| | | | Screwed junction | Bolted j junction |
| 1 | 50 | 0.07 | 0.04 | 0.05 |
| 2 | 300 | 0.05 | 0.04 | 0.07 |
| 3 | 537.5 | 0.03 | 0.01 | 0.03 |
| 4 | 650 | 0.02 | 0.01 | 0.01 |
| 5 | 1325 | 0.01 | 0.001 | 0.001 |

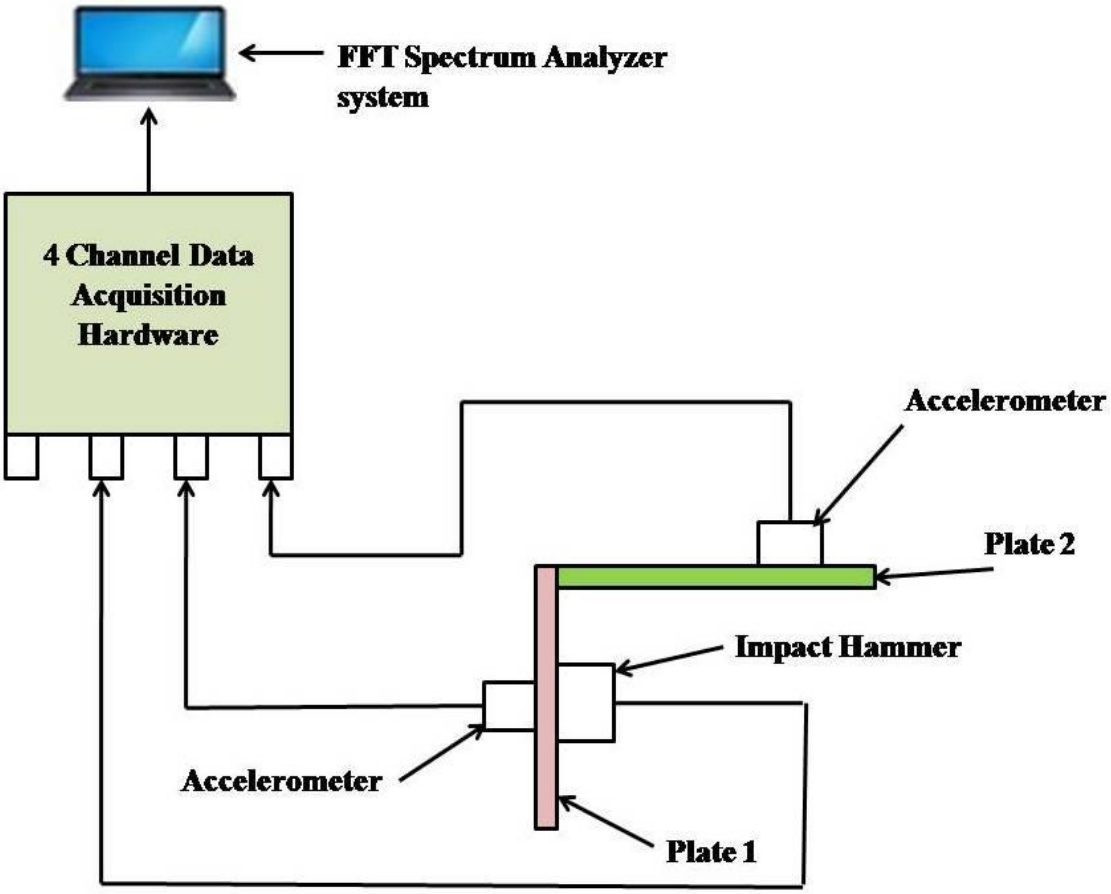


Figure 6.17 Arrangement of instrumentation for perpendicular plates


Figure 6.18 Bolted junctions for aluminium plates

### 6.6 Results and discussion

In engineering structures, structural junctions are considered a vital part because of its functionality to join and assemble the members of structure. Due to this selection of fastening techniques such as riveting, welding and bolting is important. The critical problem in mechanical structures is vibration which concern to failure of joint. So it is important to understand and know the structural junctions behavior.

#### 6.6.1 Screwed and bolted junctions of aluminium plate

In Figure 6.19 comparison of experimental results for screwed junction and bolted junction are shown. The examined connection shows lower values of CLF for screwed junction as compared to bolted junction. It has been observed from Figure 6.19 that at higher frequency the values of coupling loss factor for both screwed and bolted junctions in perpendicular plates coming close to each other. A reason for this difference is the tightening force effect in between two plates at junctions.

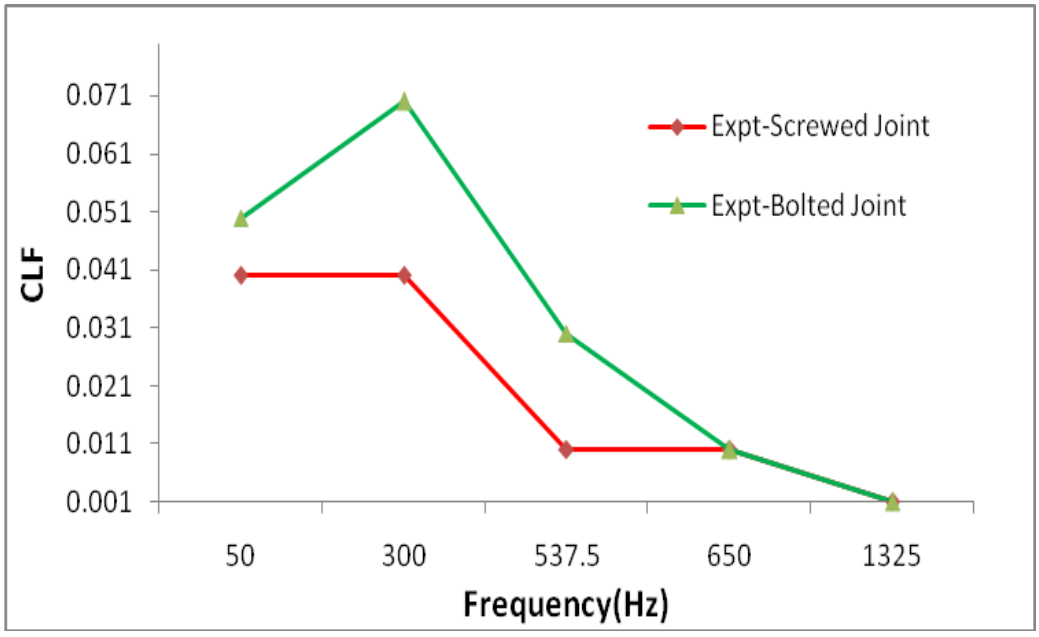


Figure 6.19 Comparison of experimental results of CLFs for perpendicular Aluminium plates

## 6.7 Experimental procedure of estimating coupling loss factors for perpendicular beams

Figure 6.20 shows the structure under test, which consists of two beams connected in such a way to form L-beam. Two beams had made of the same material, mild steel. The cross sectional dimensions of beams are 26mm x 26mm.The excitation force had applied by exciter, which had driven by a random vibration signal covering 0-5000Hz frequency range. Load cell had connected at the end of exciter for measuring the force applied on structure. The force had controlled by the oscillator.

Piezoelectric accelerometers had mounted on beams. All acceleration signals had measured by accelerometers. Bruel and Kjaer 4 channel FFT analyzer had used for measuring frequency domain and time domain spectrums. The L-beam had freely suspended on flexible supports, in order to get as close as possible to the free-free boundary condition

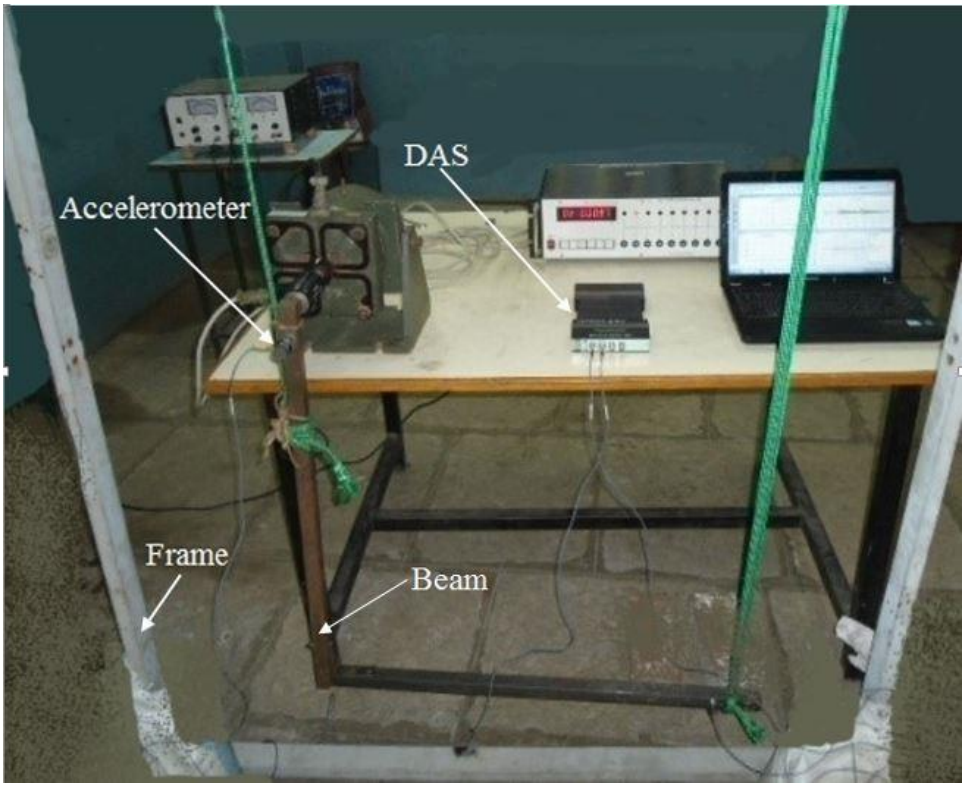


Figure 6.20 Experimental setup for beam

Two beams had joined perpendicular to each other with hinged junctions. The L-beam structure with hinged junction had excited from top side by using Exciter. The amplitude and force had controlled by oscillator. The load cell which had connected at the tip of exciter, was being used for measuring the load. Top beam had considered as a subsystem ‘p’ and bottom beam as a subsystem ‘s’. Both accelerometers had connected to four channel FFT analyzer. Systematic measurement of all sets of the examined beam connections had carried out. The accelerometer at top beam had driving accelerometer and at bottom it had driven accelerometer. The frequency spectrum for top excited beam is shown in Figure 6.21 and Figure 6.22. In Figure 6.23 and Figure 6.24 bottom excited frequency spectrum are shown. The power injection method is used for estimating coupling loss factors of perpendicular beams with line and hinge junctions.

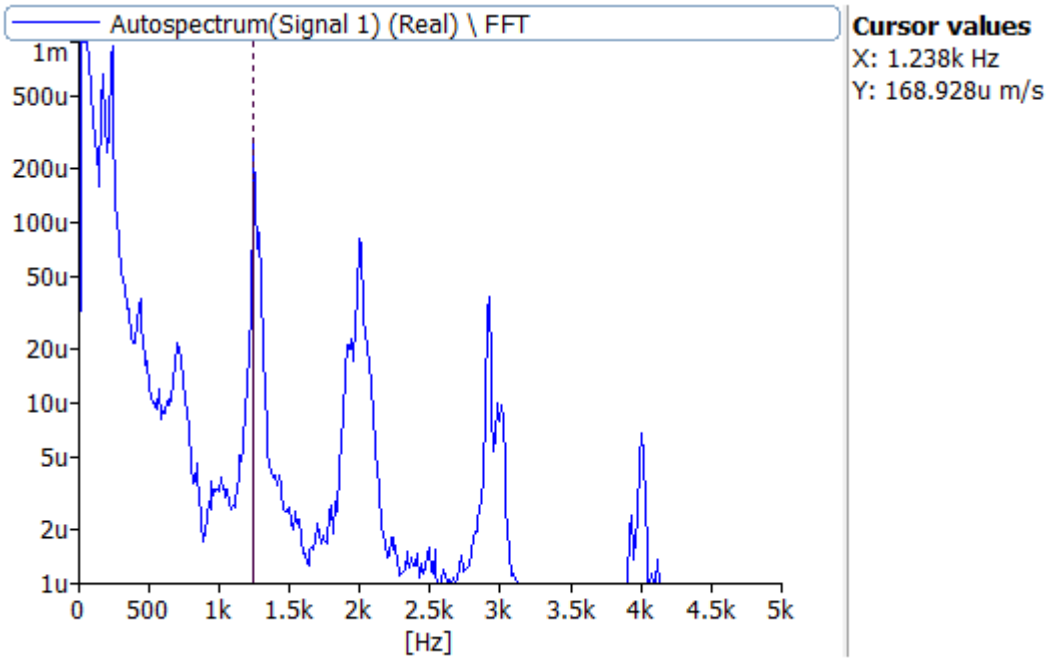


Figure 6.21 Autospectrums for top excited beam -Signal1 (Driven)

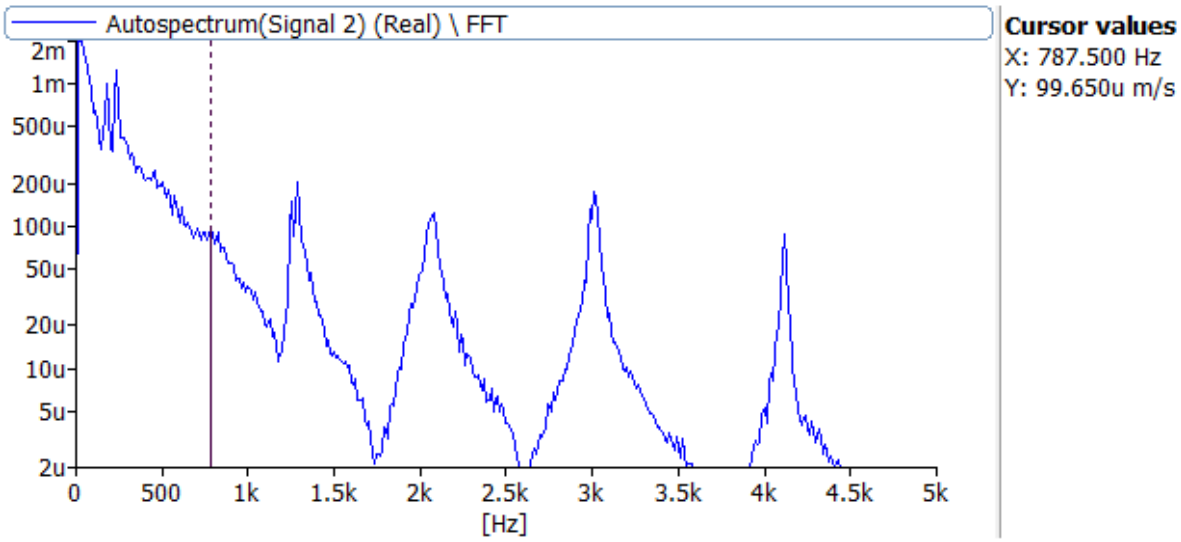


Figure 6.22 Autospectrums for top excited beam-Signal2 (Driving)

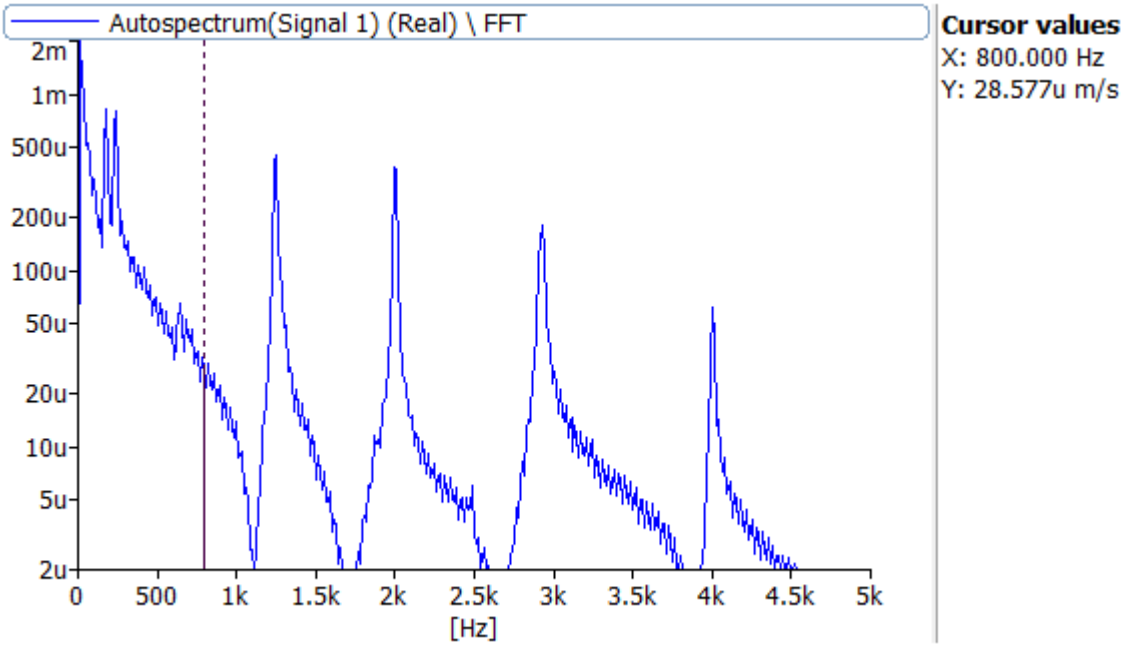


Figure 6.23 Autospectrums for bottom excited beam-signal1-(Driving)

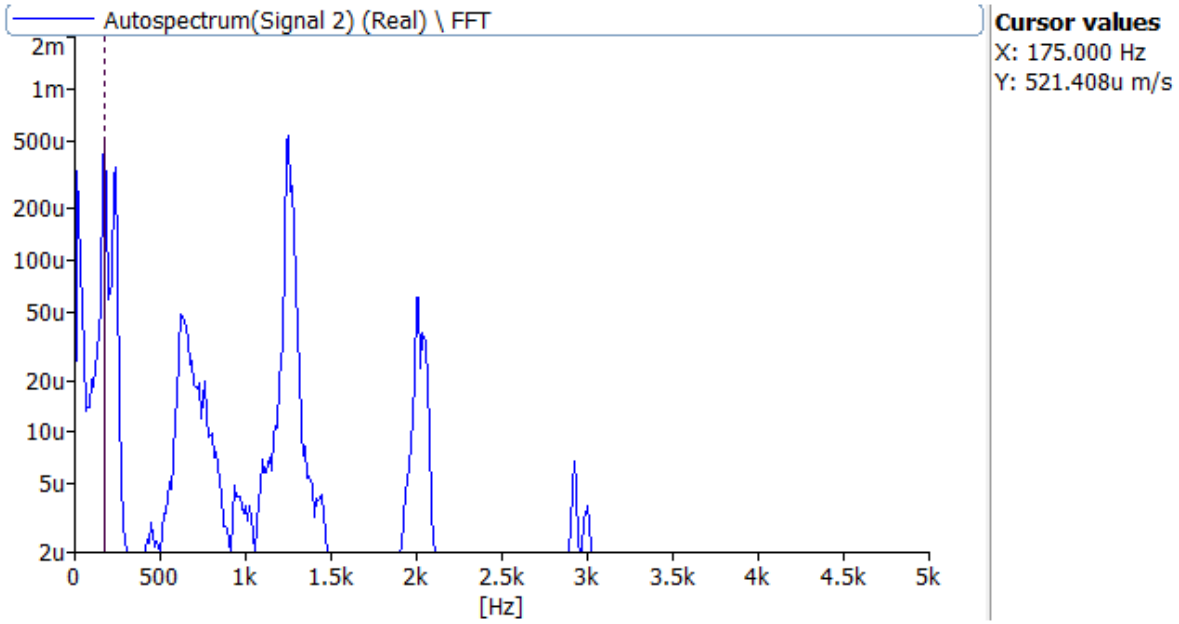


Figure 6.24 Autospectrums for bottom excited beam signal2 (Driven)

## 6.8 Results and discussion

Mechanical structures are divided into beam or plate elements for vibro-acoustic analysis. Beam structures are joined with different types of joints. So it is necessary to compare different structural junctions of beam for vibro-acoustic analysis.

### 6.8.1 Line and hinge junctions of perpendicular beams

Two beams joined perpendicular to each other by line and hinge joints. The CLF values are shown in Figure 6.25 for two perpendicular beams. Theoretical values have been calculated by wave and modal approach. Power injection method has been used for determining CLFs of line and hinge joints of two beams connected perpendicular to each other. From Figure 6.25, it is clear that CLF values for hinge joints are less than line joints. It indicates that more energy is reflected in hinge joints as compared to line joints for beams.

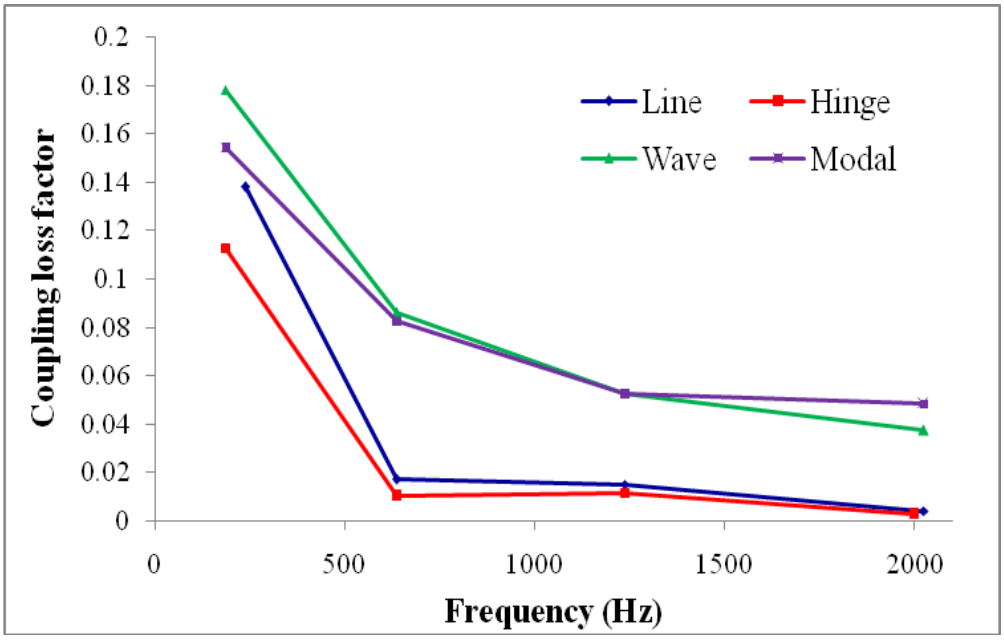


Figure 6.25 Coupling loss factors for perpendicular beams

## 6.9 Closure

Experimental readings of coupling loss factors have been taken for plate and beam structure. This chapter dealt with a comparison between theoretical and experimental results of coupling loss factors for two coupled plates by using different structural junctions. It is not a proper way to simply assume point or line connections of plates for analysis purpose, but it is required to consider specific joint in point connections of plates or beams. This shows the importance of technical understanding of connections for CLFs.

# Chapter 7

# CONCLUSIONS

The statistical energy analysis approach has been used for dynamic analysis of different structural elements. Estimation of the parameters like coupling loss factor, damping loss factor and modal density are the most important ladder in statistical energy analysis. In this work, theoretical expressions for statistical energy analysis with reference to damping loss factors and modal densities have been considered. The experimental results obtained for coupling loss factors and modal densities have been validated by the analytical results. By using same experimental methodology, around nineteen experiments have been conducted using different structural elements. Following conclusions are drawn based on the results obtained,

In order to determine the best capacity of dissipation of energy for the plates of aluminium, stainless steel, mild steel and composites with different boundary conditions have been experimentally tested. It has been found that aluminium plate has higher values of damping loss factor than stainless steel and mild steel plates for free-free, simply supported and clamped-free boundary conditions. The density of material affects the values of damping loss factor.

Unidirectional fiber orientation plate has higher damping loss factors than cross ply fiber orientation and quasi-isotropic fiber orientation plates. It has been observed that due to addition of graphene in plate made of composite materials with unidirectional fiber orientation, the capacity to dissipate vibro-acoustic energy improves. One can use this

parameter with different materials and fiber orientations for design of structural component for specific applications.

Modal density is useful to give insight into the vibro-acoustic analysis of structures when subjected to random excitations without the complete knowledge of frequencies and mode shapes. Modal densities of aluminium, stainless steel and mild steel plates are more for free-free boundary conditions than simply supported and clamped-free boundary conditions in low and mid frequency range. The effects of boundary conditions at low and mid are significant. At higher frequency range the effect of boundary conditions have not much influence.

It has been observed that cross-ply fiber orientation plate has higher values of modal density than unidirectional quasi-isotropic fiber orientation plates for free-free boundary conditions. The values of modal density of unidirectional fiber orientations plate with graphene are lower than unidirectional fiber orientations plate without graphene. Knowledge of modal density with fiber orientations and boundary conditions aid the designer in optimal design of structure.

Coupling loss factors for coupled plates of different materials have been determined analytically for point and line junctions. Two plates made of composite materials connected in same plane with point and line junctions have higher values of coupling loss factor than coupled plates of elastomer-rubber, thermoplastic-acrylics and nonferrous metal-copper. The ratio of modulus of elasticity to density of plate material affects the values of coupling loss factor.

For point junctions, the values of coupling loss factor significantly depend on type of junctions. The effects of bolted, screwed, riveted and hinged junctions on coupling loss factors have been experimentally verified. The values of coupling loss factor are higher for

bolted junctions as compared to screwed junctions for aluminium rectangular plates connected in same plane. This can be attributed to fact that bolted junctions have high transmission efficiency.

It can be concluded that higher values of coupling loss factor have been observed at higher values of tightening torques of bolted junctions for thin rectangular aluminium plates and the plates of composite materials connected in same plane. Interfacial pressure increases due to increase in preload of bolted junctions which results into increase of coupling loss factor values.

As compared to riveted junctions, higher values of coupling loss factors have been observed for bolted junctions for composite rectangular plates connected in same plane. When maximum vibro-acoustic energy is required to transmit from one subsystem to another subsystem, bolted junctions are preferably used rather than riveted junctions. Thus, vibro-acoustic energy flow can be controlled by selecting appropriate structural junctions between two components.

Coupling loss factor values changes with fiber orientation in composite plates. These values are significant at low and mid frequency range, whereas it is negligible at high frequency range.

Based on experimentations with composite plates, it is observed that the coupling loss factor is higher for cross ply fiber orientation composite plates in comparison to unidirectional fiber orientation composite plates. It can be concluded that designer can choose either cross ply fiber orientation or unidirectional fiber orientation based on desired coupling loss factor with all other considerations.

Coupling loss factor values for unidirectional fiber orientation composite plate without graphene are higher than unidirectional fiber orientation composite plate with graphene. Thus, it is possible to use estimated statistical energy analysis parameters for solving power flow equations to understand vibro-acoustic energy flow in different structures. This knowledge helps for effective design of structures in vibro-acoustic environment.

### 7.1 Future Scope

1. Studies can be carried out to understand influence of strength of connecting elements namely riveted, bolted, screwed and welded in structural junctions on statistical energy analysis parameters.

2. To design composite structures with suitable nano fillers to alter statistical energy analysis parameters as per the requirement.

3. This methodology can be extended with multiple subsystems to understand detailed vibro-acoustic energy flow.

# APPENDIX

## A) Uncertainty Analysis

Uncertainty of measurement is the doubt that exists about the result of any measurement. Uncertainty analysis involves systematic procedures for calculating error estimates for experimental data. Measurements errors arise from various sources, but they can be broadly classified as bias errors (systematic) and precision (random) errors. There are two types of uncertainties such as systematic and random uncertainties.

Systematic uncertainties are those due to faults in the measuring instruments or in the techniques used in the experiments. Systematic uncertainty decreases the accuracy of an experiment.

Random uncertainties' are associated with unpredictable variations in the experimental conditions under which the experiment is being performed or are due to deficiency in defining quantity being measured. Random uncertainty decreases the precision of an experiment.

There are two ways to estimate uncertainties,

i) Type A evaluation- Uncertainty estimates using statistics (usually from repeated readings).

When a set of several repeated readings (N) has been taken (for a type A estimate of uncertainty), the mean $\bar{x}$, and estimated standard deviation, $s$, can be calculated for the set.

$$\bar{x} = \frac{1}{N}\sum_{i=1}^{N} x_i \tag{01}$$

$$s = \sqrt{\frac{\sum_{i=1}^{N}\left(x_i - \bar{x}\right)}{N-1}} \tag{02}$$

From these, the estimated standard uncertainty, $\sigma_m$ of the mean is calculated,

$$\sigma_m = \sqrt{\frac{\sum_{i=1}^{N}\left(x_i - \bar{x}\right)}{N(N-1)}} = \frac{s}{\sqrt{N}} \tag{03}$$

ii) Type B evaluations- Uncertainty estimates from any other information. This could be information from past experience of the measurements, from calibration certificates, manufacture's specifications, from calculations, from published information, and from common sense.

a) Uncertainty in Addition and subtraction

Consider a, ….., x are the measured with uncertainties δa,…., δx and measurement is,

$$f = a + .... + d - (x + ..... + z) \tag{04}$$

$$\delta f = \left[(\delta a)^2 + .... + (\delta d)^2 + (\delta x)^2 + ..... + (\delta z)^2\right]^{1/2} \tag{05}$$

b) Uncertainty in multiplication and division

Consider a,….., x are the measured with uncertainties δa,…., δx and measurement is,

$$f = \frac{a \times \ldots\ldots \times d}{x \times \ldots\ldots \times z} \tag{06}$$

The original fractional uncertainty is given as,

$$\frac{\delta f}{f} = \left[ \left( \frac{\delta a}{a} \right)^2 + \ldots\ldots\ldots + \left( \frac{\delta d}{d} \right)^2 + \left( \frac{\delta x}{x} \right)^2 + \ldots\ldots + \left( \frac{\delta z}{z} \right) \right]^{1/2} \tag{07}$$

**1. Uncertainty analysis for Modal Density**

The sample calculation for uncertainty in modal density is given for five readings,

| Number of Modes | 51 | 53 | 48 | 49 | 54 |
|---|---|---|---|---|---|
| Modal Density | 0.017983 | 0.018688 | 0.016925 | 0.017278 | 0.019041 |

$$\bar{x} = \frac{1}{N} \sum_{i=1}^{N} x_i = 0.017983$$

$$s = \sqrt{\frac{\sum_{i=1}^{N} \left( x_i - \bar{x} \right)}{N - 1}} = 8.081 \times 10^{-7}$$

$$\sigma_m = \sqrt{\frac{\sum_{i=1}^{N} \left( x_i - \bar{x} \right)}{N(N-1)}} = 4.020 \times 10^{-4}$$

**2. Uncertainty analysis for Damping Loss Factors**

The damping loss factor is given as,

$$\eta = \frac{\omega_1 - \omega_2}{\omega_n} = \frac{\Delta \omega}{\omega_n} = 0.015347$$

Where Δω is frequency interval between two half points which are $z_1$ and $z_2$ be located of frequency where amplitude of response of this point is $\frac{1}{\sqrt{2}}$ times maximum amplitude.

$$\omega_1 = 1251 \pm 0.5Hz$$

$$\omega_2 = 1232 \pm 0.5Hz$$

$$\delta(\omega_1 + \omega_2) = \left[(\delta\omega_1)^2 + (\delta\omega_2)^2\right]^{1/2}$$

$$\delta(\omega_1 + \omega_2) = \left[(0.5)^2 + (0.5)^2\right]^{1/2} = 0.707$$

$$\frac{\delta\eta}{\eta} = \left[\left(\frac{\delta(\omega_1 - \omega_2)}{(\omega_1 - \omega_2)}\right)^2 + \left(\frac{\delta\omega_n}{\omega_n}\right)^2\right]^{1/1}$$

$$\frac{\delta\eta}{\eta} = \left[\left(\frac{0.7}{19}\right)^2 + \left(\frac{0.5}{1238}\right)^2\right]^{1/1} = 0.037 = 3.7\%$$

The absolute uncertainty for damping loss factor is 0.000571

**3. Uncertainty analysis for Coupling Loss Factors**

The coupling loss factor for screwed junction is given below,

$$\eta_{12} = \eta_1 \frac{E_2}{E_1}$$

$$\eta_{12} = 0.049$$

$$\eta_1 = 0.5759$$

$$V_1 = 418 \pm 0.001\mu m/s$$

$$V_2 = 122 \pm 0.001 \mu m/s$$

$$\frac{\delta\eta_{12}}{\eta_{12}} = \left[ \left( \frac{\delta\eta_1}{\eta_1} \right)^2 + 2\left( \frac{\delta v_1}{v_1} \right)^2 + 2\left( \frac{\delta v_2}{v_2} \right)^2 \right]^{1/2}$$

$$\frac{\delta\eta_{12}}{\eta_{12}} = \left[ (0.037)^2 + 2\left( \frac{0.001}{418} \right)^2 + 2\left( \frac{0.001}{122} \right)^2 \right]^{1/2} = 0.037 = 3.7\%$$

The absolute uncertainty for coupling loss factor is 0.001813.

## B. Codes in MatLab

The codes in MatLab for statistical energy analysis parameters are given below,

**1. Modal density of a plate-flexural vibration**

```
%[delf,nf,nomega]=md_plate_flex(rho,E,t,L1,L2)
%delf=average frequency spacing
%nf=modal density in Hz
%nomega=modal density rad/s
%rho=mass density
%E=Young's modulus of Elasticity
%t=thickness of the plate
%L1=length;L2=length
function [delf,nf,nomega]=md_plate_flex(rho,E,t,L1,L2)
c_Lp=sqrt(E/rho/(1-0.3^2));
khi=t/sqrt(12);
delf=2*khi*c_Lp/L1/L2;
nf=1/delf;
nomega=nf/2/pi;
```

**2. Program to determine beta_1**

```
%[beta]=eta_beta(eta,delf,fc)
%beta=modal damping coefficient
%eta=loss factor
%delf=frequency spacing
%k=1 for 1/3 octave band
%k=0 for octave band
function beta=eta_beta(eta,delf,fc)
  beta=fc*eta/delf;
```

**3. Driving point impedance of a plate in bending for line excitation**

```
%Z=dr_imp_plate_ln(f,rho,E,h)
%Z=driving point impedance
%f=frequency
%rho=mass density kg/m^3
%E=Young's modulus of Elasticity
```

```
%h=thickness
function Z=dr_imp_plate_ln(f,rho,E,h)
%++++++++++++++++++++++++++++++++++++++++
mu=0.3;
c_L=sqrt(E/rho/(1-mu^2));%LOngitduinal wave speed
c_p=phase_plate(f,h,E,rho);%phase speed of a plate
Z=2*rho*c_p*h*(1+j);
```

**4. Program to determine the transmission coefficient of a finite system**

```
%tau_12=trans_12(beta1,beta2,Z1,Z2)
%beta1=modaldamping factor of system 1
%beta2=modal damping factor of system 2
%Z1=Input impedance of system 1
%Z2=Input impedance of system 2
function tau_12=trans_12(beta1,beta2,Z1,Z2)
fac1=1/2/pi/(beta1+beta2);
fac2=1/2/pi*(1/beta1+1/beta2);
tau_inf=trans_inf(Z1,Z2);
tau_12=tau_inf/(fac1^2+(1+tau_inf*fac2)^2)^0.5;
```

**5. Program for converting tau_12 to eta_12**

```
%function eta_12=tau12_eta12(delf1,fc,tau12,beta1,beta2)
%eta_12=coupling loss factor
%delf1=frequency spacing
%tau_12=Transmission coefficient
%beta1=modal damping of the first system
%beta2=modal damping of the second system
function eta_12=tau12_eta12(delf1,fc,tau12,beta1,beta2)
  fac=1/pi/beta1+1/pi/beta2;
  eta_12=delf1/pi/fc*(tau12/(2-tau12*fac));
```

**6. Program to determine the line integral of a plate-to-plate connection**

```
%function I_12=I_12_line(f,h1,E1,rho1,h2,E2,rho2,Lj);
%I12=line integral
%f=frequency
%h1=thickness of plate 1
```

```
%h2=thickness of plate 2
%E1=Young's modulus of plate 1
%E2=Young's modulus of plate 2
%rho1=density of plate 1
%rho2=density of plate 2
%Lj=length of the junction
function I12=I_12_line(f,h1,E1,rho1,h2,E2,rho2,Lj)
k1=wave_number_pl(f,h1,E1,rho1);
k2=wave_number_pl(f,h2,E2,rho2);
I12=Lj/4*((k1^4*k2^4)/(k1^4+k2^4))^0.25;
```

**7. Bending number of a plate**

```
%k_b=wave_number_pl(f,h,E,rho);
%%f=frequency
%E=Young's modulus of elasticity
%rho=mass density
function k_b=wave_number_pl(f,h,E,rho)
k_i=h/sqrt(12);
mu=0.3;
cl=sqrt(E/rho/(1-mu^2));
cp=sqrt(2*pi*f*k_i*cl);%cp=phase speed
k_b=2*pi*f/cp;
```

**8. Program to find CLF for plate-plate structure**

```
clear
f=octav_third;
fc=f(:,2);
n=max(size(f));
eta=0.01;
for j=1:n,
  [delf1(j),nf1,nomega1]=md_plate_flex(2600,80e9,0.003,1,1);
  [delf2(j),nf2,nomega2]=md_plate_flex(2600,80e9,0.003,1,1);
  beta1(j)=eta_beta(eta,delf1(j),fc(j));
  beta2(j)=eta_beta(eta,delf2(j),fc(j));
  Z1(j)=dr_imp_plate_ln(fc(j),2600,80e9,0.003);
```

```
  Z2(j)=Z1(j);
  tau_12(j)=trans_12(beta1(j),beta1(j),Z1(j),Z2(j));
eta121(j)=tau12_eta12(delf1(j),fc(j),tau_12(j),beta1(j),beta2(j))*I_12_line(fc(j),0.003,80e9,26
00,0.003,80e9,2600,0.9)
eta122(j)=tau12_eta12(delf1(j),fc(j),tau_12(j),beta1(j),beta2(j))*I_12_line(fc(j),0.003,80e9,26
00,0.003,80e9,2600,0.2)
eta123(j)=tau12_eta12(delf1(j),fc(j),tau_12(j),beta1(j),beta2(j))*I_12_line(fc(j),0.003,80e9,26
00,0.003,80e9,2600,0.02)
  end
  loglog(fc,eta121,fc,eta122,fc,eta123)
  xlabel('Frequency, Hz')
ylabel(‘Coupling Loss Factor’)
title('Modal Coupling Factor')
grid
```

**REFERENCES**


1. **Lyon, R.H.,** and **Maidanik, G.** (1962) Power flow between linearly coupled oscillators, *J.Acoust.Soc.Am.*, **34**,623-639.

2. **Ungar,E.E.** (1967) Statistical energy analysis of vibrating systems, *Journal of engineering for Industry, Transactions of the ASME,* 626-632.

3. **Mercer C. A.** (1971) Energy flow between two weakly coupled oscillators subject to transient excitation, *Journal of Sound and Vibration*, 15, 373-379.

4. **Bies, D.A**. and **Hamid, S.** (1980) In situ determination of loss and coupling loss factors by the power injection Method, *Journal of Sound and Vibration ,* **70**, 187–204.

5. **Woodhouse, J.** (1981) An introduction to statistical energy analysis of structural vibration, Applied Acoustics, **14**, 455-469.

6. **Gibbs, B.M.,** and **Craven, P.G.** (1981) Sound transmission and mode coupling at junctions of thin plates, Part I: representation of the Problem, *Journal of Sound and Vibration,* **77(3),** 417-427.

7. **Craik,R.J.M.** (1983) The prediction of sound transmission through buildings using statistical energy analysis. *Journal of Sound and Vibration,* **82**, 505–516.

8. **Sablik, M.J., Beissner, R. E., Silvus, H.S.** and **Miller, M.L.** (1985) Statistical energy analysis, structural resonances, and beam networks, *J.Acoust.Soc.Am.*, **77(3)**,1038-1045.

9. **Fahy, F.J.,**and **De-Yuan, Y.** (1987) Power flow between non-conservatively coupled oscillators, *Journal of Sound and Vibration* ,**114**, 1-11.

10. **Hodges, C.H., Nash, P.** and **Woodhouse, J.,** (1987) Measurement of coupling loss factors by matrix fitting: an investigation of numerical procedures, *Applied Acoustics,* **22**, 47-69.

11. **Craik, R.** (1996) Sound transmission through buildings using Statistical Energy Analysis. *Gower Publishing Limited, Hampshire, England*.
12. **Bosmans, I.,Mees, P. and Vermeir, G.** (1996) Structure-borne sound transmission between thin orthotropic plates: analytical solutions, *Journal of Sound and Vibration,* **191(1),** 75-90.
13. **Bercin, A.N.,** (1997) Analysis of energy flow in thick plate structures, *Computers and structures*, **62**,747-756.
14. **Sheng, M.P., Wang, M.Q.** and **Sun, J.C.** (1998) Effective internal loss factors and coupling loss factors for non-conservattively coupled systems, *Journal of Sound and Vibration,* **209(4),** 685-694.
15. **Ma,Y.C., Bolton, J. S., Jeong, H., Ahn, B.** and **Shin, C.** (2002) Exprimental statistical energy analysis applied to a rolling piston-type rotary compressor, *International compressor Engineering conference*,1571.
16. **Hopkins, C.** (2002) Statistical energy analysis of coupled plate systems with low modal density and low modal overlap, *Journal of Sound and vibration*, 251(2), 193-214.
17. **Maxit,L.** and **Guyader, J.L**.(2003) Extension of SEA model to subsystems with non-uniform modal energy distribution, *Journal of Sound and Vibration,* **265**, 337-358.
18. **Seon-Woong, Hwang.** (2004) Transmission path analysis of noise and vibration in a rotary compressor by statistical energy analysis, *KSME International Journal*, **18(11)**, 1909-1915.
19. **Chieh-Yuan, Cheng.,Rong-Juin, Shyu.** and **der-Yuan, Liou.,** (2007) Statistical energy analysis of non-resonant response of isotropic and orthotropic plates, *Journal of Mechanical Science and Technology*, **21**, 2082-2090.
20. **Ji,L.**, and **Mace, B.R**. (2008) Statistical energy analysis modelling of complex structures as coupled sets of oscillators: Ensemble mean and variance of energy, *Journal of Sound and Vibration,*317, 760-780.

21. **Santos, E.R.O., Arruda, J.R.F.,** and **Dos, Santos. J.M.C.,** (2008) Modeling of coupled structural systems by an energy spectral element method, *Journal of Sound and Vibration*, **316**, 1-24.
22. **Wang, S., and Bernhard, R.J.,** (2009) Prediction of averaged energy for moderately damped systems with strong coupling, *Journal of Sound and Vibration*, 319,426-444.
23. **Ragnarsson, P., Pluymers B., Donders, S.,** and **Desmet, W.** (2010). Subcomponent modelling of input parameters for statistical energy analysis by using a wave-based boundary condition. *Journal of Sound and Vibration*, **329**, 96-108.
24. **Alain,Le. Bot.,** (2010) Statistical energy analysis and the second principle of thermodynamics, *IUTAM Symposium on the vibration analysis of structures with uncertainties*, 129-139.
25. **Lafont, T., Totaro, N.,** and **Le, Bot. A.** (2013) Review of statistical energy analysis hypothesis in vibroacoustics, *Phil.Trans.R.Soc.Lond.A*, **470,**1-20.
26. **Wilson, D.,** and **Hopkins, C.** (2015) Analysis of bending wave transmission using beam tracing with advanced statistical energy analysis for periodic box-like structures affected spatial filtering, *Journal of Sound and Vibration*, **341**,138-161.
27. **Cristina, Díaz-Cereceda., Jordi, Poblet-puig.,** and **Antonio, Rodriguez-Ferran.,** (2015) Automatic subsystem identification in statistical energy analysis, *Mechanical systems and signal processing*, 54-55, 182-194.
28. **Olaf, Täger., Martin, Dannemann.,** and **Werner, A.H.,** (2015) Analytical study of the structural-dynamics and sound radiation of anisotropic multilayered fibre-reinforced composites, *Journal of Sound and Vibration*, **342**, 57-74.
29. **Sablik,M. J.,** (1882) Coupling loss factors at a beam L-joint revisited, *J.Acoust.Soc. Am.*, **72(4),** 1285-1288.

30. **Clarkson, B. L.,** and **Ranky, M.F.** (1984) Modal Density of Honeycomb Plates, *Journal of Sound and Vibration,* **91 (1),** 103–118.
31. **Langley,R.S.** (1989) A general derivation of the statistical energy analysis equations for coupled dynamic systems, *Journal of Sound and Vibration,*135 (3), 499-508.
32. **Langley,R.S.** (1990) A derivation of the coupling loss factors used in statistical energy analysis, *Journal of Sound and Vibration,***141(2)**,207-219.
33. **Clarkson, B.L.** (1991) Estimation of the Coupling Loss Factor of structural joints. *Proc IMechE Part C: Journal of Mechanical Engineering Science,* **205**, 17-22.
34. **Fahy, F.J.** and **Mohammed, A.D.** (1992) A study of uncertainty in applications of SEA to coupled beam and plate systems, Part I: Computational experiments, *Journal of Sound and Vibration,* **158(1)**, 45-67.
35. **Cacciolati, C.** and **Guyader, J.L.** (1994) Measurement of SEA coupling loss factors using point mobilities, *Phil.Trans.R.Soc.Lond.A,* **346**, 465-475.
36. **Fahy, F.J.** (1994) Statistical energy analysis: a critical overview, *Phil.Trans.R.Soc.Lond.A,* **346**, 431-447.
37. **Tso, Y.K.** and **Norwood C.J.,** (1995) Vibratory power transmission through three-dimensional beam junctions, *Journal of Sound and Vibration*, **185(4)**, 595-607.
38. **Shankar,K.,** and **Keane, A.J.** (1995) Vibrational energy flow analysis using a substructure approach: The application of receptance theory to FEA and SEA, *Journal of Sound and Vibration,* **201(4),** 491-513.
39. **Fahy F. J.,** and **Ruivo, H.M.** (1997) Determination of statistical energy analysis loss factors by means of an input power modulation technique, *Journal of Sound and Vibration,* **203(5),** 763-779.
40. **Manik, D.N.,** (1998) A new method for determining coupling loss factors for SEA, *Journal of Sound and Vibration,* **211(3),** 521-526.

41. **Fahy F. J.** (1998) An alternative to the SEA Coupling Loss Factor: Rational and method for experimental determination. *Journal of Sound and Vibration,* **214(2),** 261-267.
42. **Hugin, C. T.** (1998) Power transmission between two finite beams at low modal overlap, *Journal of Sound and Vibration,* **212(5),** 829-854.
43. **Ming, R. S.** (1998) The measurement of coupling loss factors using the structural intensity technique. *Journal of the Acoustical Society of America,* **103,** 401–407.
44. **Mace, B.R.** (1998) The SEA of two coupled plates: an investigation into the effects of subsystem irregularity, *Journal of Sound and Vibration,* **212(3)**, 395-415.
45. **Maxit,L.** and **Guyader, J.L.** (2001) Estimation of SEA coupling loss factors using a dual formulation and FEM modal information, Part I: Theory, *Journal of Sound and Vibration,* **239(5)**, 907-930.
46. **Bosmans, I.** and **Vermeir, G.** (2002) Coupling loss factors for coupled anisotropic plates, *Journal of Sound and Vibration,* **250(2),** 351-355.
47. **Ming, R.S.** and **Pan, J.,** (2003) Approximation errors for the measurement of coupling loss factors using the ELD method, *Applied Acoustics,* **64**, 931-940.
48. **Grushetsky, I.** and **Smol'nikov, A**. (2004) FEM application for calculation of coupling loss factors used in SEA, L-shaped beams case, *Technical Acoustics*, **6**, 1-9.
49. **Grushetsky, I.** and **Smol'nikov, A**. (2005) Determination of coupling loss factors for two beams using FEM, *Technical Acoustics*,**24**,1-7.
50. **Mace B. R.** (2005) Statistical energy analysis: coupling loss factors, indirect coupling and system modes, *Journal of Sound and Vibration,* **279**, 141-170.
51. **Panuszka, R., Wiciak** and **Iwaniec, M**. (2005) Experimental assessment of coupling loss factors of thin rectangular plates. *Archives of Acoustics,* **30(4),** 533-551.
52. **Ruisen, Ming.,** (2005) An experimental comparison of the sea power injection method and the power coefficient method, *Journal of Sound and Vibration,***282**, 1009-1023.

53. **Grushetsky, I.** and **Smol'nikov, A**., (2006) Computing of coupling loss factors using FEM, probabilistic approach, *Technical Acoustics*, **10**, 1-12.

54. **Thite, A.N.,** and **Mace B. R.,** (2007) Robust estimation of coupling loss factors from finite element analysis, *Journal of sound and vibration,* **303**, 814-831.

55. **Mace, B.R.** and **Ji, L.,** (2007) The statistical energy analysis of coupled sets of oscillators, *Phil.Trans.R.Soc.Lond.A,* **463**, 1359-1377.

56. **Nunes,R.F., Ahmida,K.M.,** and **Arruda, J.R.F**. (2007) Applying a fuzzy-set-based method for robust estimation of coupling loss factors, *Journal of sound and vibration,***307,** 38-51

57. **Yoo, J.W., Thompson, D.J.,** and **Ferguson, N.S.** (2007) Investigation of beam-plate systems including indirect coupling in terms of statistical energy analysis, *Journal of Mechanical Science and Technology*, **21**, 723-736.

58. **Thite, A.N.,** and **Mace B. R.,** (2010) The effects of design modifications on the apparent coupling loss factors in SEA-like analysis, *Journal of sound and vibration*, **329**, 5194-5208.

59. **Ben,Souf. M.A., Barelle, O., Ichchou, M.N., Troclet, B.,** and **Haddar, M.** (2013) Variability of coupling loss factors through a wave finite element technique, *Journal of sound and vibration*, **332,** 2179-2190.

60. **Abdullah, Secgin.** (2013) Numerical determination of statistical energy analysis parameters of directly coupled composite plates using a modal based approach, *Journal of sound and vibration*, **332**,361-377.

61. **Lin, Ji.,** and **Zhenyu, Huang.** (2014) A simple Statistical Energy Analysis technique on modelling continuous coupling interfaces. *Journal of Vibration and Acoustics*, **136**,14501-14503.

62. **Jintao, Gu.** and **Meiping, Sheng.** (2015) Improved energy ratio method to estimate coupling loss factors for series coupled structure, *Journal of Mechanical Engineering*, **45(1)**, 37-40.

63. **DLFS Yap, F.F.,** and **Woodhouse, J.** (1996) Investigation of damping effects on statistical energy analysis of coupled structures, *Journal of Sound and Vibration,* **197(3)**, 351-371.

64. **Ahmed,Maher., Fawkia, Ramadan.,** and **Mohamed, Ferra.** (1999) Modeling of vibration damping in composite structures, Composite Structures, **46**, 163-170.

65. **Marek, Iwaniec.,** (2003) Damping loss factor estimation in plates, *Journal of Molecular and Quantum Acoustics,* **24**, 437-442.

66. **Nirmal Kumar, Mandal., Roslan Abd, Rahman.,** and **M. Salman Leong**, (2004) Experimental study on loss factor for corrugated plates by bandwidth method, Ocean Engineering, **31**, 1313–1323.

67. **Kranthi Kumar, Vatti.** (2011) Damping Estimation of Plates for Statistical Energy Analysis, Thesis submitted for M.S. at University of Kansas, March, 2011.

68. **Wang, A.,Yin,X.,Li, X.,** and **Chen,L.** (2013) Numerical and experimental study on modal damping loss factor of structural panels with damping treatments, 20th International congress on Sound and vibration, July 2013.

69. **Clarkson, B.L.,** and **Ranky M.F.** (1981) Modal density of Honeycomb plates, *Journal of Sound and Vibration,***91(1),** 103-118.

70. **Renji** (2000) Experimental modal densities of Honeycomb sandwich panels at high frequencies, *Journal of Sound and Vibration,* **237(1),** 67-79.

71. **Finnveden, S.** (2004) Evaluation of modal density and group velocity by a finite element method, *Journal of Sound and Vibration,* **273**, 51–75.

72. **Xie,G., Thomson,D.J.,** and **Jones, C.J.C.** (2004) Mode count and modal density of structural systems: relationship with boundary conditions, *Journal of Sound and Vibration,* **274,** 621–651.

73. **Ramachandran, P.,** and **Narayanan, S.** (2007) Evaluation of modal density, radiation efficiency and acoustic response of longitudinally stiffened cylindrical shell, Journal of Sound and Vibration, **304,** 154–174.

74. **Cotoni, V.,Langley, R.S.,** and **Shorter, P.J.**(2008) A statistical energy analysis subsystem formulation using finite element and periodic structure theory, Journal of Sound and Vibration, **318,** 1077–1108.

75. **Richard, Bachoo.,** and **Jacqueline, Bridge.** (2013) The modal distribution and density of fibre reinforced composite beams. *Journal of Sound and Vibration,* **332,** 2000-2018.

76. **Jingyong, Han.,Kaiping, Yu., Xiangyang, Li.,** and **Rui,Zhao.** (2015) Modal density of sandwich panels based on an improved ordinary sandwich panel theory, *Composite Structures*, **131**, 927-938.

## LIST OF PUBLICATIONS BASED ON THE RESEARCH WORK

**International Journals:**

1. Maruti B.Mandale, P.Bangarubabu and S.M.Sawant. Statistical energy analysis parameter estimation for different structural junctions of rectangular plates. Proc IMechE Part C: J Mechanical Engineering Science**,** 2016, 230(15), 2603-2610.

2. Maruti B.Mandale, P.Bangarubabu and S.M.Sawant. Damping Loss Factor estimation by experimental method for plate with convetional and composite materials, International Journal on Design and Manufacturing Technologies, ISSN 0973-9106, 2015, 09(2), 6-11.

3. Maruti B.Mandale, P.Bangarubabu and S.M.Sawant. Estimation of statistical energy analysis parameters for fiber reinforced composite plates. (Submitted to Noise and Vibration Worldwide Journal-Under Review)

**International Conferences:**

1. Maruti B.Mandale, P.Bangarubabu and S.M.Sawant, Damping Loss Factor estimation by experimental method for plate with convetional and composite materials, Int. Conf. on Industrial, Mechanical and Production Engineering: Advancements and Current Trends, MANIT, Bhopal**,** 27-29 November, 2014.

2. Maruti B.Mandale, P.Bangarubabu and S.M.Sawant, Determination of statistical energy analysis parameter of idealized subsystem with different materials, Sixth International Conference on Theoretical, Applied, Computational and Experimental Mechanics, 6th ICTACEM, 2014", IIT Kharagpur, 29-31 December, 2014.

3. Maruti B.Mandale, P.Bangarubabu and S.M.Sawant. Influence of torque at structural junction of rectangular plates on coupling loss factors. Innovative Design, Analysis and Development Practices in Aerospace and Automotive Engineering (I-DAD 2018), Veltech University, Chennai, 22-24 February, 2018.